Acknowledgments

Section 1: The Long Road to High Current Density Superconducting Conductors

David Larbalestier thanks Peter Lee for many discussions and Alex Malozemoff for a critical manuscript review. The vital help in final chapter preparation by Dmytro Abraimov is gratefully acknowledged.

Section 1.2: Alloyed Superconductors, The Type I and Type II Transition and the Collective Failure to Understand It.

A. G. Shepelev acknowledges with gratitude the discussions with academician N.F. Shul'ga, Director of NSC KIPT/Akhiezer Theoretical Physics Institute and with members of the Scientific Council.

Section 4: Bi-Ca-Sr-Cu-O HTS Wire

MWR thanks Alex Malozemoff, David Larbalestier and Bill Carter for critical review of this manuscript and acknowledges the contribution of the WDG members to advancing the understanding of BSCCO material science.

EEH acknowledges support from the DOE-HEP, NSF-DMR, and the State of Florida, as well as useful discussion with colleagues at the Applied Superconductivity Center at the National High Magnetic Field Laboratory at Florida State University.

12

Large Scale Applications

Editors: Peter Komarek, Bruce Strauss, Steve St. Lorant, Luca Bottura and Al McInturff

12.1 Introduction

Steve St. Lorant

Rarely in the history of science has so great and useful a discovery as superconductivity had so long a period of gestation before acceptance by the technical world. From the very beginning the phenomenon was burdened by the stigma of arcane science, metals such as mercury, tin and lead that are unsuitable for any practical application, nonexistent theoretical underpinnings, the very low and difficult-to-achieve temperatures, and even early doubts by the discoverer as to the practical value of zero electrical resistance. In the following two years attitudes changed so much so that by the Third International Congress of Refrigeration held in Chicago in 1913 Kammerlingh Onnes was able to speculate: "... When all outstanding questions will have been studied and all difficulties overcome, the miniature coil referred to may prove to be the prototype of magnetic coils without iron, by which in future much stronger and ... more extensive fields may be realized than are at present reached in the interferrum of the strongest electromagnets. As we may trust in an accelerated development of experimental science this future ought not to be far away ..."

But the phenomenon brooked no rapid penetration into its mysteries. In 1914 Onnes discovered that resistance was restored by a magnetic field leading to the realization that one consequence of a critical magnetic field leads to a limiting current strength supported by a superconductor. Two years

later Silsbee pointed out that the restoration of resistance in a wire was simply due to the magnetic field produced by the flowing current and not caused by any inherent properties of the metal.

The ensuing forty or so years were devoted to intense practical and theoretical investigations into the phenomenon, highlighted by the discovery of the Meissner-Ochsenfeld effect and obscured by confusing nomenclature defining superconductors as Type I, Type II, hard, dirty, sponge-like, mixed, intermediate, etc., thereby demonstrating its complexity. This confusion reached a zenith at the 1963 International Conference on the Science of Superconductivity where the participants unanimously petitioned the IUPAP to rule on the use of the symbols H_{c1} and H_{c2}! And that happened two years after the discovery of the properties of niobium-tin. At the same conference, in his closing remarks Pippard said: "... we are in the process of handing over to engineers the problem of superconductivity. If engineers have got to be trained to the point where they are competent to understand a time-dependent Ginzburg-Landau equation, or perhaps BCS theory and Green function formalism, I suspect they'll have precious little brains left for the useful arts and will become bad scientists and worse engineers."

How wrong was he! Another dynamic was at work—the needs of physicists and engineers in other fields, in energy, in particle physics, in transport, in industries not usually associated with state of the art engineering. Mere months after the discovery of the high-field properties of niobium-tin, the particle physics community (they were not yet HEP in those days) met to discuss the potential use of this new material for the construction of magnets, for detectors initially. For accelerators conventional magnets were still de rigueur. Meanwhile in the industrial sector an intense search for suitable materials followed, with the result that niobium-zirconium became what we may call the first superconductor produced on an industrial scale, Avco Everett's NbZr Supergenic Strip, SG 700, consisting of nine wires embedded, in parallel, in a copper substrate, boasting of a current density of 2.78×10^4 A/cm^2.

We should not forget the simultaneous search for high T_c compounds, Nb_3N, V_3Si, V_3Ga, Nb_3Ge and ultimately, at ~21 K, the heroic $Nb_{79}(Al_{73}Ge_{27})_{21}$! Of the alloys, NbZr and NbTi remained and of these only the latter survived, but not before a NbZr magnet became for a short while the first and largest superconducting magnet, built by Avco, a 3 meter, 4 tesla device, a working model of a type that would be used in a large-scale commercial MHD generator. The saddle-shaped magnet was constructed of five concentric modules, each containing two concentric winding layers and used 20,700 meters of conductor. In announcing this event, the Avco Everett Public Relations Department release casually noted that "... should the windings develop a resistive "hot" spot, the Avco design transfers the current out of that area and into the copper with no change in field strength. In effect, the copper acts as a shunt, allowing the current to bypass the "hot" spot until the spot cools and resumes superconductivity". And thus was the concept of cryostatic stability formally announced to the world.

Shortly thereafter Avco abandoned NbZr and reformulated its "Supergenic" strip with NbTi, in company with a number of other manufacturers. In parallel, the RCA and GE companies began manufacturing niobium-tin ribbon, marketed by the former as "Vapodep", the latter as plain "GE Superconductive Tape", together with a range of tape-wound high field superconducting laboratory solenoids, so much so that by the end of 1966 glossy product catalog literature was being distributed. The industrialization of superconductivity had begun.

This advertising literature interspersed with technical papers makes fascinating reading. One is struck immediately by the obvious lack of understanding of the principle of cryostability; somehow the importance of the triad of field, current and temperature was not fully appreciated, and the presence of an "excess" copper was regarded more as a trick of the trade rather than something which had a sound physical basis. But this changed in the summer of 1968 when at the Brookhaven Summer Study where the theoretical underpinnings of stability in cooled superconducting magnets were discussed at the same time as the first tests of the Argonne 12-foot bubble chamber magnet were presented, a magnet which was designed with this principle in mind. Also at this meeting the participants were treated to another, quite unanticipated, criterion, that of "intrinsic" stability. Taken

together, this gathering of scientific and engineering talent in the name of superconductivity quite negated Pippard's earlier concerns, a solution of GLAG equations was obviously not required to build useful superconducting magnets!

Every science needs a forum. Initially progress in the technical field of superconductivity was announced in the pages of the proceedings of the Cryogenic Engineering Conference. Then in November 1966 a euphemistically called National Superconductivity Information Meeting was hosted by the Brookhaven National Laboratory, sponsored by the US Atomic Energy Commission, which quickly morphed into the Applied Superconductivity Conference. For several years this gathering sought a home for the publisher of its proceedings, in 1974 it finally found refuge in the IEEE and proudly displayed its logo and that year's papers on the front cover of an issue of *IEEE Transactions on Magnetics*. ASC papers are now published in an issue of *IEEE Transactions on Applied Superconductivity*. Of course in any nascent science or technology there is a growing demand for publication space, our science being no exception, so that in the succeeding years the number of journals and publishers demanding our emanations proliferated.

Let us return now to hardware. In the four years following Brookhaven 1968, we saw intense activity in the DC magnet construction business as well as the first tentative entries into pulsed magnets, catalyzed by the work at the Rutherford Laboratory, to which we owe the eponymous conductor design we all, or almost all, use today. During this time also numerous proposals for the use of superconducting magnets in fusion research, levitation, medicine, power generation and transport were made. Who can forget the daring superconducting electromagnetic guns intended to hurl equipment into space, the high speed levitated trains and the promise of new medical applications for intravascular navigation or tumor therapy? Unfortunately this period also saw the demise of a number of promising conductor fabricators whose products, while conceptually well designed, were often far too expensive for the meager demand. Yes, the applied superconductivity community was replete with wonderful ideas, enthusiastically presented at the ASC meetings, but by and large they were paper studies, prompting the late Paul Reardon to remark on one occasion that he was "... but a part of the theoretical applied superconductivity community".

This state of affairs did not last long; various governments with deep pockets began to understand the importance of superconductivity and began to support projects in which the phenomenon played an important part. In the following pages we will read about the history of fusion magnets, about the efforts the power generation industry made to introduce novel concepts into established and very conservative utilities and about successes in industries which once seemed to be at the most remote end of the interest spectrum: ore beneficiation, and metal treatment. High energy physics due to its high demand for magnets quickly subsumed the major conductor development in an effort to satisfy the growing need for larger and more powerful accelerators and detectors; not only were improvements in the conductors sought, but industrialization of the entire facility construction process was invented. We will be reminded by our contributors that the road to the Large Hadron Collider, HEP's most ambitious undertaking was often littered both with niggling failures and monumental mistakes, and we expect that the next major project involving superconductivity, ITER, will encounter similar bumps in its road to a successful demonstration of its potential.

Several articles will be conspicuous by their absence, magnetohydrodynamic power generation, levitated transport and some facets of medical applications. Magnetic resonance imaging systems will be found elsewhere in this book; and while the design and fabrication of the superconducting magnets for this application is by now a major, worldwide industrial endeavor, the initial attempts to produce a patient-friendly diagnostic system make fascinating reading.

Magnetohydrodynamic power generation seems to have receded into the background, obscured no doubt by the extensive attention focused on fusion. Nevertheless some impressive superconducting magnets for MHD were designed and built, none more notable than the Argonne production of the magnetic channel for use in the bypass loop of the U-25 MHD facility in Moscow, a part of the 1976 US-USSR magnetohydrodynamics information exchange. Regrettably this program never came to fruition and whatever data were obtained disappeared into forgotten archives. A compara-

bly sized dipole magnet was designed and built by the same team for the UTSI Coal Fired Flow MHD Research Facility in 1981; channel corrosion problems as well as NO_x formation and control led to the termination of the program in 1995.

Magnetohydrodynamic drives were popularized by the *Star Trek* universe and were featured in a number of science fiction stories, the best known being the film adaptation of the *Hunt for Red October* which described the drive as a "caterpillar drive" for submarines, a stealthy, silent propulsive system. In the novel of the same name the drive was a "pumpjet", a variant of which appeared in reality in Japan, in 1992. The Ship and Ocean Foundation set up a research organization in 1985 to demonstrate that a ship can actually be propelled by MHD thrusters: the *Yamato 1* was the result. This 185 ton ship had a drive consisting of six dipole superconducting magnets of 4 tesla each, linked together in a hexagonal pattern around the seawater ducts and a small but complete cryogenic recondensing facility on board. The magnets were operated in the persistent mode. Its design speed was about 8 knots. On the basis of this program, the participants concluded that to make superconducting MHD ship drives a practical proposition, very much larger magnets with higher fields were required, but, even more importantly, a higher electrical conductivity of the sea water was essential!

Turning to levitation, particularly of people movers, we find intense initial interest in the superconductor community, an interest which inevitably always seemed to be on the verge of a major breakthrough. The Magneplane of 1972 epitomized this thinking and for virtually the first time addressed issues not directly connected with magnets, superconducting or otherwise: passenger comfort, the needs of the infrastructure, rights of way and the like. Subsequently a number of short track demonstration projects were launched in Europe and Asia culminating in the opening for public service in 2004 of the Shanghai Maglev Train, a 30.5 km long track covered at a commercial maximum speed of 431 km per hour; its EMS system however powered by resistive magnets.

As we will learn in more detail in the following pages, the phenomenon of superconductivity has earned its place in the world of magnet engineering, power management and varied industrial applications. It is not a universal panacea for things magnetic, but it is a very benign phenomenon when approached with understanding and treated with respect.

12.2 The History of Superconductivity in High Energy Physics

Steve A. Gourlay and Lucio Rossi

12.2.1 Introduction

Scientists spent the last half of the century putting together what is called the Standard Model of particle physics. The Standard Model, which explains the basic interactions of fundamental particles that make up everything we see, is the most complete physical theory in history, yet it leaves 95% of the universe unexplained! Particle physicists use accelerators to recreate the conditions of the early universe in an attempt to piece together the complex puzzle of how we got to where we are today. These huge machines are used to accelerate particles like electrons, protons and ions of various masses to high energies where they are brought together in collisions that generate particles that only existed a few moments after the Big Bang that created the universe 15 billion years ago.

An electron or proton accelerated by a potential difference of 1 V acquires an energy of one electron-volt or 1 eV. Typical accelerators today operate in the range from millions of electron-volts (MeV) to Tera electron-volts (TeV). Accelerators enable particle physicists to explore the fundamental nature of matter and gain insight into the rules that govern their interactions.

The Large Hadron Collider, or LHC, is located near Geneva, Switzerland and is the largest and most powerful particle accelerator in the world with a circumference of 27 km. Protons with energies of 7 TeV will be brought to collision inside giant detectors used to reconstruct the complex collisions that consist of hundreds of particles. This gargantuan "time machine" will generate conditions that existed approximately 20 billionths of a second after the Big Bang, and, if nature is kind, will uncover phenomena never seen before.

Accelerators were invented at the beginning of the 1930s and soon became key instruments for nuclear and particle physics. Ernest O. Lawrence, who won the Nobel Prize in 1939 for the invention of the cyclotron, a circular accelerator that opened the door to high-energy physics, was the first to use the new technology for medical applications.

In this history of accelerators, of high-energy physics, (HEP) seen from the point of superconductivity we would be remiss if we failed to mention the first purpose built accelerator, the Bevatron. When operations started in 1954, this weak focusing proton synchrotron with resistive magnets had initially but one mission: to demonstrate the existence of the antiproton. It achieved that goal signally and in the years following gave the nascent HEP community an incredibly useful tool with which to explore the nuclear realm. Figure 12.1 is a picture of this historic particle accelerator during decommissioning, a sight guaranteed to evoke many a memory in the readers of this book, and at the same time highlight the remarkable progress which the phenomenon of superconductivity has brought to HEP.

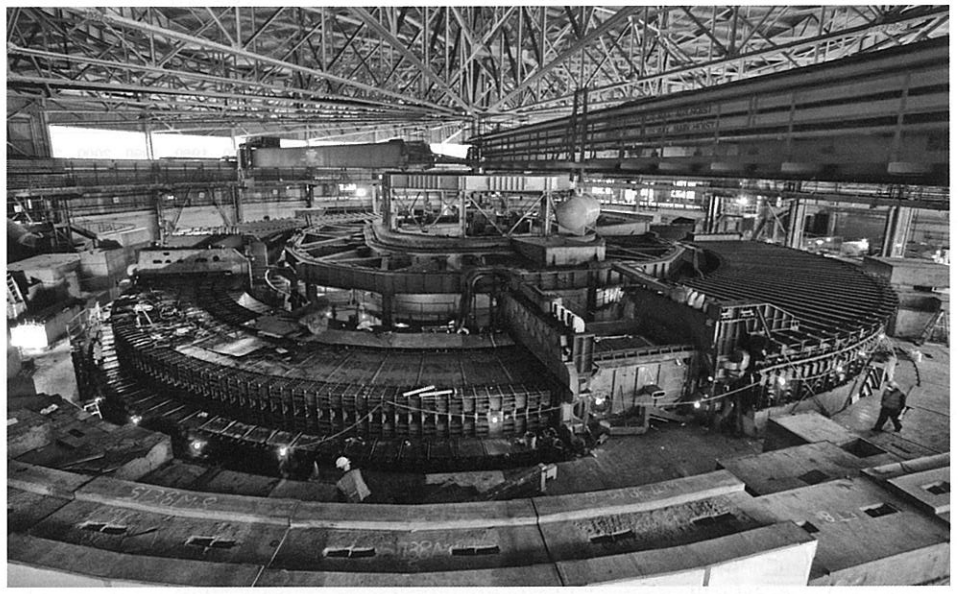

FIGURE 12.1: The Bevatron. (Courtesy LBNL.)

Figure 12.2, the so-called Livingston Plot, illustrates the increase in accelerator energy over time; it charts the evolution from Lawrence's cyclotron, capable of 0.03 to 0.1 GeV, in the early 1930s, through the Cosmotron and Bevatron to today's LHC and on to possible future projects. As can be seen from the plot, starting in the 1980s, superconducting magnets have been a major enabling technology in the development of particle accelerators.

The adventure started in the mid-1960s, thanks to the pioneering work of W.B. Sampson at Brookhaven National Laboratory (BNL), who built a 76-mm-aperture, 85-T/m quadrupole magnet model wound from Nb_3Sn ribbons and cold tested in January 1966. The feasibility and reliability

of large superconducting magnet systems was demonstrated by the Tevatron at FNAL, which was commissioned in 1983. The Tevatron paved the way to commercial applications of applied superconductivity (such as Magnetic Resonance Imaging or MRI systems) and to a series of ever more ambitious projects (HERA, SSC, UNK, RHIC and now LHC), which have continuously pushed the technology forward.

A wide variety of acceleration methods have been developed over the years, but they all require a means of generating a time-varying electric field to accelerate the charged particles. Modern accelerators come in two main configurations. Linear accelerators or "linacs" built from a series of radio frequency (RF) structures that generate the accelerating field and circular machines (cyclotrons and synchrotrons) that contain the particles using magnetic fields, sending the particles through the accelerating structure again and again until they have reached their final energy. Each can operate with a single beam, as pure accelerators, or as a collider, where two oppositely directed beams are focused and brought into collision inside the particle detectors placed around the ring. In the collider mode the center of mass energy is maximized, but the beam stability and accuracy of the trajectory must be one to two orders better than that in a pure accelerator, and the size and position of the beam at the collision must be controlled from the micro- to the nanometer level.

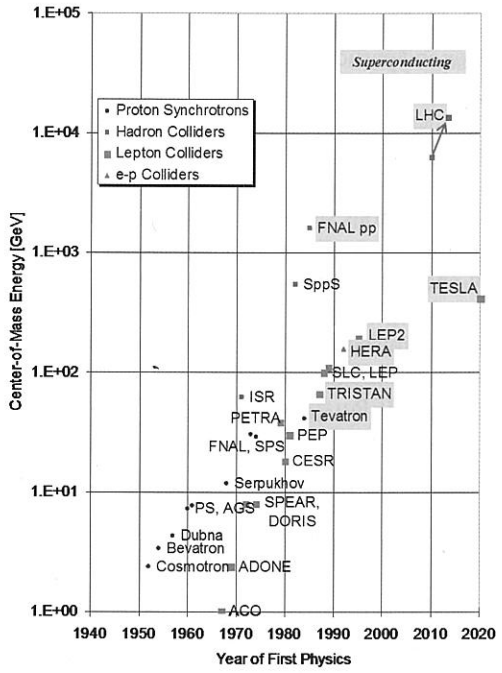

FIGURE 12.2: The Livingston Plot for accelerators and colliders.

It was quickly realized that in these machines, superconductivity could be used to obtain much higher energies. Resistive magnets have a maximum field of < 2 T and, in principle, if a ring of magnets were large enough, could be used to achieve extremely high energies, but the power consumption would be enormous, not to mention the capital costs of building the tunnel to contain them. Without superconductivity, the field of high energy physics (HEP) would not be what it is today. However, the advantages of superconducting magnets did not come without considerable challenges. Superconductivity, that is the loss of electrical resistance in matter, is a phenomenon largely restricted to the very low temperature regime. Thus superconducting magnets must be kept "cold", very cold indeed, and the operation of small and large cryogenic systems to do so is one of the major challenges. The materials which are superconducting themselves are another; at the beginning of the era of practical applications there were a number of candidates, of these various alloys of niobium and titanium still dominate conductor species used for HEP magnets. For applications requiring magnetic fields beyond the properties of niobium-titanium alloys, the so-called A15 compounds, true chemical compounds of niobium and tin, Nb_3Sn, are being considered, as well as the so-called high temperature superconductors (HTS). The latter materials, discovered about twenty five years ago have unique properties but unfortunately all high field materials are inherently brittle and strain sensitive, a particularly regrettable situation given that higher fields lead to higher forces and thus a higher stress and hence strain on the conductors.

12.2.2 Accelerators

Manipulation of particle beams is based on electric and magnetic fields. The basics of cyclic accelerators, by far the most common accelerators in the physical sciences and in medicine, are depicted in Figure 12.3. Electromagnetic fields are shaped to have the electric components parallel to the particle trajectory and in phase such that when the particle crosses the gap between the electrodes it receives a positive kick of energy. Magnetic fields perpendicular to the particle trajectory are shaped in such a manner as to bend the particles and recirculate them into the gap repeatedly, thereby adding continuously to the energy kick.

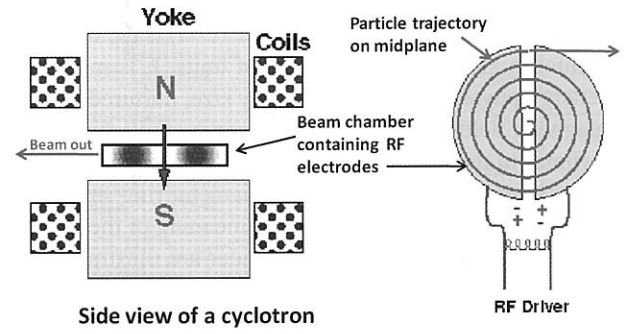

FIGURE 12.3: The principle of the cyclic accelerator.

Obviously the voltage between the electrodes must vary in sign; whatever dc voltage is impressed initially, it cannot always be positive, in order that the particle is accelerated at each crossing of the gap. This means that the field polarity must reverse with a frequency ranging from tens of MHz to a few GHz, according to the type of particle, energy and size of the accelerator. In addition to guiding the particle beam, usually accomplished by a uniform transverse dipole field, magnetic fields have to provide the necessary focusing elements to stabilize the beam against inevitable perturbation of the trajectory, of the main field or against intra-beam and inter-beam effects.

This restoring or focusing force is given by a field gradient, usually in the form of a quadrupole field. Figure 12.4 illustrates this action. "Higher order" magnetic fields are required to nudge the beams and keep the particles in a stable orbit in the machine throughout the acceleration phase and

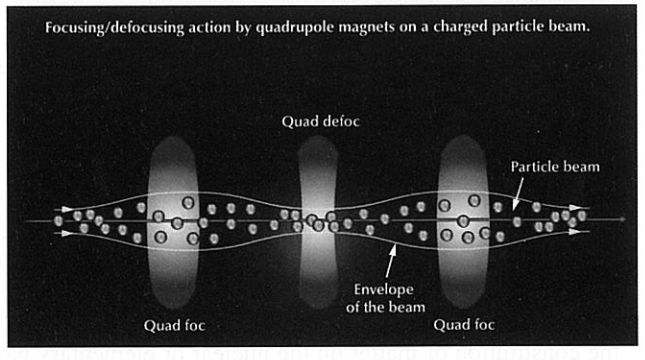

FIGURE 12.4: The properties of a quadrupole magnet. (Courtesy CERN.)

during storage. The focusing of a quadrupole depends on the energy of each particle and particle beams have a spread in energy and momentum. This leads to an effect called "chromaticity" and requires the use of a sextupole field to compensate. An octupole field provides special features, damping of certain beam instabilities for example, but it needs to be carefully controlled. In colliders, where the beam maintains its top energy for hours and millions of turns, higher order multipole magnetic fields need to be carefully controlled to avoid resonant behavior and instabilities. For example, in the LHC the magnetic fields are carefully controlled as far as the dodecapole component, a requirement which sets particularly stringent specifications on the magnet builders, with concomitant demands on manufacturing quality control.

In the case of a circular accelerator the main parameter is the bending strength, that is the product of the field strength, B, and length, L, of each dipole magnet. For relativistic accelerators one can show that the top energy scales as $E \sim 0.3BR$, where B (in Tesla) is the maximum field in the dipoles and R is the bending radius (in km). With this choice of units, E is measured in TeV. No wonder that the history of high energy physics has been driven by size, nurtured by increasing beam energy. Despite that, the high magnetic fields provided by superconductivity help mitigate this rush toward larger size, the current winner in the accelerator race, the LHC, is a ring of 27 km in diameter. Not surprisingly, in the name of science, even 200-300 km diameter ring structures have been proposed in recent years, the Eloisatron and the VLHC, where the meaning of the name or of the letters is left to the discerning reader. The main components of a collider are illustrated in Figure 12.5, which is a schematic representation of the LHC collider.

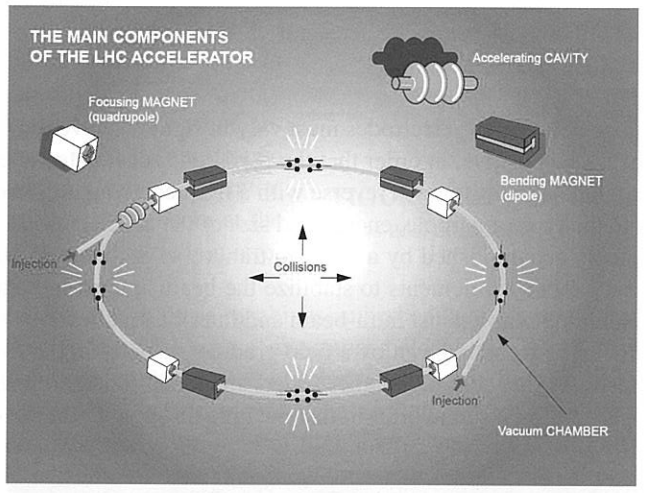

FIGURE 12.5: A picture of the LHC: the combination of an accelerator and a collider.

An impressive number of accelerators have been built for various uses, from basic research to medicine and industry, many of them not even recognizable as such. Even the ubiquitous X-ray machine is a miniature accelerator and the detector a film or a semiconducting screen. Industrial accelerators serve a large range of applications, as simple irradiation tools in the food industry for preservation, to sophisticated ion implantation devices in the semiconductor industry. As Figure 12.6 shows, the end "product" of an accelerator is not necessarily only the advancement of our understanding of the constitution of matter on the nuclear or elementary particle level, but it is also a rich field of applied techniques for the benefits of society. We note further that a detector is not necessarily an essential component except in fundamental research where accelerators provide

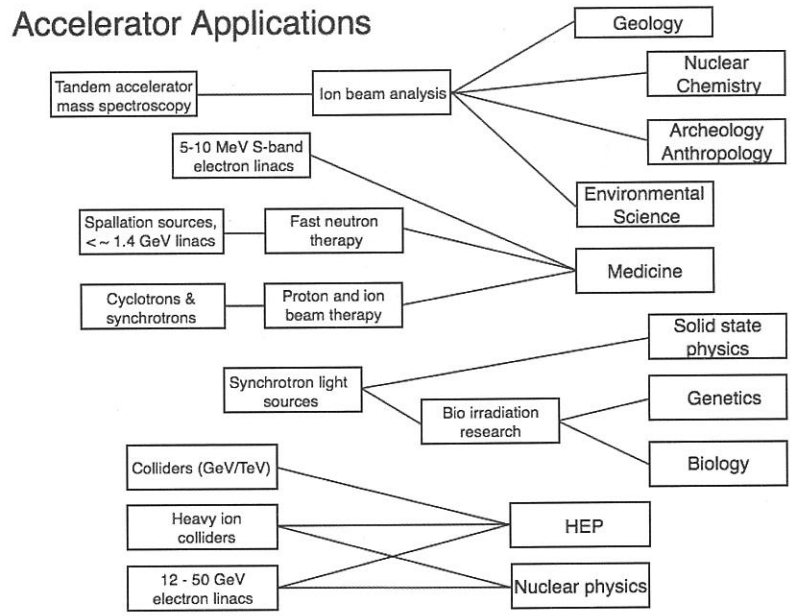

FIGURE 12.6: The world of accelerators.

new particles and new conditions that must be detected by special devices, to be described in the following section.

12.2.3 Detectors

Detectors have a part that is pure calorimetry that is the measurement of the particle energy and a part that we call spectrometry, which measures the charge and the momenta of the reaction products. While the total deflection of a particle is of course proportional to the product of the field and the length of a magnet, $B \times L$, the main parameters of the accelerator as mentioned above, HEP detectors usually measure the amount of bend (proportional to the particles' momentum), with

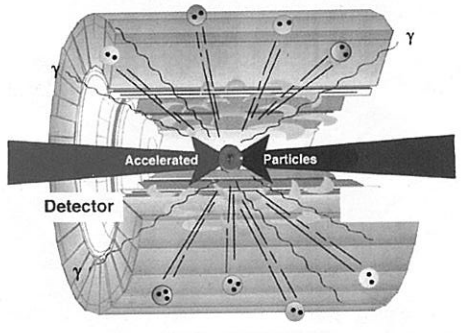

FIGURE 12.7: The detector at the collision point of two opposing beams of particles. (Courtesy CERN.)

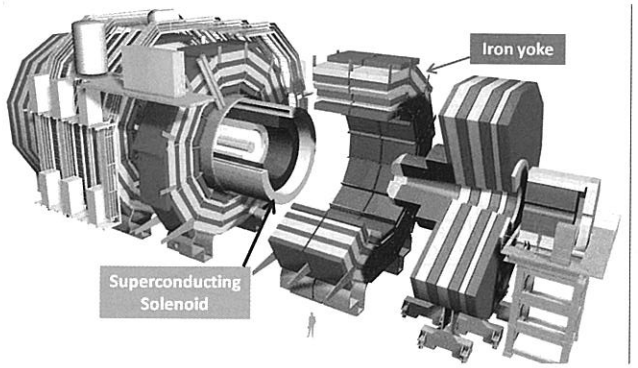

FIGURE 12.8: The CMS detector at the LHC. The superconducting magnet is usually a relatively small, less complex, though very important, component of a typical detector. (Courtesy CERN.)

detectors positioned inside the magnetic field to reconstruct the particle trajectories. In such a case the resolution of a magnetic spectrometer is proportional to $B \times L^2$: therefore large volumes pay off more than high fields. That is why the magnet size in detectors is huge: the largest magnetic system, the one for the ATLAS detector at the LHC, is a cylinder 20 m in diameter and 25 m long!

The principle of a detector at a typical collider is illustrated in Figure 12.7. Two opposing beams of accelerated particles, they can be electrons or protons or ions, or even a mix for example, are made to interact, collide head on in effect, inside an evacuated beam pipe. The products of the collision are then analyzed with a collection of specialized instrumentation chosen to maximize the information yield.

Given the magnetic field and spatial requirements, it is not surprising that despite the medium field level, 1 T average, 4 T peak, the construction challenges are enormous. Another detector magnet for the LHC, the one for the CMS experiment, Figure 12.8, is a detector with a classical solenoid.

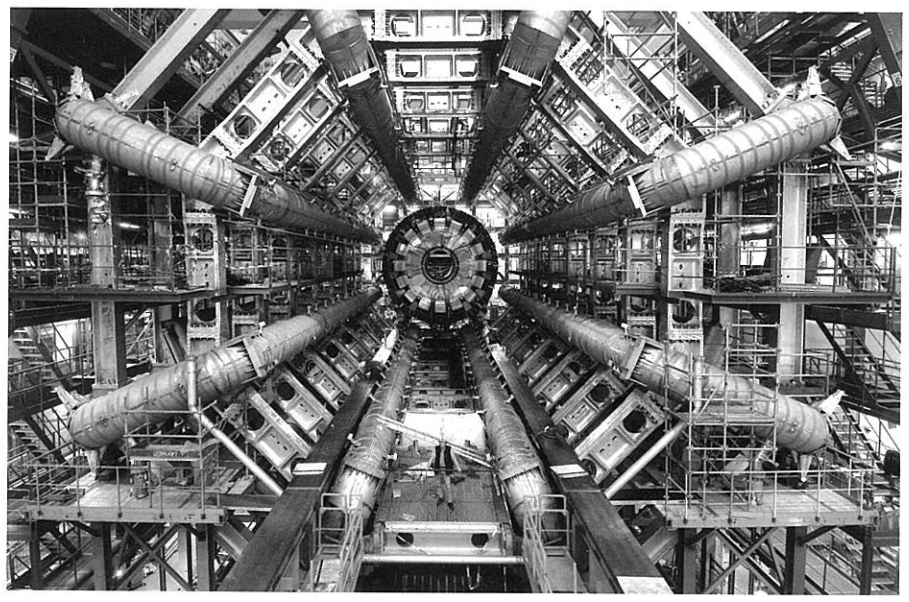

FIGURE 12.9: The ATLAS detector. The superconducting magnet is contained in the eight toroidal cryostats. (Courtesy CERN.)

However its size with an internal diameter of 6 m, a length greater than 12 m and field, 3.8 T, gives it a world record 2.5 GJ of stored energy in a single superconducting magnet circuit. The other challenge inherent in detector magnets is that they are intimately integrated with the various particle subdetectors, electronics, wiring and other subsystems that constitute the main components of the detector. Often the magnet becomes the supporting structure around which the detector is built. Figure 12.9 shows the Barrel Toroid coils of ATLAS after their assembly and of the immensity of the detector as a whole.

One has to imagine that all the empty space must then be filled by a variety of subdetector electronics and other very complex systems, among which a larger liquid argon chamber, end cap toroids for spectrometry in the forward direction, and an inner thin superconducting solenoid must all be integrated into the detector.

12.2.4 Main Characteristics of Accelerator Magnets

The coils of the dipole magnets used in HEP accelerators may be arranged in different configurations to generate the desired uniform transverse field. These basic shapes are illustrated in the top half of Figure 12.10. A uniform field may be generated either by a constant current density with a geometry given by oppositely intersecting ellipses, or by a shell in which the current density is maximum at the midplane and vanishes toward the pole region with a current distribution given by $J = J_0 cos\theta$. In practice, real magnets are composed of shells of constant current to fit the cosine distribution. Quadrupoles need a $cos2\theta$ current distribution and so on. The lower half of Figure 12.10 illustrates the coil cross-section of the actual LHC dipole.

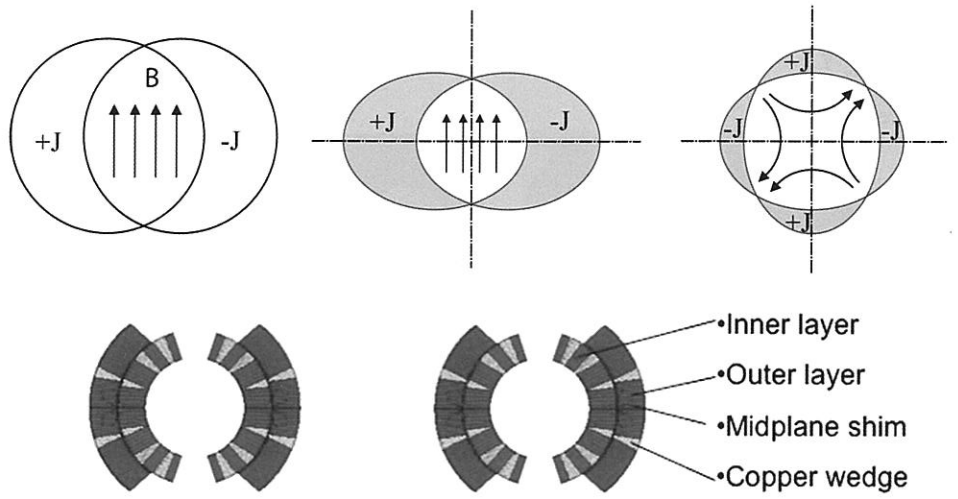

FIGURE 12.10: Top: Ideal current distributions to generate dipoles and quadrupole fields. Bottom: The LHC twin dipole configuration.

12.2.5 The Benefits of Superconductivity

The central field produced by a cosine distribution scales as $B \times J_0 \times a$, where J_0 is the current density and a is the thickness of the coil package. Obviously, the higher the current density, the higher the field. In addition, the coil volume increases faster than the field level. In other words the current density is by far the most important engineering parameter of accelerator magnets. Table 12.1 lists the ranges of values of the most important characteristics of magnet systems, superconducting as well as resistive. We note that while the tokamak systems have higher field and stored energy values, accelerator magnets require the materials capable of providing the highest possible current densities.

TABLE 12.1: The Typical Overall Current Densities of Various Magnet Systems

Magnet System (DC only)	Current Density ($J_{overall}$ A/mm^2)	Operating Current (kA)	Typical Field Range, (T)	Stored Energy in the System (MJ)
Resistive—air cooled	1–5	1–2	1	0.01
Resistive—water cooled	10–15	1–10	2	0.05
Large S.C. coils for detectors	20–50	2–20	2–6	5–2,500
S.C. MRI Magnets	20–50	1	1–10	1–40
S.C. Tokamaks for Fusion*	25–50	5–70	8–13	5–40,000
S.C Laboratory Solenoids	100–200	0.1–2	5–20	1–20
S.C. Accelerators	200–400	1–12	4–10	1–10,000

The benefit of superconductivity is evident from the previous considerations and the LHC can be used to quantify this benefit and to emphasize the virtues and advantages of the technology of superconductivity.

The LHC ring is 26.7 km long and requires some 126 t of liquid helium inventory to operate its 8.3 T superconducting magnets. The power required by the refrigeration system is about 40 MW. If the LHC had been built with classical resistive magnets having fields of 1.8 T, the circumference would have been more than 100 km and have required about 900 MW of installed power. This would have led to prohibitive construction and operating costs; 900 MW is the output of a fairly good sized nuclear power plant. In addition it would have had an unacceptable impact on the environment since the 900 MW would be rejected as virtually unusable, warm water.

Using the LHC as a specific example, the main characteristics for accelerator magnets are:

- High overall current density is the first key parameter. This is obtained through a high value of the critical current density, J_c where by J_c we mean the critical current (I_c) at a particular field divided by the area of the superconductor (I_c/A_{Sc}); this is of course of prime importance. Not only must the intrinsic J_c performance be high, but clearly we need to operate the system at a small fraction of the critical current. For example, the LHC dipoles run at 85% of the load line intersecting the critical surface, but they have been designed, and many of them tested, to operate up to 93%. Therefore even a small variation in the J_c performance, usually negligible in other systems, may have a direct effect on the magnet performance.

* High numbers refer to ITER under construction.

- Low stabilizer content. Copper is of course necessary but we need to keep it to a minimum, compatible with stabilization and protection requirements. Usually the copper to superconductor ratio, or Cu/Sc (or $A_{stabilizer}/A_{nonstabilizer}$ in a more complex system) ranges between 1.5 to 2 for NbTi-based systems and 0.9 to 1.5 for Nb_3Sn magnets. The stored energy can be as high as 8 MJ for each of these magnets.

- High compaction cable. Following initial attempts to use fully transposed braids, flat double faced cable, of which the so-called Rutherford cable is the prime example, is the invariable choice. It has a 90% compaction factor, which can increase to 93–94% after coil curing. The interstices between the strands are such as to allow helium to percolate inside to increase stability, particularly in NbTi magnets. Such a high compaction is not trivial considering the necessity of multi-kilo-Ampere cables as we will see later.

- Thin insulation. Total inter-turn thickness is less than 250 μm in modern accelerator magnets, usually consisting of polyimide tapes, to maximize the current density of the coil while withstanding discharge voltages in the kilovolt range.

- Collaring systems to withstand the forces. Dipoles, like toroids, are not self-supporting systems with respect to the forces generated by the magnetic field, as Figure 12.11 indicates. For accelerator magnets the restraining system must be outside the coils, to avoid reducing the current density. This is provided in the form of collars tightly surrounding the coils to prevent any motion which could lead to quenches (transition from the superconducting to resistive state caused by motion and subsequent heat generation) and provide the precise coil geometry for the required field quality.

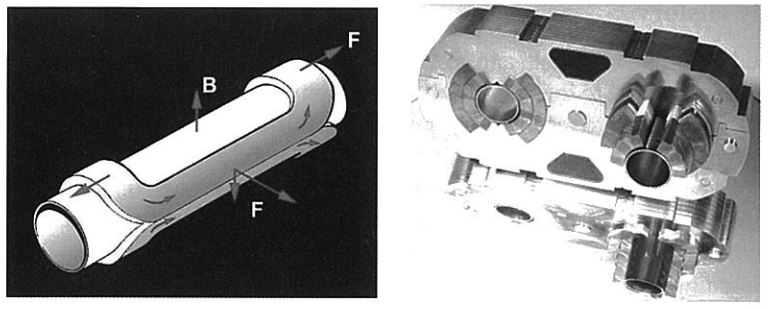

FIGURE 12.11: Forces on a dipole, left; a section showing the LHC dipole retaining structure, right.

- Very low stability margin. This is a consequence of the high Joverall, and translates into a very small stability margin, of the order of 10 to 1000 μJ. When we compare this to the 8 MJ of stored energy in the magnet, it is not surprising that accelerator magnets are designed to train and to withstand multiple quenches. Training is the process by which a magnet approaches the theoretical maximum operating current through a series of quenches, relieving stress in the coil and converging on a more stable mechanical configuration.

- It is important that the magnet has the ability to maintain memory of the process, and once trained to operating field, it can reach this field level with little or no further training. Since

energy release is mostly generated by movement of the coil, the very low stability margin dictates not only a good system of force restraint but also a very accurate mechanical construction, which as we will see later, affects field quality.

- Protection through active heaters and bypass diodes to reduce the current in 100 to 500 ms to avoid dangerous hot spot temperatures. Magnets quench when a small volume of the coil, usually due to a microscopic movement of the conductor, transitions to the normal state. The current, formerly carried by the superconductor, shunts into the copper matrix generating a current density in the copper (J_{Cu}) of 1000 A/mm^2 which is not sustainable without damaging the magnet. Once such an event is detected, heater strips, placed within the coil are fired, causing the entire magnet to become normal and thus dissipating the stored energy throughout the entire mass of the coil, while at the same time the current (13 kA in the case of the LHC dipoles) is bypassed around the magnet via cold diodes. Development of 13 kA cold diodes and heaters near the coil, which are exposed to the same forces and stresses, has been a major endeavor of the LHC.

- Field quality. First of all, the magnets in the ring must all have the same field within a few units, a unit being 100 ppm of the main field, or about 1 mT for the LHC magnets at full field. Then, all higher order harmonics must be controlled at a level better than one unit, in some at the level of 0.1 units. Such a goal is relatively easy to achieve with electromagnets where the iron pole plays the primary role in shaping the field, but this is a real challenge in superconducting magnets as it requires the control of the conductor position to ±50 μm. Coil geometry dominates the field quality at the collision energy and thus requires control of the persistent currents, snapback effects and the coupling currents in the cable, that is governed by the interstrand resistance, to a very high degree. These superconducting effects are very important at low field during injection, and during ramp up.

12.2.6 Early History

Probably the first truly large scale application of superconductivity was in particle physics. As a technology eminently suited to the purpose, it allowed physicists initially to build detector magnets of a prodigious size and later to reach energies not accessible by any other means. Even so, it was not always taken for granted: as a former DOE Program Manager, David F. Sutter frequently remarked, rather acidly, "Never use superconductivity unless you absolutely have to!" Superconductivity was not fully embraced by the High Energy Physics community either, an experimentalist once remarked that, "superconductivity will be the death of High Energy Physics!"

The long relationship between superconductivity and high energy physics began with the discovery of Nb_3Sn in 1961, 50 years after Onnes' discovery. Shortly after the publication of this latest discovery appeared, Lawrence Berkeley Laboratory (LBL) laid out plans for development of bubble chamber magnets with fields of 10 T or more. This was a rather ambitious goal given that the initial conductor samples were microscopic and far from the "engineering" material required for magnet fabrication and the magnets were never realized. This sort of bold extrapolation has been repeated with the discovery of every new superconductor since, with mixed success. There is always a huge gap between the appearance of a new superconducting material and the subsequent actual engineering application. Despite the visionary goals of the LBL team, the first viable superconducting device used in high energy physics, a 25 cm bubble chamber magnet, was built at Argonne National Laboratory (ANL) in 1965. At this time there was a growing realization among high energy physicists that future experiments would require superconducting technology. In the early 1970s, three groups in Europe, three in the U.S. and one at KEK in Japan were studying the high energy superconducting accelerator. This flurry of activity was eventually reduced to two main projects in

the late 1970s: ISABELLE and the Fermilab Energy Doubler/Energy Saver/Tevatron. The Tevatron was the machine that was ultimately built and it has been in operation since 1983.

A pivotal event in the application of superconductivity in high energy physics came in 1968, at a summer study held at Brookhaven National Laboratory (BNL). During this six week meeting, international experts examined many application-related challenges and laid the groundwork for the future of superconductivity in high energy physics.

In 1972 a team of physicists and engineers at the Rutherford Laboratory in the UK, under the leadership of Martin Wilson, figured out that superconducting cables could be made to work for accelerator magnets (and a host of other applications!) if the wire were made of a filamentary composite, in which very fine filaments of superconductor are embedded in a matrix of copper. The theory associated with the invention of this "Rutherford Cable" was written up by Wilson as Rutherford Memo A26, but never published! Magnets powered with superconducting coils can produce much higher fields, enabling higher energies to be reached for a given machine size. This key development ignited a new wave of HEP magnet applications. Government support has played, and continues to play, a large role in the development of superconductivity.

In the 1970s, the leaders in high energy physics considered superconductivity a necessity for growth of the field. The main focus at that time was filling in the missing pieces of the Standard Model of particle physics.

During that period Fermilab Main Ring was the largest operating proton synchrotron with a radius of 1 km, a peak field of 2 T, a power consumption of more than 50 MW and an operating energy of 400 GeV. Type II superconductors were becoming available that offered the prospect of operating at fields higher than 4 T with no resistive losses. Superconductivity would allow Robert R. Wilson, the founding director of the laboratory to double the energy while reducing power consumption. Hence the original name Energy Saver/Doubler, which was later changed to Tevatron. The opportunity was too good to pass up: Wilson brought the initial accelerator project in considerably under cost and planned to use the left over funds to build a second superconducting ring with an energy of 1 TeV. The approach in designing the machine can be seen in a paragraph from the The Energy Doubler Design Study: The design process, and if carried out, the construction of the Doubler, builds upon our experience at NAL. We have not proceeded on the basis of deciding what is readily practicable, designing to that, adding up the cost and attempting the result. Instead, we have set a cost goal and keep designing, redesigning, haggling and improving until we have done what we set out to do. Occasionally, we are forced to admit that we are not clever enough to achieve our cost goal and admit defeat, but not without a struggle. This was a fruitful time in accelerator development with several other applications being considered by the community. A 4 GeV experimental ring, ESCAR, was under construction at LBL, Brookhaven was developing a 400 × 400 GeV proton-proton collider called ISABELLE, and the Rutherford Laboratory undertook some crucial development of superconducting cable while studying the possibility of building the Super Proton Synchrotron at CERN with superconducting magnets, an effort that was eventually discarded in favor of conventional technology.

The construction of the Tevatron initiated the development approach and basic engineering that is still used today. This would be the first time that industrial-scale production of a superconductor became a necessity. Over 1,000 superconducting magnets were required: a model magnet program, based on short model magnets, was used to rapidly produce magnets with varying parameters. This program was the basis for development of fabrication techniques such as cable and insulation and ways to consistently produce magnets with the required field quality. In parallel, a long magnet production program was taking input from the short model program to develop full length magnets. Over 200 model magnets were produced in the two programs. Much of the technology developed for the Tevatron has been used on subsequent accelerators with minor evolutionary improvements.

HERA at DESY began construction in 1984, soon after the Tevatron came on and pushed the technology further. The HERA magnets were longer at 8.824 m as opposed to 6.4 m and worked at a higher field, 4.7 T versus 4 T at the Tevatron. The HERA magnet had an adequate amount of

margin that was used later on to run the magnets at 5.5 T, boosting the proton ring energy from 800 to 920 GeV.

Among several innovations resulting from these projects, HERA was the first to have the magnets assembled industrially. This involved transferring the design to industry and carefully monitoring the product through the production cycle. The construction started in 1984 and the machine became operational in 1990.

During the period from 1985 to 1995 there was a great deal of intense work on superconducting magnets at other locations. The Relativistic Heavy Ion Collider (RHIC), at Brookhaven National Laboratory developed a very simple single shell coil that used the iron collars directly to contain the winding (Figure 12.12). Another project of the early nineteen eighties was the Superconducting Super Collider (SSC), the most ambitious application of superconductivity ever conceived. This machine involved all of the US National laboratories and much of the technology we have today was developed for it. Alas, a victim of politics and poor management, it died a sad death in 1993.

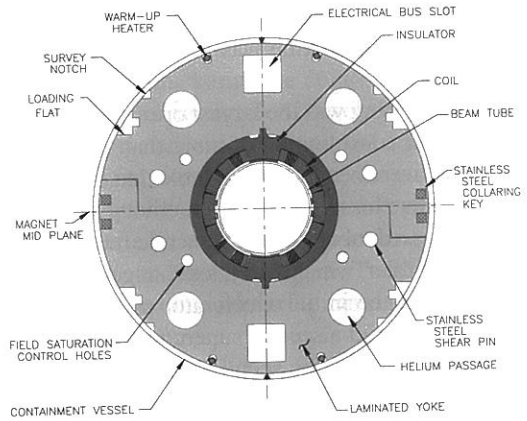

(a)

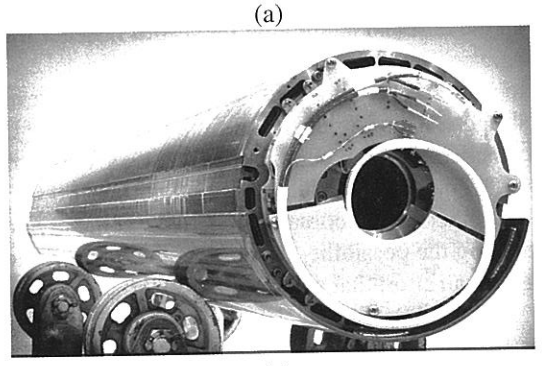

(b)

FIGURE 12.12: (a) Cross section of a RHIC arc dipole. (b) The cold mass of a RHIC helical dipole. (Courtesy of Brookhaven National Laboratory-RHIC Collaboration.)

12.2.7 The Large Hadron Collider

The demise of the SSC proved to be a boon to the Europeans, who were in the process of developing the Large Hadron Collider at CERN in the ring space then occupied by LEP. Building on

the technology of the SSC, the LHC contributed some key developments in accelerator technology: solving the problem of putting two magnets in one yoke and cryostat, operation in super fluid helium and large-scale industrial production. Beset with teething problems, the initial expectations were not fully met, but with an operating field of 8.33 T it will have the highest field value to date once the idiosyncrasies of this very complex machine are fully understood. Situations like this, where technology is pushed to the limit and fallen short of initial expectations, are common and have been repeated many times in the past. Establishing the parameters of such a complex system, trying to squeeze the best possible performance while trying to reduce cost, is a complex process only understood in hindsight. Let us look at the history in a little more detail. The original specification was for nominal 10 T, 50 mm bore, 10 m long, twin aperture with a separation of 180 mm, using a 17 mm wide, 15 kA cable. By the time of the EPAC'90 conference it was in the range 8 to 10 T. The work had started around 1983 with some winding tests at CERN, but the 1 m models were made in industry. At the time it was thought that it would be a good idea to whet the appetite of industry in order to drum up enthusiasm and increase the chance of being funded. It is not so clear now that that was a good idea: progress would probably have been much faster if the models had been made at CERN. Industry is more interested in large scale manufacturing than model work. In the early 1990s, when the SSC was canceled, things got serious and it was realized that the aperture was too tight; it was increased to 56 mm and at the same time the beam separation was increased to 194 mm. The 17 mm cables were hard to wind, so were reduced to 15 mm, and the magnet length was increased to 15 m in order to reduce the total dead space between magnets so as to maximize the integrated dipole field around the ring. It was then that 8.33 T (7 TeV) was decided, with 9 T "ultimate"—i.e., ancillary equipment designed so that if 9 T could be reached in the dipoles there wouldn't be a bottleneck elsewhere.

The LHC represents the summit of 20 years of development of Nb-Ti based accelerator magnets. The main characteristic is the two-in-one structure, i.e., the fact that two magnets are contained in the same cold mass, to accommodate the counter-circulating particle beams.

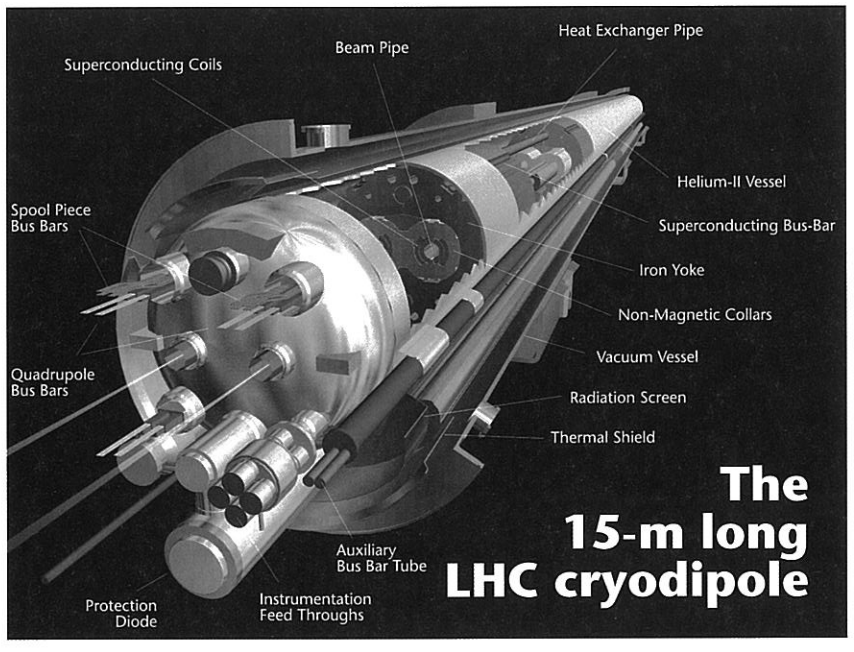

FIGURE 12.13: The LHC two-in-one dipole magnet. (Courtesy CERN.)

Figure 12.13, an artist's impression of the main LHC dipoles, shows this unique concept. The magnets are cooled by superfluid helium pressurized to 1 bar to boost the performance of NbTi. The collider uses the 27 km long tunnel of the previous CERN accelerator, LEP, and given the fact that the tunnel length was fixed, increasing the field as much as possible was instrumental in getting approval for the project. Moreover, the transverse tunnel dimensions were fixed as well, so a compact structure became essential, dictating the two-in-one design. In addition, it turned out to be a cost-saving factor: the twin aperture design fully magnetically and mechanically coupled, giving maximum compactness. Subsequent analysis has shown that this design feature saved at least 15% of the cost, or 200 MCHF.

Ultimately the LHC magnet R&D, design, construction and installation lasted more than 20 years. Figure 12.14 illustrates the LHC magnet roadmap with the main milestones. A few of the most interesting highlights in this process are presented here in order to illustrate the challenges in large-scale production of extremely complex scientific devices.

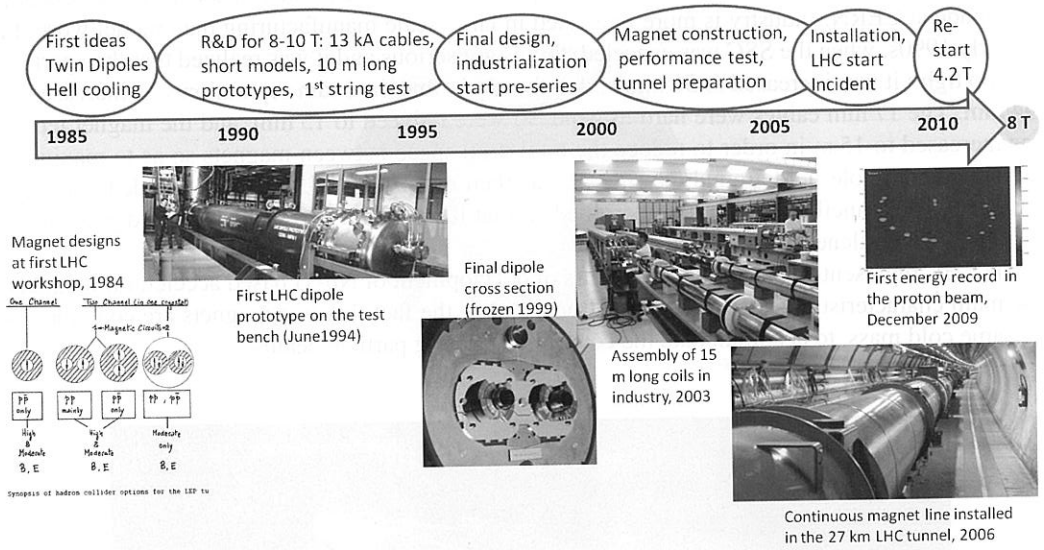

FIGURE 12.14: The path to success: a glimpse at the milestones and accomplishments of the LHC project.

There are more than 1200 dipole magnets in the collider which in principle must all be identical, in practice this is impossible. As there will always be manufacturing deviations from the ideal, the fabrication process must include all the lessons learned from the extensive prototyping process in which the various spatial and prestress correlations are established and elaborate quality assurance controls established. Considering that more than 5,000 dipole coils were produced, the coil size variation along its 15 meter length of better than 30 μm is a superb achievement. The field quality, the most essential parameter of all, is even better than originally desired which taken together with the superconductor fabrication, is one of the most striking achievements of the whole project.

The success of the LHC superconducting magnet construction, within schedule and with a negligible extra cost of less than 2%, meeting or exceeding all specifications shows the maturity of this technology. The entire installation with its huge detector magnets working very satisfactorily is yet another step in the quest of knowledge, a step that has been made possible by superconductivity.

12.2.8 Applications in Japan

Superconducting magnet systems play a key role in the Japan Proton Accelerator Research Complex (J-PARC). The experimental facilities utilize three superconducting magnet systems; a muon transport solenoid, a superconducting spectrometer and a 150 m superconducting beam line in the Neutrino Experimental Facility.

An excellent example illustrating that there is still room for creativity and improvement is a superconducting combined-function magnet developed by the Japan High Energy Research Organization, KEK, to optimize the magnet performance with a strong emphasis on cost effectiveness. This magnet, which features a coil radius of 170 mm, provides dipole (2.6 T) and quadrupole (19 T/m) fields superimposed in the same bore. The optics in the bending section of the beam line is simplified by using 14 pairs of these combined-function magnets. Also, it offers the advantage of requiring only a single component to design instead of separate dipoles and quadrupoles. The magnet design has been greatly simplified by the choice of a single layer coil surrounded by plastic collars and an iron, flux-return yoke.

The KEK-B BELLE detector is of course well known for its extensive use of superconducting elements in its B meson factory experimental program. The original detector, now in the process of being dismantled in preparation for a proposed upgrade, is shown in Figure 12.15. The beam pipes for the two counter-rotating electron beams are clearly visible in the foreground.

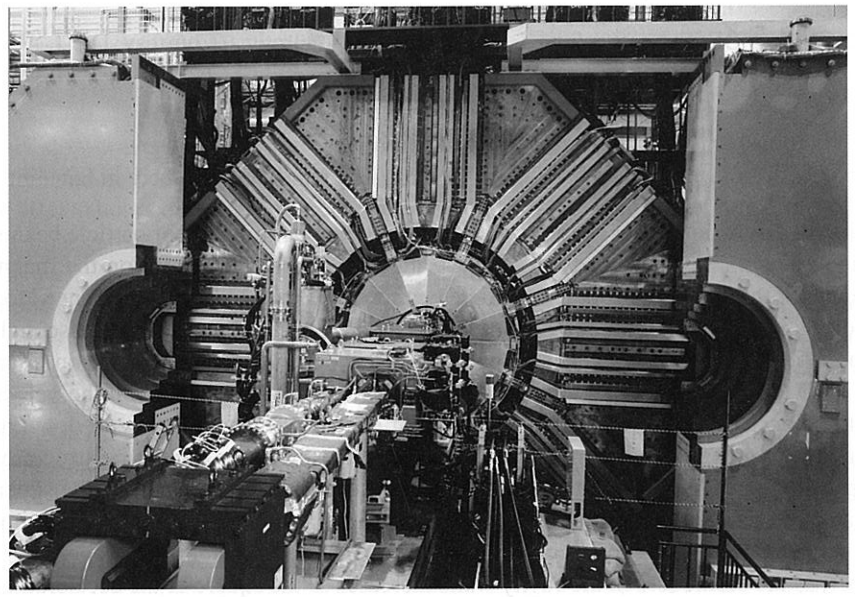

FIGURE 12.15: The KEK-B BELLE detector. (Courtesy KEK, Japan.)

Another Japanese innovation pushing the limits of existing technology is an extremely thin superconducting solenoid magnet launched via balloon to high altitudes for more than 2 weeks, used to investigate cosmic-ray antiparticles. Called the Balloon-borne Experiment with a Superconducting Solenoid or BESS, the design goals were extreme: maximize the volume, minimize the mass and heat load, and be able to survive up to 10 g. The magnet has a coil thickness of only 3.4 mm to minimize particle interactions and is wound with advanced aluminum stabilized superconductor to achieve the required strength to weight ratio. The central field is 1.2 T in a volume of 0.9 m and a

length of 1.4 m. Figure 12.16 is a photograph of the preparations for launch in the Antarctic of this imaginative experiment.

FIGURE 12.16: BESS on the launch gantry in the Antarctic. (Courtesy Dr. J. W. Hitchell, NASA.)

12.2.9 RF Superconductivity

In our initial discussion of accelerators we stated that the manipulation of particle beams is based on electric and magnetic fields and thus far our attention has been focused on the magnetic field requirements for this manipulation. But particle beams once produced by a source need to be accelerated and this is where another component of the modern accelerator plays an essential role, the electromagnetic cavity resonator. The resonant frequency depends on the application, usually lying between 100 MHz and 3000 MHz, the type of cavity used in turn depends on the velocity of the particles to be accelerated. Initially cavities made of copper were universally used, but as our understanding of superconductivity progressed, the advantages of superconducting structures became increasingly obvious. One of the attractions is that the dissipation in the walls of the superconducting resonator can be many orders of magnitude less than that in a copper unit of the same species which is particularly attractive for accelerators which operate in the continuous wave (CW) mode. In other words, as the ohmic loss in the cavity walls increases as the square of the accelerating voltage, resistive cavities become increasingly uneconomical. In such a case as the surface resistance of a superconducting cavity is generally five orders of magnitude less than that of copper, even when the refrigeration needs are taken into account, there is a net gain of many hundreds. Figure 12.17 illustrates a collection of accelerator cavities. Clockwise from the left a 345 MHz double spoke resonator (ANL), an 800 MHz, 6 unit elliptical cell (JLAB/MSU), the pioneering Stony Brook Heavy Ion Accelerator resonator, and a variety of superconducting cavities. In the left foreground the DESY 9 cell TESLA cavity, on the right a CESR 500 MHz cavity, a small-Sscale version of which is on the left. The large Nb-Cu cavity in the background is a 200 MHz resonator developed by Cornell and CERN for future muon accelerators and neutrino factories.

The application of the technology of RF superconductivity to particle accelerators traces its beginnings to about 1965 with the acceleration of electrons in a lead plated resonator at Stanford. Contem-

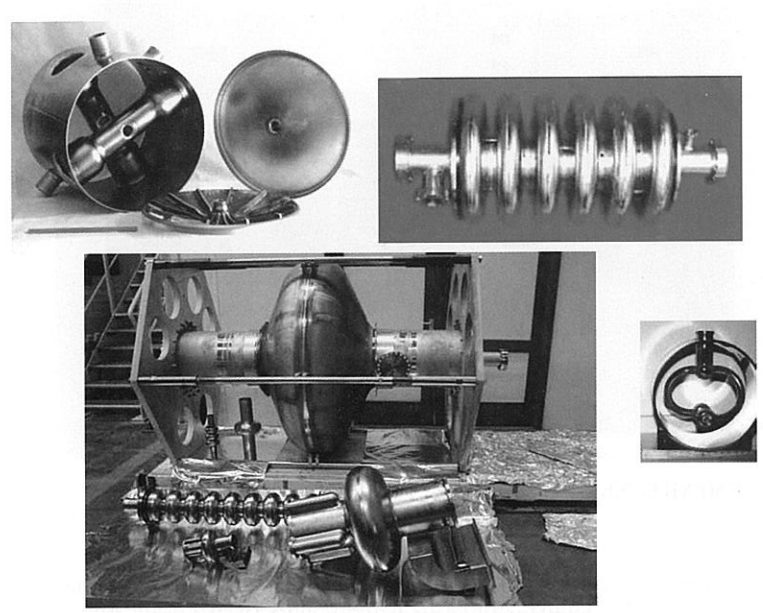

FIGURE 12.17: A selection of superconducting accelerator cavities for different applications. (Courtesy Dr. H. Padamsee, Cornell University.)

poraneously slow-wave structures were beginning to be developed at Argonne National Laboratory which culminated in the heavy ion linac known as ATLAS. By 1989 this machine had accumulated more than 40,000 hours of beam-on-target operating time, in the company of numerous other superconducting linacs around the world, accelerators designed not only for heavy ions but for proton and electrons as well. As a result of this collective experience it could be demonstrated that the dramatic reduction of the RF surface resistance could be achieved even in complex resonator geometries.

In the 1 to 10 GeV range, superconducting cavities have special advantages for electron accelerators intended for nuclear physics: a continuous beam, high average current with excellent beam quality. Such a machine would be used for precision measurement of electromagnetic cross sections and for coincidence detection of reaction products in electron-nuclear collisions. CEBAF at the Thomas Jefferson National Accelerator Facility in the USA and LEP-II at CERN in Europe became the two largest superconducting RF installations: at CEBAF, originally designed for 4 GeV, a beam energy of 6.5 GeV was achieved in five recirculating passes with a CW beam current of 200 μA. LEP-II installed a total of 465 meters of superconducting RF cavities. The accelerating gradients in

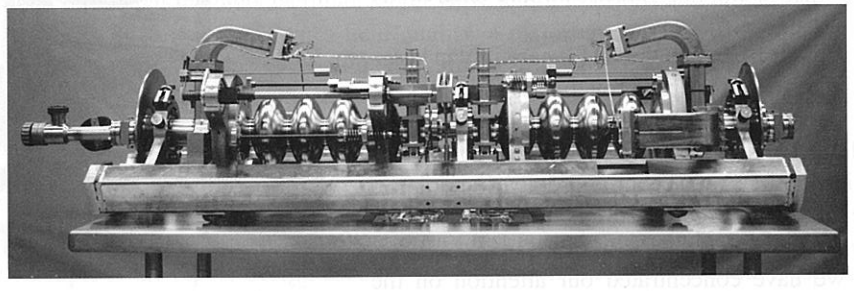

FIGURE 12.18: CEBAF 5-cell cavities, 50 cm in length. (Courtesy Jefferson blostcy.)

FIGURE 12.19: 350 MHz Nb/Cu cavities for LEP-II. (Courtesy CERN.)

the cavities rose commensurately, at CEBAF from the initial 5 MV/m to more than 7 MV/m with major improvements readied for the planned upgrade. Figure 12.18 illustrates the original assembly of 5-cell cavities operating at 1497 MHz.

In contrast, the LEP-II cavities consisted of a thin film of niobium sputtered onto a copper cavity shell which was initially capable of 6 MV/m, to be later upgraded to 7 MV/m. By mid 2000 the average sustainable gradients approached 7.2 MV/m. An assembly of these 350 MHz Nb-Cu cavities is shown in Figure 12.19.

The history of the remarkable progress achieved at continuous electron beam accelerator facility (CEBAF) is particularly interesting. When the decision was made to make the recirculating electron machine superconducting, it was based on a Cornell single cell design developed for storage rings. This cavity had routinely achieved a gradient of 5 MV/m and was proven in a beam test at cornell electron storage ring (CESR). The accelerator was built with major input from industry which provided the essential high purity niobium in unheard-of quantities, enough to make more than 400 cavities, establish mass production protocols for manufacture and assembly of these devices under exacting conditions and execute them.

The Spallation Neutron Source (SNS) at Oak Ridge National Laboratory is driven by a high intensity proton linac: the 1.4 MW machine is based on eighty-one 804 MHz superconducting cavities and accelerates protons from 200 MeV to 1000 MeV. Los Alamos and Jefferson Lab were partners in the development effort; Figure 12.20 illustrates the assembly of a 1 m long cavity string.

FIGURE 12.20: A 1 m long SNS RF cavity during assembly. (Courtesy Jefferson Laboratory.)

The LHC with 14 TeV in the CM is certainly in keeping with the historical energy growth rate. It too has the necessary complement of superconducting RF cavities: at 400 MHz, 16 Nb-Cu cavities in four cryomodules will provide 16 MW per beam and deliver about 180 kW of beam power. Figure 12.21 is a composite view of such an assembly.

So far we have concentrated our attention on the needs of high and very high energy machines but the world is full of other machines which over the years

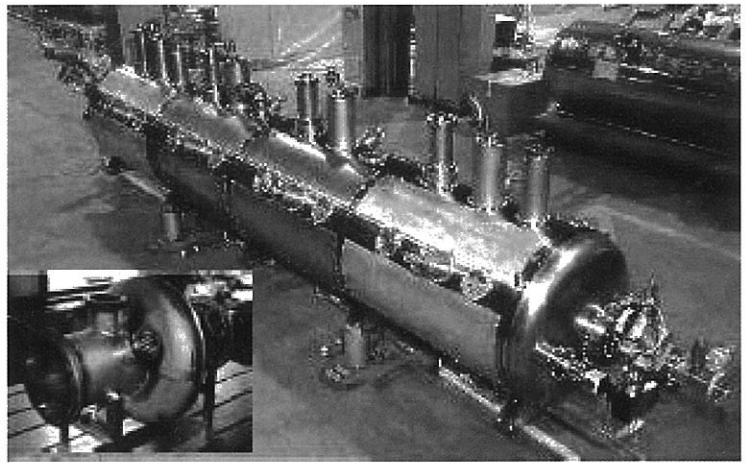

FIGURE 12.21: A superconducting RF LHC cryomodule. (Courtesy CERN.)

have become dependent on superconducting RF structures. High luminosity machines so equipped, noteworthy among others is CESR in the US and KEK-B in Japan. At the latter the two beams intersect at a finite angle to reduce the background at the interaction point and to simplify the local beam optics, but this reduces the luminosity and has other undesirable influences on the circulating beams. So called "crab" RF cavities were invented to deflect the bunches and thus position them for head-on collisions. Four 500 MHz cavities are required for this beam manipulation.

Another application is storage ring light sources whose numbers grew from just a few machines in the 1960s to about 70 machines worldwide either in various stages of development or built and fully operational. Not included in these numbers are the free electron lasers and SASE FELs such as the TESLA Test Facility at DESY in Germany, all of which depend on one or more superconducting RF components. In other words, RF superconductivity has also come of age.

12.2.10 New Applications

Wigglers and Undulators

The demand for more sources of synchrotron radiation is growing, leading to the construction of new laboratories and upgrades of existing facilities in order to provide higher performance beams. Light sources depend on undulators to provide high brilliance beams of tunable radiation. Currently short period undulators based on permanent magnet technology represent the state-of-the art but performance beyond the limits imposed by permanent magnets will require superconducting technology. Superconducting magnets facilitate larger gaps, shorter periods and higher fields, but aside from the obvious issues associated with field quality, a major challenge will be the development of a cryogenic system that supports small gap operation in the presence of beam heating. In addition, there will be a premium on cryogen-free operation using cryocoolers since most existing light sources do not have a cryogenic infrastructure.

Fast-Cycling Magnets

Until recently, there have been few applications of fast pulsed superconducting accelerator magnets. One example is the dipole design used for the Nuclotron at JINR in Dubna. Despite the complications of field quality degradation and cryogenic losses caused by persistent currents in the superconductor and eddy currents in the cable, iron and surrounding structures, the increasing de-

mand for high intensity beams requires superconducting magnets with high ramp-rate-capability. Note that all the designs considered for this purpose rely on NbTi technology. The international Facility for Antiproton and Ion Research (FAIR), currently under construction at the Helmholtzzentrum für Schwerionenforschung (GSI), consists of two synchrotrons in one tunnel, the SIS 100 (100 T-m rigidity) and SIS 300 (300 T-m rigidity). The SIS 100 is the heart of the machine, accelerating protons and ions at a high repetition rate and distributing them to other parts of the complex. The required dipole ramp rate is 4 T/s up to a field of about 2 T for SIS 100 with a 1-Hz duty cycle and 1 T/s up to 6 T for SIS 300, with a duty cycle of 50%.

Future Applications

Superconducting magnet technology is continually evolving in order to meet the demanding needs of new accelerators and to provide necessary upgrades for existing machines. A variety of designs are now under development, including high fields and gradients, rapid cycling and novel coil configurations. The performance, or physics "reach" of a colliding beam accelerator is determined by the energy of the particles and the luminosity, where, for a given energy, the luminosity is a measure of the production rate for a particular process. The particles are brought to collision in the interaction regions by sets of quadrupoles placed on either side of the collision point. As machines go to higher energies, there is a trend toward higher gradients. In many cases, it is aperture that dominates the requirements, leading to higher fields on the conductor. Also, the high radiation/high heat load environments in which these magnets are expected to operate, make them very challenging.

Recent progress in the development of Nb_3Sn has encouraged the prospects for use in accelerator magnets but the application for the LHC upgrade adds additional issues to the already formidable list. The magnets will operate in a high radiation environment, subject to unprecedented beam induced heat loads, that will require development of radiation hard materials for coil construction and understanding the heat transfer characteristics of composite coils. The design process will necessitate working closely with accelerator physicists to understand trade-offs between magnet performance limits and the interaction region upgrade options.

Magnet applications for future colliding beam machines can be separated into two categories; upgrades of existing facilities such as the LHC, described below, and new facilities. High fields are the obvious choice for an upgrade scenario, while other factors such as tunnel cost, cryogenics, logistics and location are factors that have to be considered along with magnet performance and cost at a green-field site.

The second phase of the LHC upgrade proposal is to increase the energy in the existing LHC tunnel. This will require major changes to the LHC arcs, new dipoles and quadrupoles, as well as the injector chain. Increase in energy a factor by two implies an operating dipole field of at least 16 T, quadrupoles with a gradient of 450 T/m and apertures of ~50 mm. A program to develop these magnets may take 15 to 20 years and will necessarily focus on cost as well as technology.

So far, superconductivity has not been the death of high energy physics, but rather a crucial enabling technology. New materials tempt HEP to continue its relationship with this fickle partner. It remains to be seen how it ends.

12.3 Magnet Engineering—Study in Stability and Quench Protection

Luca Bottura and Al McInturff

12.3.1 Outline

This chapter documents the historical perspective of stability and the closely related subject of protection in superconducting magnet engineering. We will follow the historical path, showing how the parallel development of materials suitable for building magnets and the achievement of increased current density, was related to conductor stability. The interplay of high current density and stability features drove the increasing sophistication of the magnet/device protection systems.

12.3.2 The Infancy of Superconducting Magnet Technology

Soon after his discovery of superconductivity, H. K. Onnes realized the potential for generating high magnetic fields using negligible electrical power. The concept was rapidly tested using Sn and Pb wires. But his announcement at the Third International Congress of Refrigeration, held in Chicago in 1913, that a 10 T solenoid was close at hand[1], was rapidly *quenched* by the realization that any of the material used would not carry any significant current at magnetic fields exceeding 50 mT [2]. Onnes himself concluded that superconducting magnets were not practical, and this can be regarded as the first and certainly not the last superconducting magnet project canceled. It was not until 1954 that Yntema at the University of Illinois wound superconducting coils with cold-worked niobium and produced magnetic fields close to 1 T [3], a range of practical application. The results were published in a short abstract[4] that was nearly ignored, but for a few scientists like John Hulm at Westinghouse who is credited with making the second superconducting magnet in 1955, an air-core solenoid that achieved 0.6 T.

The pace increased in the 1960s. Autler of the Lincoln Laboratory at M.I.T is reported to have made in 1959 iron-cored niobium magnets reaching a field of 1.4 T, to provide the magnetic field required by a solid state maser. It was then that Kunzler, at Bell Labs, filed the first patent for a 1.5 T superconducting magnet wound in layers with a molybdenum-rhenium wire and cooled in a cryostat by a bath of liquid He [5]. His patent on "Superconducting Magnet Configuration" was filed on September 19, 1960, beating a similar patent request by Autler by 2 weeks. This patent[6], issued 4 years later, in April 1964, can be regarded as the actual start of superconducting magnet technology. Early in 1961, Kunzler's group reported the discovery of superconductivity in Nb and Sn compounds up to field of 8.8 T [7], and the race for the original dream of Onnes was on again.

The groups at the respective laboratories of Bell, Westinghouse, Atomics International, Lincoln Laboratory, and Oak Ridge were competing for the highest field achieved by the time of the 1961 International Conference on High Magnetic Fields at MIT[8]. Field records were broken daily throughout that week. Kunzler's group, reportedly spurred by a bet at Bell that would result in a bottle of

1 H.K. Onnes, *Commun. Phys. Lab. Univ. Leiden* 34b (1913) 55
2 H.K. Onnes, *Commun. Phys. Lab. Univ. Leiden* 139f (1913)
3 G.B. Yntema, *IEEE Trans. Magn.* 23 (1987) 390
4 G.B. Yntema, *Phys. Rev.* 98 (1955) 1197
5 J.E. Kunzler et al., *J. Appl. Phys.* 32 (1961) 325
6 J. E. Kunzler, US Patent 3,129,359, filed September 19, 1960, received April 14, 1964
7 J. E. Kunzler et al., *Phys. Rev. Lett.* 6 (1961) 89
8 H. Kolm et al., *High Magnetic Rields*,Cambridge, MA, Nov. 1-4, 1961, New York, NY, Wiley, 1962

Scotch for every 0.3 T above 2.5 T [9], was the one achieving the highest field at the time, 6.8 T using a wire made of Nb tubes filled with crushed powder of Nb and Sn, and heat treated at 1000 °C to chemically react the precursors into Nb_3Sn. This barely surpassed the two main competitors, Hulm from Westinghouse and Hake and Berlincourt from Atomics International, who each reported fields of 6.6 T using Nb-Zr in their windings. Using the Nb_3Sn technique, Kunzler's group later achieved a record field of 10 T, finally reaching the goal of H. K. Onnes, 60 years after it was speculated. Superconducting magnet engineering was born.

12.3.3 The Appeal of Nb_3Sn and the First Stumbling Steps

The high level of interest for Type II superconductors resumed because the new form of Nb_3Sn conductor produced by Kunzler and colleagues had excellent $J_c(H,T)$ characteristics. Indeed, superconducting magnets need current density and a large part of the race for the first 10 T magnet was the search for a superconducting material with a sufficiently high current density. The cold-worked Nb wires used by Yntema for his magnet had critical current density J_c just below 1 kA/mm^2 in an applied field of 0.5 T and at 1.7 K. The Mo_3Re wires in Kunzler's initial magnets had a J_c of 500 A/mm^2 at the operating field of 1.5 T. The first samples of Nb_3Sn barely achieved 40 A/mm^2 at 9 T and 1.5 K, but that was soon raised to values of 1000 A/mm^2 at 9 T [7], an impressive achievement for the time. There was limited interest in superconducting magnet construction prior to the 1950s primarily because most of the research into superconductivity concentrated on an understanding of the theoretical underpinnings of the phenomenon. Particle physics was still dependent on resistive components for its accelerators and beam lines. Superconductivity in niobium tin was discovered in 1950, yet for a decade aroused no interest.

From the magnet construction point of view the engineering current density J_E, the prime requirement for magnet design, is directly related to the critical current density $J_c(H,T)$; the ability to modulate the amount of superconductor in the winding area was far too low for most practical applications. Superconducting devices become economically viable and efficient when the engineering current density is in the range of few hundred A/mm^2. Although this was met by the 0.5 mm diameter, Nb_3Sn conductors produced by Kunzler and coworkers, it was industry, especially RCA and GE, that produced tape and filamentary material on a substantial scale, opening a whole new range of magnetic fields for engineering applications and devices, and the concomitant surge in the drive to exploit them. (See Appendix 1 of this section) Once again, though, the sudden and enthusiastic rush to wind and test the new materials was somewhat reduced by the issues of flux-jumps, stability and training. Indeed, early coils failed to reach the same current level of short samples of conductor. This was eventually traced to a problem in a conductor where the heat generated by the movement of the magnetic flux was too large to be conducted out of the superconductor before it reached the critical temperature, i.e. an unstable flux-jump. We will elaborate further on this issue. The result was a serious limitation on the use of the early Nb_3Sn wires, made in large filaments and with high current density. However, it was also discovered in magnetization studies in the mid to late 1960s that a wire sample powered in a high background magnetic field produced in a different flux arrangement in the conductor and much improved stability. An ingenious solution to the problem of unstable flux-jumps was to subdivide the coil in multiple winding sections that were independently powered. For example in a solenoid the outer windings would be wound with a wire of lower current density conductor (more stable against flux jumps) than the inner sections (where high current density was needed). Powering the outer coil before the inner one would lower the magnetization of the inner section at a given current, and thus allow reaching higher fields. (See Appendix 2 of this section) The technical literature as well as the glossy advertising produced by industry was full of examples of this type of "research magnet." These magnets could now be found in every properly

[9] J. E. Kunzler, *IEEE Trans. Magn.* 23 (1987) 396

equipped low temperature laboratory as well as in various experiments at accelerator establishments such as Brookhaven or the Bevatron at Berkeley.

12.3.4 Malleable Nb-Based Alloys: Technology Goes to Industry

The supremacy of Nb_3Sn, and other more exotic and brittle intermetallic compounds such as Mo_3Re, did not last long. Already in the first half of the 1960s, Type II malleable alloys were commercially available. The first wire offered commercially, in 1962, was Nb-Zr at Avco Everett Research Laboratory[10], soon after followed by Nb-Ti at Westinghouse[11]. These two alloys were mechanically very tough, as they were originally developed for high strength rivets. Among the two, Nb-Ti was easier to manufacture, had superior mechanical strength, and had a 2-Tesla advantage in the upper critical field. For these reasons Nb-Ti became the dominant conductor used in device designs and construction[12]. This domination can be ascribed to two factors: ease of fabrication and the ability to sustain the Lorentz forces without loss of current carrying capacity. Fabrication of NbTi became an industrial-type process with the advent of the multifilamentary conductor first commercially produced by Imperial Metal Industries Ltd. The price to be paid, when compared to the intermetallic, brittle A15 structure superconductors, Nb_3Sn, Nb_3Al, and V_3Ga, was only an approximate factor of two reduction in critical temperature and field. At that time this was a minor issue when compared to the degradation of coil performance with respect to the theoretical current carrying capability of short samples.

12.3.5 Training and Degradation, the Discovery of Stability

The first superconducting magnets built in the decade around 1960 had their first transition to the normal state, that is quenched, much before reaching the expected critical current, largely disappointing the constructors. At the first powering only the early magnets reached a small fraction of the critical current of the single wire after which they quenched. The following attempt to power the magnet resulted in a higher current before a quench. The process continued, more or less regularly, at each attempt, and the maximum current that could be reached increased quench after quench, slowly approaching a plateau. This behavior became known as training,[13] and the curve of quench current vs. powering attempt became known as the training curve. The plateau current reached, however, was still below the expected maximum current carrying limit of the wire. The current limitation observed was originally thought due to bad spots in the wires or cables, and thus contributed to poor homogeneity in the quality of the superconductor. This idea produced the concept of degradation of the conductor performance. Although training clearly showed that a physical degradation could not be responsible for the bad performance, the misleading name remained as an inheritance of the misty understanding. Particularly puzzling was the fact that the degradation depended on the coil construction and on its geometry. A principle not yet fully understood at the time was that of stability of the cable with respect to external and internal disturbances. Insufficient stability and large disturbances were the key issues to the failure of the early experiments on superconducting magnets. (See Appendix 3 at the end of this section)

The pieces started to come together in the early 1960s when it was recognized that the perturbations that were limiting the achievable currents in small solenoids were originating from magnetic instabilities called flux-jumps. Magnetization studies of these conductors showed that under certain circumstances, the magnetization of the wire in a varying field could collapse suddenly and catas-

[10] Avco Supergenic Strip SG 700

[11] J. K. Hulm and R. D. Blaugher, *Phys. Rev.* 123 (1961) 1596

[12] T. G. Berlincourt, *Cryogenics* 27 (1987) 283

[13] M.A.R. LeBlanc, *Phys. Rev.* 124 (1961) 1423

trophically. The flux linked with the filaments could change nearly instantaneously, jump, and cause local energy dissipation in the wire. The source was identified and was shown to be a function not only of field and field change, but was also dependent on the conductor geometry with respect to the field. Numerous workers began to consider ways in which these instabilities could be controlled and their reports and conjectures appeared in the literature of the day. The devices that were being designed and constructed in this mid-to-late 1960s were based on one or more forms of stability enhancement.

In the midst of this bubbling atmosphere, Brookhaven National Laboratory sponsored in 1968 a Summer Study on Superconducting Devices and Accelerators, which did an excellent job of bringing the various contributors to this state of the art and represents a veritable historical milestone. The proceedings of the workshop[14], as well as the summaries and highlights[15], provide an excellent record which traces well the understanding and progress made.

12.3.6 Stabilization Strategies

With improved understanding of the causes of instability, it was finally possible to design a coil so that it would be stable. In the following sections we will review some of the main stability strategies developed in a selection of the previously mentioned references and authors. Each strategy added to the change in understanding and in some cases effected a change in the direction of design or construction of a device even after their start.

12.3.7 Cryogenic Stability

The first and earliest form of stabilization was used in a large MHD generator magnet model at Avco Everett. This magnet with windings in a saddle-shaped configuration produced 4 T over a region 3 m long and 0.3 m in diameter. Constructed of Avco SG 700 9-strand NbZr conductor embedded in a copper strip, the dipole had a stored energy of 5 MJ at a current of 785 A [16]. Although the device never contributed to the advancement of MHD technology, it gave the superconducting community a new principle for the construction of stabilized superconducting coils[17], a principle which became known as *cryogenic stability* and the conductors dubbed as *cryostable*. Simply stated, a cryogenically stable conductor has a sufficient amount of low electrical resistivity material in parallel, and a sufficiently large surface in contact with an adequate volume of liquid or pressurized helium, so that even if the superconductor is driven into the normal state, whatever the cause, it is cooled down and can recover the superconducting condition below the current sharing temperature T_{CS}. Taking as a simple example, a single strand of cross section A operating at a current I, the maximum joule heating per unit length is given by $I^2\rho_n/A$ where ρ_n is the normal state resistivity, averaged over the whole strand cross section. The minimum heat flux per unit length to the helium bath can be written as $hP(T_c - T_{OP})$, where h is the heat transfer coefficient to the helium, P is the wetted perimeter, T_c the critical temperature and T_{OP} the temperature of the helium. Stekly[18,19] was the first to formulate the condition of cryogenic stability as:

$$\frac{\rho_n I^2}{A} \leq hP(T_c - T_{OP}) \tag{12.1}$$

[14] *Proceedings of the 1968 Summer Study on Superconducting Devices and Accelerators*, Brookhaven National Laboratory, June10–July 19, (1968)

[15] H. R. Hart, *Proceedings of the 1968 Summer Study on Superconducting Devices and Accelerators*, Brookhaven National Laboratory (1968) 571

[16] Avco-Everett Research Laboratory press release, *Cryogenic Engineering News* (1966)

[17] A. R. Kantrowitz and Z. J. J. Stekly, *Appl. Phys. Lett.* 6 (1965) 56

[18] Z. J. J. Stekly and J. L. Zar, *IEEE Trans. Nucl. Sci.* 12 (1965) 367

[19] Z. J. J. Stekly et al., *J. Appl. Phys.* 40 (1969) 2238

or the equivalent conditions $\alpha_{Stekly} \leq 1$ in terms of the parameter α_{Stekly}:

$$\alpha_{Stekly} = \frac{\rho_n I^2}{hPA(T_c - T_{OP})}. \tag{12.2}$$

The above criterion provides a limit for the maximum current up to which the conductor operates in cryo-stable conditions. In a strand of radius R, cross section $A = \pi R^2$ and wetted perimeter $P = 2\pi R$, the maximum cryo-stable engineering current density $J_{cryostable}$ is:

$$J_{cryostable} = \frac{2q''}{\rho_n R}. \tag{12.3}$$

Once the strand size, R, the materials and their fractions are chosen, T_c and ρ_n, we see that the heat flux q'' is key to the stability of the winding. An average value of heat flux normally found for a 50% wetted surface in a pool of liquid helium is $q'' \approx 0.4$ Wcm^{-2}. Minimum values are obtained for very small channels and less than 10% wetted surface, for which $q'' \approx 0.1$ Wcm^{-2}. The upper extreme is the case of completely open bath and more than 60% wetted surface being $q'' \approx 0.8$ Wcm^{-2}. Yet higher values can be obtained in transient or super-critical helium, with the heat flux reaching values $q'' > 1.0$ Wcm^{-2}.

The corresponding engineering current density $J_{cryostable}$ is in the range of 100 to 200 A/mm^2. This form of stability, which is also the most conservative form of magnet winding protection, is normally adopted in large coils where the size/and or bulk of the winding is not an issue. It is still used in modern devices and systems on the buswork and interconnects, and to guarantee stable operation of large-scale magnets subjected to a large energy spectrum such as the ITER coils. On the other hand, when the current density needs to be high, as close to the magnet bore as possible, and the winding is tightly packed with little helium (i.e., in accelerator magnets), cryostability is not applicable.

A dramatic example of a cryo-stable magnet was the Big European Bubble Chamber (BEBC) at CERN[20,21]. Illustrated in Figure 12.22, BEBC was a 4.7 m bore split solenoid with a 0.5 m gap producing a maximum field in its center of 3.5 T, corresponding to a maximum field at the conductor of 5.1 T, and a stored energy of 800 MJ. At nominal operating conditions (5700 A) the conductor was operating at a Stekly parameter α_{Stekly} of approximately 0.5, i.e., largely in the cryo-stable regime. (See Appendix 4 at end of this section)

12.3.8 Adiabatic Stability

The concept of enthalpy stabilization in adiabatic winding is at the other extreme of the strategies of stabilization. The idea is that the conductor has the enthalpy to absorb the heat locally, without exceeding the current sharing temperature, preventing the instability to initiate. This concept applies to tightly packed, impregnated windings that are not permeated by the helium coolant (adiabatic windings) and operate at high current density, a bonus for the economics of the magnet system. The price to pay is that the enthalpy of a strand between typical operating temperatures of 1.9 to 4.2 K, and current sharing conditions is small, a few mJ/cm^3. Correspondingly, the superconductor can survive events depositing only very small energy, and great care must be put to reducing all sources of magnetic and mechanical perturbations. By contrast, a cryo-stable conductor can in principle survive any perturbation.

This form was presented in early papers by Hancox[22], Chester[23] and Smith[24] and is normally

[20] E. U. Haebel and F. Wittgenstein, *Proc. 3rd Int. Conf. Magnet Technol.* (1970) 874

[21] F. Wittgenstein et al., *Cryogenics* 9 (1969) 158

[22] R. Hancox, *Phys. Lett.* 16 (1965) 208

[23] P. F. Chester, *Rep. Prog. Phys.* XXX (1967) 561

[24] P. F. Smith, *Proc. 2nd. Int. Conf. Magnet Technol.* (1967) 543

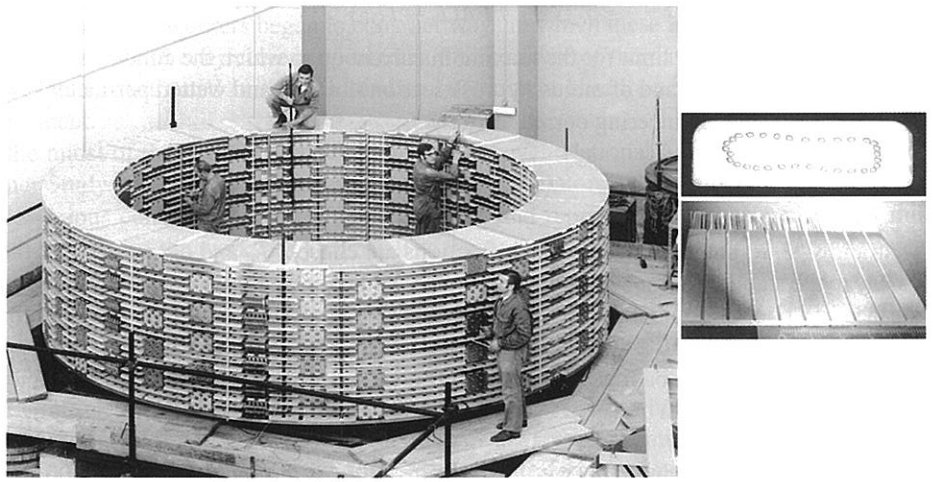

FIGURE 12.22: The solenoid of the Big European Bubble Chamber during winding, and a cross section of one of the conductors used, consisting of straight Nb-Ti filaments in a large Copper matrix. (Reproduced by permission of CERN. Courtesy CERN.)

used to evaluate the upper bound on the size of a superconducting filament that can sustain a flux-jump. Their analysis considered the effect of a small temperature increase δT on the magnetization of a superconductor in an external field. The decrease of J_c at increasing temperature, i.e., a negative derivative dJ_c/dT, causes a reduction of the magnetization and an energy dissipation δE in the superconductor. This energy in turn leads to a further temperature increase $\delta T'$. An instability is initiated when $\delta T' > \delta T$, a flux jump. This condition was presented as an upper limit on the superconductor characteristic size d:

$$d \leq \frac{1}{J_c} \frac{3CT_0}{m_0} \tag{12.4}$$

where T_0 is given by $J_c/(dJ_c/dT)$ and falls in the range of $T_c/2$ and the difference between the critical and operating temperature, i.e., $(T_c - T_{op})$. The above criterion was derived for the case of a superconducting slab, but can be used as an approximation of the diameter of a round filament. For the highest current density NbTi the maximum diameter compatible with flux jumps and adiabatic stabilization is approximately 25 μm. Wires made with single filaments of this dimension are clearly not practical for applications requiring ampere-turns at the level of few hundreds of kA-turns that is necessary, as for example, in accelerator applications.

12.3.9 Dynamic Stability

The successful experience on magnets built with ribbon or tape superconductors, tapes obtained by vapor deposition of Nb_3Sn on Hastelloy or silver, the "Vapodep" ribbon from RCA, or the diffusion processed niobium tin tape from GE, of dimensions exceeding the flux jump limit but sandwiched with a copper tape, demonstrated that the adiabatic stability condition given above is too

conservative. An important realization was that while the magnetic flux diffusion time in a superconductor is a few orders of magnitude faster than the thermal diffusion time, for very pure conductors such as Al and Cu the situation is the opposite. Therefore, if the correct combination of pure metal foils and thin layers of superconductor are combined in a winding, it is possible to "freeze" the magnetic flux for time sufficiently long to allow cooling. Such a package is hence stable thanks to a dynamic heat balance, whence the name of dynamic stabilization given to this strategy. A report by Dahl[25] lists several early Nb_3Sn magnets with on this form of stability. In the dynamic case the stability limit on the superconductor size d (the tape thickness or filament diameter) was modified as follows:

$$d \leq \frac{1}{J_c} \frac{6k(T)T_0}{\rho_n} \frac{1-\lambda}{\lambda} \tag{12.5}$$

where λ is the fraction of superconductor in the strand, and $k(T)$ is its effective thermal conductivity and all other quantities were defined earlier. The factor $(1-\lambda)/\lambda$ for a strand with 50% superconductor is equal to 1. The above limit is much less restrictive than the adiabatic limit, resulting in maximum filament sizes larger by one order of magnitude (i.e. around 200 μm). It is evident that distributing the superconductor in a low resistance matrix metal has multiple advantages. Small filaments in one multifilamentary strand had lesser tendency to adiabatic flux jumps, and even if they did they could be dynamically stabilized.

12.3.10 MultiFilamentary Wires and Twisting

Most of the work so far described originated in the early to mid 1960s. By this time multifilamentary copper/NbTi wires with good steady state stability properties began to be available, and new issues were found related to field ramps. (See Appendix 5 at end of this section) The use of small filaments embedded in a matrix of high conductivity material was sufficient to prevent flux-jumping to trigger an instability, but it was clear that this was not the end of the story. (See Appendix 6 at end of this section) We return once more to that seminal event, the "Woodstock of Superconductivity", the 1968 Summer Study on Superconducting Devices and Accelerators, and in particular to the work of the Superconducting Applications Group at the Rutherford Laboratory in England[26].

12.3.11 Cable Stability: The Invention of Rutherford Cable and CICC

Wires and tapes can carry currents in the range of few hundreds of amperes and are appropriate to wind small magnets, when the magnet inductance and stored energy are not an issue as we will see in a later discussion on protection. On the other hand, the large-scale magnets of interest for accelerator or fusion applications store energies that can reach hundreds of MJ. It was soon realized that it was important to decrease the magnet inductance, so to limit the operating voltage. This calls for the use of cables made of several wires in parallel, capable of carrying much larger currents, typically in the range of 10 kA. Similar to a multifilamentary strand, the strands in the cable need to be electromagnetic de-coupled through geometric transposition[26]. Early efforts at effecting this transposition of filament elements in superconducting cables in the manner of high frequency litz cables proved unsatisfactory, but eventually the eponymous cable geometry developed at the Rutherford Appleton Laboratory[27] became the standard. A Rutherford cable is composed of two dimensionally transposed, twisted wires, which ensures good current distribution. The main advantage of this geometry is the possibility of achieving a tight twist and a high compaction ratio

[25] P. F. Dahl, BNL Report BNL50498 (1976)

[26] P. F. Smith et al., *Proceedings of the 1968 Summer Study on Superconducting Devices and Accelerators*, Brookhaven National Laboratory (1968) 913

[27] G. E. Gallagher-Daggitt, Rutherford Laboratory Memorandum No. RHEL/M/A25 (1973)

without degrading the strand performance. In practice, 80 to 90% of the cable cross section is filled with strands, with minimal loss of engineering current density. In addition, the cable can be shaped to a precisely defined and tightly controlled geometry. Rutherford-type cables soon dominated the design of accelerator magnets. All superconducting accelerators to date have been built using this type of cable. Figure 12.23 shows the example of an LHC Rutherford cable used to wind the main dipoles.

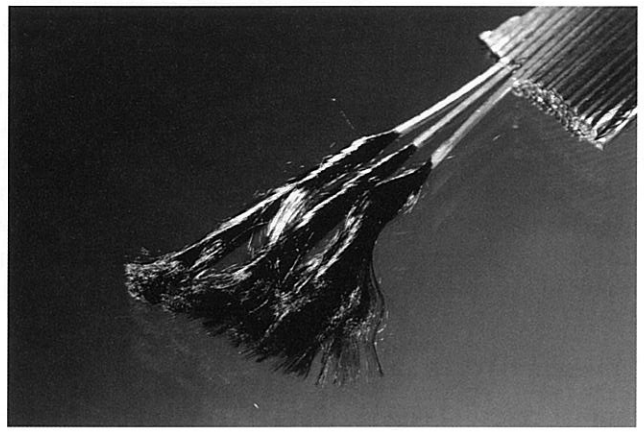

FIGURE 12.23: A recent example of Rutherford-type cable, used for the construction of the LHC magnets. A few strands have been etched to expose the 7 μm thick Nb-Ti filaments. (Reproduced by permission of CERN. Courtesy CERN.)

Compacted cables such as those of the Rutherford type rely on the same stability concepts as single tapes and wires. A shift in paradigm was achieved with the concept of a cable-in-conduit conductor (CICC), which evolved from the internally cooled superconductors (ICS) that had found applications in magnets of considerable size between the late 1960s and early 1970s in particular the work of Morpurgo[28]. In ICSs the helium is in a cooling pipe that either includes or is in intimate contact with a superconductor, very much like standard water-cooled copper conductors. This conductor can be wound and insulated using standard technology, a considerable advantage for large systems requiring high dielectric strength. A major drawback of this concept, however, was the fact that in order to achieve good heat transfer and thus stability and high operating current density the helium would either have to be in the supercritical state or have to flow at very high flow rates. The advantage of the increase of the wetted perimeter obtained by subdivision of the strands was clear already at the beginning of the development of ICS[23]. In 1974 Hoenig, Iwasa and Montgomery proposed the first CICC concept, whose properties were successively elaborated by Hoenig and collaborators[29,30,31,32,33].

[28] M. Morpurgo, *Proc. 1968 Summer Study on Supercond. Devices and Accelerators*, Brookhaven National Laboratory (1968) 953

[29] M. O. Hoenig and D. B. Montgomery, *IEEE Trans. Magn.* 11 (1975) 569

[30] M. O. Hoenig et al., *Proc. 5th Int. Conf. Magnet Technology* (1975) 519

[31] M. O. Hoenig et al., *Proc. 6th Int. Cryo Eng. Conf.* (1976) 310

[32] L. Dresner, *IEEE Trans. Magn.* 13 (1977) 670

[33] L. Dresner and J. W. Lue, *Proc. 7th Symp. Eng. Problems* (1977) 703

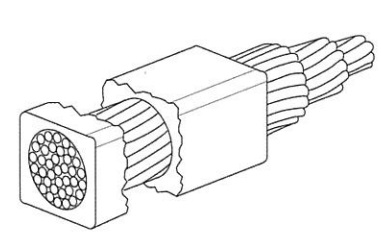

ROUND BUNDLE WITH 37 STRANDS ENCLOSED IN RECTANGULAR CONDUIT - SHOWING TRANSPOSITION OF STRANDS

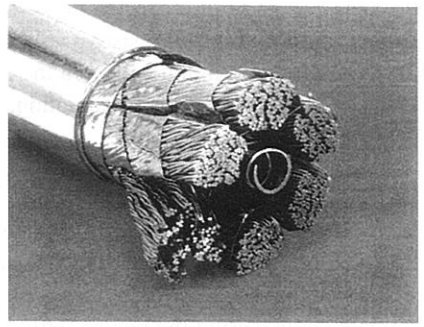

FIGURE 12.24: The first proposal of a CICC configuration, by Hoenig (left), contrasted to a prototype ITER TF CICC with central cooling channel. (Courtesy of ITER.)

A bundled conductor is obtained cabling superconducting strands, with a typical diameter in the mm range, in several stages. The bundle is then jacketed into a helium-tight conduit that provides structural support. Helium flows in the conduit within the interstitial spaces of the cable. The small hydraulic diameter insures a high turbulence, while the large wetted surface achieves high heat transfer, so that their combination gives the known excellent heat transfer properties. CICCs were initially designed to satisfy the Stekly criterion. Strictly speaking, a CICC cannot be considered to be cryostable because the amount of helium available for its stabilization representing the dominant heat capacity is limited in any case to the volume in the local cross section. A large enough energy input will always cause a quench, so the question is the magnitude of the minimum energy input producing a quench in a particular operating condition. This parameter is the stability margin[34]. A typical behavior of the stability margin was found in measurements of Nb-Ti CICCs as a function of the operating current[35]. For a sufficiently low operating current a region with high stability margin, named by Schultz and Minervini[36] the *well-cooled* regime of operation, is observed. In this regime the stability margin is given by the total enthalpy available in the cross section of the CICC up to current-sharing, including both strands material and helium. As the current increases a fall in the stability margin to low values, the *ill-cooled* regime, appears. The proper naming of this regime received much attention by many native language reviewers at conferences and international journals, proposing various, more grammatically correct alternatives, such as *poorly-cooled* or *badly-cooled*, demonstrating yet again that the smallest perturbations to a system arouse the widest consequences, just as in a superconducting circuit! The fundamentals are that in this regime the stability margin is one to two orders of magnitude lower than in the well-cooled regime and approaches the enthalpy of the superconducting strands. A good CICC design is hence optimum from the stability point of view when operating just below the well-cooled/ill-cooled transition.

Stability was the main argument that won the conductor competition in the European Fusion Program of the late 1980s. The CICC concept that was prototyped in Europe by Brown-Boveri Switzerland lived through a few minor changes during the first years of the ITER Conceptual Design Activities. It was modified to the present form which includes a central cooling channel during the ITER interregnum of P. H. Rebut, the official motivation being the fear that the cable would act as a filter and eventually be clogged by particles or impurities in the helium coolant. Although the overall current density was reduced, and the fear of impurities may not be justified, the present ITER cables

[34] M. O. Hoenig and D. B. Montgomery, *Proc. 7th Symp. Eng. Problems Fusion* (1977) 780

[35] L. Dresner, *Cryogenics* 20 (1980) 558

[36] H. Schultz and J. V. Minervini, *Proc. 9th Int. Conf. Mag. Technology* (1985) 643

are extremely robust with regard to their stability properties. This is also due to the fact that the cable can sustain a significant resistive voltage without quenching because of the fairly low resistive transition index with common values in the range of 5 to 10, a feature that makes magnet engineers refer to the ITER coils as "hyperconducting."

12.3.12 Stability in the New Millennium

As we write, we are profiting from the spectacular development of Nb_3Sn multifilamentary conductor for High Energy Physics that took place at the turn of the millennium: the J_c of this material has increased by a factor of three within the last decade The implication of this development can be appreciated considering the record setting dipoles D20 and HD1, built at the Lawrence Berkeley National Laboratory in the 1990s and 2000s, respectively. In 1997, the D20, a 4 layer cos-θ coil, produced a central field of 13.5 T using a Nb_3Sn conductor with J_c of approximately 750 A/mm^2 at 12 T and 4.2 K [37]. In 2004, the HD1 dipole reached a bore field of 16.1 T by virtue of a conductor with J_c of approximately 3000 A/mm^2 at 12 T and 4.2 K [38]. If D20 had used the conductor available for HD1, and ignoring issues of electromagnetic forces, it would have been a two-layer coil, and would have attained significantly higher field.

Although beneficial, this boost of J_c has also led to the rediscovery of the importance of stability, its relation to filament and strand diameter, and the electrical properties of the stabilizer. Specifically, magnet engineers are being reminded of the early finding that we have described in this chapter. Filament sizes in high-J_c internal tin wires are in excess of 100 μm, i.e., on the edge of flux-jump stability, and caution is in order. A modest residual resistivity ratio (RRR) is in itself not a problem if it is uniform in the wires, and in general magnets built with low-RRR wires, say in the range of 15, are easier to protect as they are characterized by a faster quench detection, thus easier to spread the energy and a faster dump. However, it was found that the presence of local spots with low RRR caused by tin leakage from the subelements damaged during cabling can lead to poor stability and magnet performance limitations in the intermediate field region of 8 to 12 T.

A few more lessons have been learned and are common practice in superconducting magnet engineering. It is important to hold the winding pack in compression in all directions, with a force that is greater than the Lorentz load, including an appropriate safety factor. This is done to reduce the energy inputs of mechanical origins that can trigger instabilities. Good conditions are attained when the winding does not have freedom to move and is always in contact with the force-bearing surface. An initial load is applied on this surface, sometimes just a few MPa sufficient to remove the fluff. Caution must be used to avoid cracking or tearing at the interfaces, and in particular those bonded or glued during an impregnation process. In some cases it may be of advantage to intentionally remove the bond between the windings and the surfaces that are not supporting the Lorentz load, especially at the surfaces that tend to separate. In this case the coil would be allowed to move as much as required, e.g., by field quality considerations. These principles may be difficult to apply in cases where the force distribution is complex, e.g., the large coil systems of future fusion experiments, or in high order field configurations such as the multipole corrector magnets of particle accelerators. Such magnets are then designed with a larger operating margin to cope with the increased perturbation energy spectrum. High-temperature superconductors are just at the beginning of this process of learning again from the past, and will eventually have to deal with stability at liquid Helium temperature. They are ideal perspective candidates for high field inserts in magnets where the background field is generated by coils wound from A-15 or Nb-Ti conductors. For reasons of magnet economy, HTS conductors still need an increase of J_c by a factor of 5. Assuming that this is successfully achieved, and if the present effective filament size does not decrease, HTS should reach the known

[37] R. Scanlan et al., *Inst. Phys. Conf. Ser.* 158 (1997) 1503

[38] A. Lietzke et al., *IEEE Trans. on Appl. Supercond.* 14 (2004) 345

stability boundary conditions. Stability as it concerns filaments in a matrix via dynamic criteria á la Chester or an enhanced cryostability scenario á la Stekly will result again in a criterion on the maximum dimension of the filament that we quoted earlier. History repeats itself.

12.3.13 Quench and Protection—a Burning Issue

A quench is an inherent part of the life of a superconducting magnet system. Quenches happen either accidentally, as we have described at length earlier, or intentionally, e.g., during a magnet test. A normal zone starts suddenly or gradually, the resistance and Joule heating grow, the temperature, initially barely above the superconducting transition, starts rising more and more rapidly, and a normal voltage appears at the coil terminal. Whatever the initiation, the final result of a quench is always a coil dump. The burning question is how rapidly the current is reduced to zero. As early as 1963, that is right after the superconducting rush for high field applications, Smith documented the concern that: "...the dissipation of the stored energy of the coil gives rise to local heating which, for large coils, may be sufficiently great to damage the insulation or permanently alter the properties of the wire ..." [39]. Indeed, recall that a superconducting wire carrying a current of 100 A can have a typical diameter of 0.5 mm, i.e., no larger than the wire in a household fuse that breaks at 15 A in fractions of a second. This comparison was inspiring to those that were finding criteria for magnet design. Conductors were considered adiabatic, and the temperature increase was computed equating the power produced by Joule heating $I^2\rho_n/A$ to the rate of enthalpy change $AC\frac{dT}{dt}$, where C is the volumetric heat capacity. With minimal manipulation, the same design used for fuse wires, it is possible to relate the peak conductor temperature at the end of the current dump, also called hot-spot temperature T_{hot}, to the integral in time of the square of the current:

$$\int_{T_{op}}^{T_{hot}} \frac{C}{\rho_n} dt = \int_0^\infty I^2 dt. \tag{12.6}$$

The interest in the equation above is the integral on the left. It is a property of the conductor geometry and materials only, while the integral on the right depends only on the current waveform during the dump. The equation thus defines the relation between the hot-spot temperature and the current rating of a specific dump. The units of the above integrals are those of squared current times seconds. A new, convenient definition of this unit was found at Fermilab in the 1970s: the MIITS, which measures the current integral in 10^6 (A^{2}s), a practical number for conductors that carry a few kA and need to be dumped in fraction of a second to avoid over-heating. (See Appendix 7 at end of this section.) The use of the MIITS curve caught-on very rapidly. This is a relatively easy criterion to apply, and somewhat conservative as a conductor is not adiabatic inside a coil. One difficulty remains, though, namely that to predict temperature one has to know the current waveform during a coil quench. This, in turn, depends on the coil resistance, that is on the size of the normal zone and the temperature in the coil which we are seeking to determine, on the coil inductance, a geometrical parameter that is affected by the cable size through the number of turns, as well as on actions external to the coil such as power supply or switch response. This difficulty shows the typical iterative process associated with the choice of a suitable protection strategy for a magnet system. In broad terms, a good protection strategy is a balance among a safe temperature increase (material integrity), limited temperature gradients (thermal stresses), coil voltage level (electrical standoff) and the complexity of the quench detection and protection circuitry. We can distinguish two extremes when considering different protection strategy. At one extreme the magnetic energy inventory is fully dissipated within the magnet cross section. This is appropriate for small magnets that store little energy compared to the material damage level. The main issue in this case is how

[39] P. F. Smith, *Rev. Sci. Inst.* 34 (1963) 368

to spread evenly the energy, and to increase the resistance rapidly so that the coil discharges fast. The best situation is that of quick quench propagation in the coil. At the opposite end of protection strategies we have the case in which the magnetic energy is nearly completely drawn from the coil and dumped, e.g., in extraction resistors or diodes switched into the circuit. This is mandatory in large systems that store quantities of energy far exceeding the local damage limit. The issue in this case is whether the external circuit can be fast enough, i.e., essentially a question of allowable MIITS and terminal voltage. It is now clear why in large coil systems it is beneficial to reduce the magnet inductance by winding the coil with large conductors. Of course, the two extreme strategies are not mutually exclusive, and can be combined as appropriate. These ideas developed fast in the early days. It is remarkable that the earlier work of Smith[39] already reviewed protection strategies ranging from self-protection, subdivision, coupling to additional circuits and fast insertion of resistors, covering most conditions of relevance, and including considerations of magnets in persistent mode, and concern on the maximum voltage developed internally and externally to the coil by the various methods. Apart for the use of quench heaters embedded in the coil, an expedient to speed-up quench propagation in the high current density and high field magnets connected in the kilometer-long strings of modern accelerators such as the LHC, most of the fundamental work had been completed.

12.3.14 Hot Helium Bubbles

Electrical and thermal considerations are not the only issues during a quench. In most cases the energy deposited to the helium is so large that trying to contain the ensuing pressure increase would neither be practical nor safe. A closed volume of liquid helium would pressurize to about 400 bar upon warming up to 100 K, which is still a modest temperature for a typical quench. This explains why all cryogen-cooled superconducting magnets are duly equipped with quench pressure relief lines. While in the early days these would blow cold helium into the atmosphere of the laboratory, they presently vent to a helium recovery system, a much more environmentally and economically correct solution. Internally cooled cables, and especially CICCs represent a special case for the process of helium heating, pressurization and expulsion. If a quench happens within the coil, the helium in the normal zone is heated and pressurized. The quench relief line in this case is the cable itself that sees a rush of warm helium trying to escape the normal zone. In doing so, the helium actually propagates the quench with a speed that is comparable to the flow velocity. This is in fact the dominating quench propagation mechanism in coils built from ICSs and CICCs. The understanding of this phenomenon was strongly motivated by the work on the CICC coils for fusion, and in particular the Westinghouse coil built within the framework of the Large Coil Task Program, a toroidal assembly of 6 coils built at major world laboratories and industries and tested at Oak Ridge National Laboratory[40]. It was Dresner who proposed the "hot helium bubble" mechanism to explain quench propagation in CICCs[41]. Miller and Lue, systematically tested Dresner's theories in specially constructed sub-scale conductor experiments[42,43,44]. In the years around 1980, this team addressed most of the issues in CICC design, stability, quench and protection, thus providing a well-founded background to the design of the large coil system that will be at the core of ITER. An interesting sidelight to this work is the thermo-hydraulic quench-back. A process such as quench in a CICC, involving heat transfer in the cable and compressible fluid-dynamics, is not a trivial analytical task, and it is natural to resort to computer modeling for this type of work. Computing quench

[40] D. S. Beard et al., *Fus. Eng. Des.* 7 (1988)
[41] L.Dresner, *Proc. 10th Symp. Fusion. Eng.* (1983) 2040
[42] J. R.Miller et al., *Proc.8th Int. Cryo. Eng. Conf.* (1980) 321
[43] L.Dresner, *Proc. 9th Symp Eng. Prob. Fusion Research.* (1981) 618
[44] L.Dresner, *Proc. 11th Symp Fusion Eng.* (1985) 218

evolution as a function of operating conditions, Luongo[45] found that under certain circumstances the quench propagation speed could increase from the few m/s typical of heating-induced flow to tens and hundreds of meters per second. The first obvious reaction was skepticism in the results, initially attributed to an issue in numerical convergence. As understanding improved, it was again Dresner[46], and two mathematicians, who identified analytically conditions upon which the adiabatic compression and frictional heat could generate a thermo-hydraulic quench-back wave traveling in the coil up to the sound of speed in helium[47]. Lue reproduced this condition experimentally in 1993 [48], thus demonstrating that computer simulations can indeed be useful.

Helium expulsion can be an effective means to identify a quench. Flow conditions in a cryogenic circuit depend strongly on local heating, and already modest power cause flow locking and thermally induced flow. These effects can be measured easily and used as a backup quench detection system. (See Appendix ix at end of section)

12.3.15 Coda

One hundred years since discovery, the promise of exceedingly large magnetic fields at little cost still inspires the imagination. Invariably, though, among the many facets that are vital to the successful engineering of a superconducting magnet system, stability and protection are two key issues that determine performance, reliability and safe operation. In our first sentence here we indulge in a little hyperbole: exceedingly large magnetic fields are definitely not available at little cost, projects involving them have become international ventures involving participating specialists numbering in the thousands. The results are spectacular, for they all rest on the shoulders of the small band of dreamers, thinkers and tinkers of yesteryear.

12.3.16 Appendix: Recollections and Reminiscences

A.M. = Al McInturff, L.B. = Luca Bottura

1. On the Discovery of High Field Superconductivity, A.M.

I remember my thesis advisor Professor Charles Roos discussing the possibility of obtaining a measurement of H_{c2} of Kunzler type Nb_3Sn in a 200 kGauss pulsed solenoid by converting the Michigan State University old surplus RF capacitor bank into a pulsed power supply with another Vanderbilt graduate student Clay Whetstone and I, using "war surplus" radar parts. This pulsed power supply we would in turn use to power the spare "Bitter Type" solenoid (15–25T 30 millisecond pulse) I was using to keep the photo-produced electron pairs out of my emulsion stack exposed at the Cal Tech Synchrotron that were to be scanned for photo produced sigma particles at Vanderbilt's Scanning Laboratory. We would turn the magnet on its end, so that the axis was vertical and then mount a double liquid volume glass cryostat (Dewar) in the bore with the reservoirs of liquid nitrogen and liquid helium above the magnet with the glass Dewar resting on a cork washer sitting on the upper magnet end plate. The Nb_3Sn sample mounted on a couple of current leads held by a G10 clamp supported on a stainless steel threaded rod. It was a four-terminal measurement to determine H_{c2}. The plate at the top was clamped to an external support to hold the sample in the right spot during the magnet pulse to measure their H_{c2} resistively. Our "Kunzler" type samples were fabricated by our ORNL colleagues Drs. G. Kniepe, J. Betterton and R. Boom. Of course we were unaware that the pulsed field was going to increase the temperature of our sample. As I remember,

[45] C. Luongo et al., *IEEE Trans. Magn.* 25 (1989) 1589
[46] L.Dresner, *Cryogenics* 31 (1991) 557
[47] A. Shajii and J. P. Freidberg, *Int. J. Heat Mass Transfer* 39 (1996) 491
[48] J. W. Lue et al., *IEEE Trans. Appl. Supercond.* 3 (1993) 338

the samples were a cross between dried black spaghetti and hard rubber and to add to the challenge about as easy to solder! Our first LHe level gauge was an Ever-Ready flash light and a ruler. First rotate the non-silvered strip of the outer cryostat to align with the inner one and put the light behind to reflect off the helium surface and then measure. The liquid helium was obtained from ORNL in a rental truck driven by Clay or myself to Vanderbilt in Nashville from Oak Ridge. Our measured value was a few Tesla low but still served to give the highest early H_{c2} for the A15 compound. Such a high value only increased the interest in applications.

2. On the AGS K Meson Beam Line, A. M., in Connection with Early High Field Magnets:

"One such example was the solenoid at the BNL AGS K-beam line designed and constructed by William Sampson. This device was used in an experiment (1967–1968) at the BNL AGS K-beam line to measure the magnetic moment of the short life time Ξ^- hyperon. Due to the life time the Ξ^- traveled only 10 cm on the average. The split pair solenoid magnet would be located right behind a solid H_2 target which together would be located inside a "Cerenkov" counter. A spark chamber followed behind the magnet centered on the beam line. This magnet was a four split-coil array stabilized by anodized high purity Al foils separating the layers for two sections and a Mylar/cu-foil/Mylar for the other two sections and protected against high voltages by copper shorting foil strips across each layer. The conductor was a vapor deposited Nb_3Sn on a Hastelloy ribbon. The stability of the higher J_c inner section was enhanced by the field of the lower J_c outer sections. The magnet produced 12.5 T bore field and had a persistent switch across the input leads during HEP operations, a very early feature which has become common place nowadays. The magnet had an eight degree conical inner bore (3.8 to 6.6 cm id), the production angle of the Ξ^-, 0.89 million pictures were taken during the HEP data run and 1.7×10^4 possible Ξ^- events were found.

3. Training and Degradation, Recollections of J. Hulm:

"Those tiny, primitive magnets were, of course, terribly unstable [...] One had to have faith to believe that these erratic toys of the low temperature physicist would ever be of any consequence as large engineered devices."

J. K. Hulm, "Superconductivity research in the good old days," Talk given at the banquet of the Applied Superconductivity Conference, Knoxville, TN, Dec. 1, 1982. The talk is available for download at : http//www.sainc.com/asc04/johnHulm.htm

4. On the BEBC at CERN:

A dramatic example of a cryo-stable magnet was the Big European Bubble Chamber (BEBC) built and operated at CERN (Haebel, 1970). BEBC was a 4.7 m bore split solenoid with a 0.5 m gap producing a maximum field in its center of 3.5 T, corresponding to a maximum field at the conductor of 5.1 T, and storing an energy of 800 MJ. The magnet was cooled in a bath of 17,000 l of liquid helium, and the bubble chamber sitting in the bore contained 35,000 l of liquid hydrogen. These dimensions are spectacular even on the scale of modern HEP detector magnets, BEBC was the largest European superconducting magnet at that time, and long after. Each coil was wound in 20 pancakes out of a flat monolithic conductor with 3 mm thickness and 61 mm width. This conductor was itself a composite containing 200 untwisted NbTi filaments with a diameter of about 200 μm in an OFHC copper matrix. At nominal operating conditions (5700 A) the conductor was operating at a Stekly parameter α_{Stekly} of approximately 0.5, i.e., largely in the cryo-stable regime. The construction of the magnet started in the late 1960s, only a few months before the P. Smith and the Rutherford Group discussed the necessity of twisting the filaments to decouple them (see later). In the recollection of the BEBC magnet project engineer, Francois Wittgenstein, by that time the conductor production in Germany (Siemens) and France(CGE) was too advanced to introduce a major change in the manufacturing sequence, such as twisting of the filaments. Besides, earlier

prototype conductor testing in a small-scale solenoid model built for this purpose did not show evidence of performance issues (Wittgenstein, 1969). Hence, the production commitment could not be stopped, especially when such a minor issue such as the threat of flux-jumps was to be compared to the strikes organized by the French Unions in May 1968, right in the middle of the extrusion of 2 km conductor lengths required for winding. The group managed to overcome these very practical difficulties, and wound the solenoid that reached nominal operating conditions, as expected. Indeed, thanks to cryostability, the BEBC coil could be energized up to the operating current in spite of the fact that the conductor with large untwisted NbTi filaments had very large magnetization associated with the currents that flowed in the electromagnetically coupled filaments. A feature that was built in the coil design was a set of heaters that could be fired to suppress the large magnetization produced by these coupling currents. In practice, however, the heaters were never used in routine operation. But there was another effect associated with the large magnetic moment of the conductor, namely the force distribution in the solenoid was not as expected. As a result, at locations the solenoid shrank in diameter, instead of expanding. This caused mechanical interference with the cryogenic pipe work and the appearance of shorts that, strangely enough in the eye of the operators, would disappear after the ramp was stopped (and the induced currents in the conductor would decay). The problem was cured by adding mechanical support and reinforcing electrical insulation during a technical stop, when finally, in light of the evidence, the influence of the induced currents was recognized.

5. On Magnetization Studies, A.M.

I was doing magnetization studies on various conductors that were available and had already figured out that the field/current path geometry was driving the instabilities that I saw. I was primarily using tapes (even fabricated NbTi tapes for comparison). The first MF samples that I tested were very stable until I reached very high rates of field change.

6. On Impressions of Smith's Exposition of Filament Twist in Relation to Stability of Wires, A.M.

As I listened to him explain the twisting arguments canceling the filament-to-filament current coupling, a light went on and I understood the problem with the MF mini-coils I had made for the next stage of magnetization studies. I went back to the lab and took one sample coil apart and put it on a lathe with a brake and pulled it through a 10% reduction die and back on the sample holder. I then tested the small coil and the magnetization was about a magnitude lower and at twice the rate of change of background field. I was convinced and I called my old colleague Whetstone to tell him to twist the multifilament conductor that Cryomagnetics, Inc. was making for the outer NbTi winding of a bubble chamber coil in partnership with IGC who would provide the inner Nb_3Sn tape coil. The NbTi outer coil would provide a 7 T field to be added to the inner Nb_3Sn coils 4 to 5 T resulting in an 11 T field for the bubble chamber data. IGC had used the "dynamic" scheme for stabilizing the 30 cm id inner winding plus of course the background field of the outer NbTi coils contributing to the stability. The magnet during test after a quench or two reached a bore field of 11.5 T and it was decided to mount the bubble chamber inside and run at 11 T in the CERN K-beam line. The contract was with the Max Plank Institute in Munich and was in collaboration with our former Professor Charles Roos. This bubble chamber and high field magnet system designated "HYBUC" ran in the CERN PS Kaon beam line for over a year resulting in a statistically accurate determination of the Σ^+ and Σ^- magnetic moments. I had set the twist rate high in my magnetization check and used that same value for the HYBUC magnet, but another colleague (G. Morgan) in our group at BNL actually worked out a model and published a result for the critical pitch length. In order to decouple the filaments in a composite, the twist pitch "$l_c(max)^2$" $\leq (10^8 \lambda \rho a J_c d)/[(dH/dt)_c(a+d)]$ where λ is a geometry factor which equals 1 for Cu, "a" is the filament separation, and ρ is the resistivity of the matrix, according to G. H. Morgan, *J. Appl. Phy.*, 41, p. 3673 (1970). Actually the

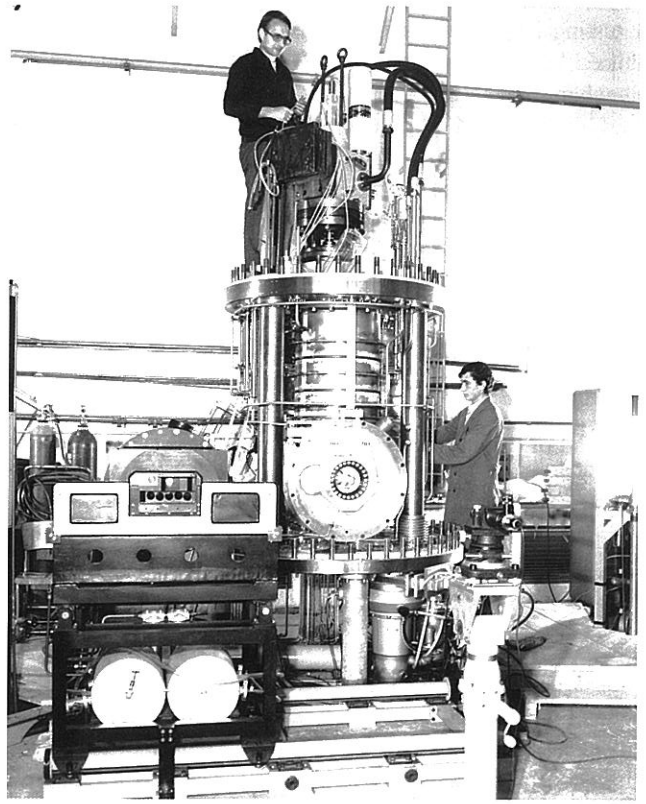

FIGURE 12.25: A remarkable little bubble chamber, called HYBUC, was built to measure magnetic moments of hyperons. It was one of the first rapid cycling chambers, and, using a superconducting magnet achieved very high fields of 11 Tesla. (Courtesy CERN.)

magnetization data indicated about a third of that pitch length for a normal charge rate is ok.

7. On MIITS, A. M.

Early in the prototyping of the Energy/Saver Doubler (Tevatron) work, Moyses Kuchnir and Joe Tague measured this type curve for the E/S cable. Moyses and Joe mounted an E/S cable on a long sample mount, which they instrumented with thermometry, voltage taps, and a heater in the middle of the cable. After covering the cable and associated instrumentation with insulating silicone grease, they placed the rig in a cryostat which subsequently was filled with LHe. A power supply was connected to the conductor and a DAQ unit continuously monitored and recorded cable current, voltage between taps, cable temperature, and the pulsed heater's current and voltage versus time. The heater was manually pulsed until the cable quenches, this quench voltage appearance causes the DAQ to speed up and after a few seconds to stop taking data. The data stored is a few seconds before the quench and a few after the quench. The data logged yields the peak temperature versus MIITS curve. I do not recall if they actually degraded or burnt any of the cables, but I would assume so. When I arrived at Fermilab after accepting a position to work on the Energy/Saver Doubler, I computed the MIITS curve for the E/S cable using Martin Wilson's "Quench" code and compared it to Moyses' data and found the computed values to be slightly conservative especially at the start (which is what one might have expected for an adiabatic calculation).

8. On Helium Expulsion Effects During a Quench of a CICC Conductor, L.B.

We were testing the ITER PF Conductor Insert at the CS Model Coil Test Facility in Naka, and one important item in the test preparation, before any serious powering, was to make sure that a quench could be detected timely. To this aim the Insert was equipped with a rather involved quench circuitry that included cowound wires to provide a reliable cancellation of inductive voltages. These instrumentation wires are embedded in the winding, and can fail under thermal stresses or electromagnetic forces. One such issue at the start of the test was solved by rewiring the instrumentation, modifying the balanced bridges, adjusting them slowly and carefully until the team had confidence enough that a quench would be suitably protected. The whole balancing procedure took very many hours, under the pressure of those who wanted to have a quick answer on the cable performance limits. Finally, with enough confidence in the adjusted quench detection, the cable quench current was measured, right at the expected value, 45 kA at 6.3 K and 6 T. The quench was detected by an interlock on the inlet massflow, much earlier than the voltage threshold. In fact, all but one of the quenches were detected by flow interlocks, not by the voltage signals!

12.4 The History of Fusion Magnet Development

Jean-Luc Duchateau, Peter Komarek and Bernard Turck

12.4.1 General Introduction

The need for superconducting magnets in large fusion devices was already recognized in the middle of the 1970s and the initial major development programs were started based on the first definitions for the required magnet parameters. These programs followed two lines. First was the development of conductor and magnet systems for small and medium sized plasma devices such as T-7 and T-15 in the Soviet Union, TRIAM in Japan and most prominently TORE SUPRA at CEA in France. Second, in the form of an international project, was the development of a conductor and magnet arrangement with parameters pertinent to large fusion devices and their test in a dedicated special facility, the Large Coil Task (LCT) project, within the framework of an agreement by the International Energy Agency (IEA). These projects were followed in Europe, Japan and the US by the basic development of poloidal field coils with principal emphasis on conductor development.

Following the successful execution of these projects, the design and construction of larger fusion devices with superconducting confinement magnets were started. Some are already in operation—tokamaks EAST in China and KSTAR in Korea, the stellarator LHD in Japan—or are still in the final construction stage, the SST1 in India, tokamak and the stellarator Wendelstein W7-X in Germany. Finally, the international fusion community felt brave enough to start the development, in a worldwide effort, of ITER, a tokamak-type reactor accompanied by a somewhat smaller tokamak, JT-60SA, in Japan, with major contributions from Europe. This chapter gives a brief survey of these developments and the present status of superconductivity for thermonuclear fusion.

12.4.2 The Large Coil Task (LCT)

As the result of an invitation from US Department of Energy, EURATOM and Switzerland, at that time not yet a member of EURATOM, joined in 1976 the so-called Large Coil Task (LCT)[49].

[49] D.S. Beard et al., *Fusion Engineering and Design* 7 (1998) 1

This project involved the development of a torus with six superconducting D-shaped coils with a bore of about 2.5 m × 3.5 m. Three coils were to be developed in the US, one in Japan, invited as an additional partner, one by EURATOM, and one by Switzerland. The work was formally organized through an Implementing Agreement of the International Energy Agency (IEA). All but one of the LCT magnets were constructed with a NbTi conductor meeting quite exacting specifications; one US coil was designed with Nb_3Sn conductor, a technology still unproven at that time. In contrast to the almost standard design at that time, namely pool boiling cooling for large coils, the advantages of a forced flow cooling concept within a strong conduit were emphasized. Its advantages are optimal force transmission to the coil case, well defined heat transfer and fully predictable voltage properties. This was a big challenge for the project groups involved and for their industrial partners. Budget and the time table became very critical, but all groups stayed on schedule and all 6 coils were operated together very successfully in 1986–87, Figure 12.26, in a test facility constructed for that purpose at the Oak Ridge National Laboratory. During extended tests some coils reached up to 9.1 T at 3.6 K before transitioning smoothly to normal conductivity, a record magnetic field value at that time.

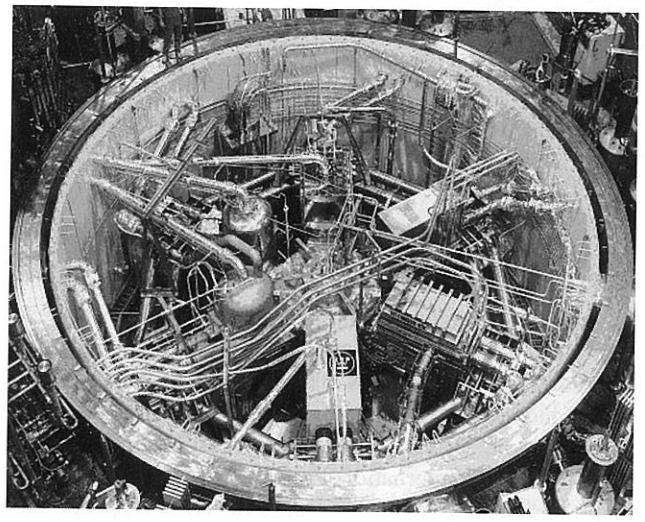

FIGURE 12.26: View of the toroidal arrangement of the LCT coils in the test cryostat at ORNL. (Courtesy ORNL.)

One major finding of this project was that for large fusion magnets, forced flow cooling of the conductor was the right choice to cope with the huge mechanical forces and the losses, and all later fusion projects followed this path. Another important experience was that this project was the beginning of very well working, formalized, international collaboration in the area of fusion magnets, greatly needed for resource sharing in projects which were growing larger and larger.

In connection with the LCT project, a smaller test facility TOSKA, a cryostat with a 4.5 m bore and 8 m in height, was built at FZ-Karlsruhe, now Karlsruhe Institut für Technologie, for the first tests of the EURATOM LCT coil as a single coil prior to shipment to the USA. This facility was also planned for future upgrades and future European fusion coil projects, a very wise decision as we will see later.

After its operation at ORNL, the EURATOM LCT coil was shipped back safely to Karlsruhe. As an extension of the existing program, the FZ-Karlsruhe team proposed to investigate the coil performance at reduced temperatures, down to 1.8 K, to demonstrate the feasibility of higher field

operation of such coils with a NbTi superconductor. Following some hard negotiations, the EURATOM authorities finally approved this experiment. For this purpose the coil had to be reinforced with external thick steel bands to withstand the huge mechanical forces existing in a single coil operation. The tests were performed in the TOSKA facility and proved to be very successful. While the highest operation point at ORNL had been 16 kA at 3.6 K, achieving 9.1 T at the winding, the coil was now operated up to 19 kA at 1.8 K, achieving 11 T. The coil quenched only slightly above that value, close to the critical current load line. With these results in 1998 everybody in Europe was now happy that this coil could be used later as a background coil for the testing of an ITER TF Model Coil and the Wendelstein W7- X demonstration coil, as will be described later in the appropriate sections.

12.4.3 Early Work on Poloidal Field Coils for Tokamaks

The challenge of this coil system is the need for pulsed operation in the same mode as the plasma current. Shortly after the LCT, the international collaboration began to establish initially a number of medium sized programs to meet these needs, mainly concentrating on conductor problems, with particular attention on the reduction of AC losses. Due to the fact that the magnetic field here is much smaller than in the toroidal field coils, NbTi can be used for the conductor, but sophisticated cabling of the conductor strands and strand coating with less conductive material is essential, requiring a special conductor development program. Even today, including the ITER design, several approaches are under investigation resulting in complicated and more expensive conductors. One of the largest test coils, 3 m in diameter, was developed at FZK earlier and tested in 1996 in the TOSKA facility. Currently a cost and effort intensive program is devoted to the ITER project as we will see in a later section.

12.4.4 *Tore Supra*

Introduction and Context

Until the beginning of the 1980s, all the fusion magnet systems were resistive with silver alloyed copper conductors to improve their mechanical properties and to resist the large electromagnetic forces. This kind of solution was possible due to the small size of the machines and to their pulsed mode of operation. The largest machine of this type was the Joint European Torus (JET) with a major radius of 2.98 m. Here the power required to energize the system was more than 1 GW, produced by flywheel generators, a solution possible only because of the short duration, 10 to 30 s, of the JET plasma discharges.

The first significant introduction of superconducting magnets into magnetic fusion systems was the construction of the 2.4 m diameter Tore Supra (TS) tokamak in France and of the T-15 in the Soviet Union. In both machines the magnetic field on the conductor was nominally around 9 T, making the classical use of NbTi conductors at 4.2 K impossible.

This led to a debate at the end of the 1970s centered around two possible choices:

- the use of forced flow Nb_3Sn conductors at a temperature in the range of 4 K,
- the use of bath cooled NbTi conductors with pressurized helium at 1.8 K through a new technique developed at CEA in France.

The inadequate industrial maturity of Nb_3Sn technology was clearly seen during the acceptance tests of T-15 where resistive parts in the magnets prevented steady state operation of the tokamak, which ultimately stopped operation in 1991.

The main design goal for the toroidal field system of Tore Supra at the beginning of the eighties was to extend the application of the NbTi superconductor, a cheap material, insensitive to mechanical strain, to a magnetic field of at least 9 T using superfluid helium, at 1.8 K and 1 bar, as a coolant.

This industrialization of refrigeration at 1.8 K was really a breakthrough, furthering the production of higher field NbTi as well as Nb_3Sn magnets. Only the toroidal field coil system was chosen to be superconducting, with the cryostat walls as close to the coils as possible All the other pulsed coils were conventional copper coils operating at ambient temperatures. This choice proved to be the correct one; as operational experience with the plasma control systems increased, it was possible to run with plasma discharges as long as 6 minutes.

Tore Supra and the Invention of Pressurized Superfluid Helium as a Cooling Technique for Superconductivity

Tore Supra was the first large sized superconducting machine using a substantial volume of superfluid helium, 5 m^3 at 1.2 bar of He II, mainly contained within the 18 toroidal field coils. The cooling of the pressurized baths is achieved through heat exchangers feeding the saturated baths. The design and sizing of all the 1.8 K refrigeration circuits were the result of studies at CEA during the 1970s, particularly the low temperature pumping of the saturated baths by two stage centrifugal compressors. This technique, used here for the first time in the world, was selected to obviate the intensive development of the low-pressure exchangers which necessarily must have a very small pressure drop. The choice of warm oil ring pumping was also the result of comparative studies from the technical, investment and operating cost points of view.

This novel cooling technique[50], developed at CEA, Grenoble, not only provided a lower operating temperature and thus a higher critical current density but the superfluid helium under atmospheric pressure has outstanding heat conduction properties. Also the total enthalpy between 1.8 K and 2.16 K, approximately 3×10^5 J/m^3, is available to ensure the stability of the conductor against disturbances.

In order to make a compact winding with good overall mechanical characteristics while reducing ac losses and increasing the wetted perimeter, a rectangular monolithic conductor wound edgewise in double pancakes was chosen. The superconducting filaments were extruded in a mixed matrix of copper and cupronickel in order to limit coupling losses by cupronickel barriers. The copper amount was also reduced as a result of the superfluid helium cooling resulting in a current density in the conductor of 89.2 A/mm^2.

The superconducting winding, Figure 12.27, was made of 26 double pancakes of conductor edge wound on the narrow side and made as rigid as possible, especially in the radial direction, to take the large void associated with superfluid helium into account. Each turn was electrically insulated with a pre-impregnated glass-fiber epoxy tape cowound with the conductor. The interconnects were located on the outer part of the coil, in a low field and low mechanical stress region.

The pancakes were separated by insulating spacers, providing additional mechanical cohesion of the winding while ensuring a very large volume of helium in direct contact with the conductor. After completion of the assembly process, the winding was heated to polymerize all pre-impregnated parts and to ensure a rigid coil.

Tests of a Prototype Coil and Difficulties Linked to the Acceptance Tests of the Assembled System

Once the superfluid helium cooling at 1.8 K and 0.12 MPa process was established, and a half scale model coil had been fabricated and its performance checked, a prototype coil was fabricated and tested at CEA, Saclay. These tests constituted the essential step to confirm the performance of the coils and to finalize the process for operation, with particular attention devoted to protection.

A stability test showed that, apart from a more elevated temperature zone around the initiating heated point, the coil was entirely quenched in 2 or 3 seconds after the opening of the circuit breaker,

[50] G. Claudet et al., *Cryogenics* 26 (1986) 443

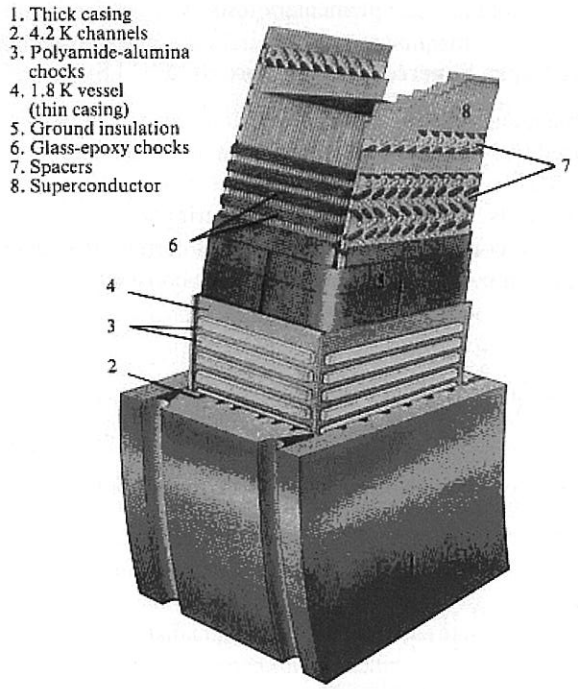

FIGURE 12.27: Sketch of one coil of Tore Supra showing the bare conductors immersed in superfluid helium confined in a thin casing. (Courtesy CEA.)

at a temperature of about 25 K. This proved that the quench propagation was very fast thanks to strong helium convection throughout the magnet. This process was driven by the increase of pressure and the escape of the helium through a safety valve located at the bottom of the coil in the low field zone. The final average temperature of the coil was 45 K, while the highest temperature located on the second pancake at the opposite of the gas outlet was estimated to be 130 K. Similar results were confirmed later in 1989, when during operation at 1400 A the coil BT4 suddenly quenched and triggered the magnet safety discharge system. This quench incidentally was the only quench observed during the 20 years of the Tore Supra operation. It was caused by the heat deposited by a fast electron beam from a severe plasma current disruption.

It may be recalled that in 1988 the acceptance tests of the entire system at CEA, Cadarache, were interrupted at 600 A by the appearance of a short circuit in coil BT17 during a test of the safety discharge system. This fault produced constant power dissipation in the coil. Pulsed operation of the coil was initiated during the next few months with a dedicated power supply to begin the first plasma runs in the machine. Then BT17 was replaced with a spare coil, the former prototype coil BT19, a process which took some 6 months. The damaged coil was removed, inspected, repaired and tested at CEA Saclay to be used as a possible spare coil. Only a limited part of it was damaged: 4 out of a total of 52 pancakes. In addition a more sophisticated analysis of the stability and quench test results of the prototype coil was undertaken, based on the experience with the toroidal field coil protection system. The purpose was to find a way to protect the magnet effectively while reducing the discharge voltages to a lower level. After analysis and additional testing, a complete revision of the protection scheme and a modification of the electrical circuit was instituted; it was demonstrated that the voltages could be divided by a factor of 10 in cases of fast safety discharges. This conclusion was reached after an in-depth examination of the specific behavior of the coil in He II after a quench,

shown in the prototype tests and in the supplementary tests.

Commissioning the Tore Supra Superconducting Toroidal Field System at Nominal Current

After the coil replacement and revision of the protection scheme, in November 1989 the current was progressively increased to 1455 A, corresponding to a magnetic field on the strand of 9.3 T and to a stored energy of 650 MJ [51].

During these acceptance tests, several discharges were triggered to test the safety system at increasing current levels. In the course of this phase, the coil current was reduced by extracting the magnetic energy through a dump resistor with a typical time constant of 120s.

One Day of Operation

On December 4, 2003, a day specifically chosen to study the impact of plasma operation on the cryogenics, two 4-minute plasma discharge runs were made with 1 GJ energy injected in the plasma.

Figure 12.28 represents the impact of a plasma operation on the temperature of coil BT15, this coil being representative of the behavior of the 18 coils of Tore Supra.

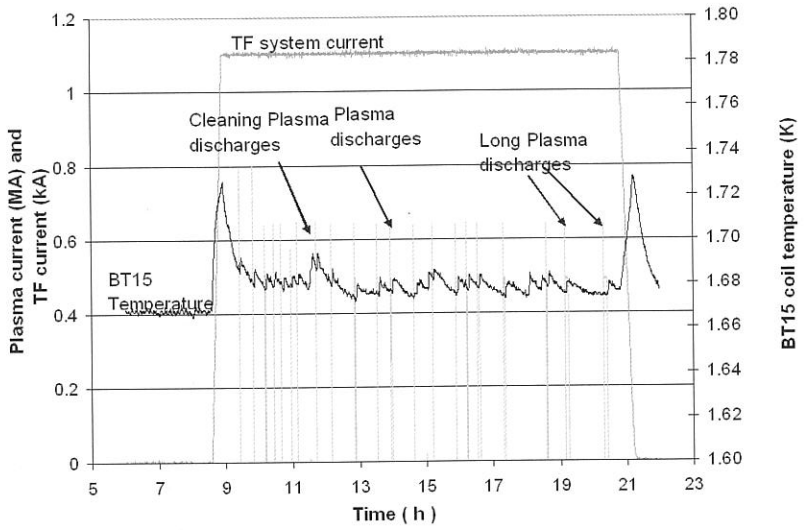

FIGURE 12.28: BT15 temperature during one day of operation.

On a normal day of operation the current in the toroidal field system was raised at the beginning of the day and kept constant during the whole day until reduced at the end of the day. The changes in the current levels had but a small impact on the coil temperature, the changes being about 0.06 K, recovery from which took place within half an hour.

The effect of plasma operation on the coil temperature is due to hysteretic and coupling losses, induced in the toroidal field conductors by the associated field variations. These field variations also induce eddy currents and heat dissipation in the thick coil casings. During the day, a phase of cleaning plasma discharges to recondition the vacuum vessel after a disruption produces a typical temperature increase of 0.25 K in the thick casings, needing about half an hour for the system to

[51] B. Turck, *IEEE Trans.* Mag. 25 (1989) 1473

recover. The rest of the operation has little impact on the cryogenics. Heat dissipation is always associated with plasma current initiation but the related temperature increases are small, less than 0.01 K for the coil temperature and approximately 0.08 K for the thick casing. It should be noted that the two last plasma discharges of the day, the 1 GJ discharges, had no particular impact on the cryogenics.

Summary

After more than 20 years of operation and 45000 plasma discharges without a major failure, this first marriage between fusion and superconductivity proved to be very positive[52]. It is also worth noting that while only one quench in a coil had been experienced during the whole life of the system, about 100 fast safety discharges of the magnet system occurred, resulting each time in a shutdown of the system for about two hours. These fast safety discharges were always triggered for reasons not associated with the magnet but rather by interference events in the sensors or in the electronics. Minimizing this type of disturbance must be an objective for the operation of all large devices including ITER.

The Tore Supra experience has demonstrated that superconducting magnets can safely and successfully be operated in long term plasma physics research. Far from being a burden, the steady state operation of the toroidal field system leads to a simplification in the preparation of the plasma discharges. No significant heat load is apparently associated with long plasma discharges but the circular shape of the Tore Supra plasma may attenuate the thermal load associated with plasma control, a phenomenon which must be confirmed on a machine with an elongated plasma. Future long pulse operation of the later tokamaks such as EAST and KSTAR will help to clarify this important point. The steady state operation of a large magnet system is also an advantage with regard to the mechanical integrity, fatigue life and aging of the coil. In Tore Supra no sign of mechanical aging was apparent judging from the mechanical measurements.

Clearly, the path is really open for a long and extensive program for superconducting machines for fusion. Certainly the superconducting magnet system of Tore Supra, with its 20 years of safe operation, has demonstrated and emphasized the way for a necessary and fruitful relationship between superconductivity and fusion.

12.4.5 Tokamaks with Superconducting Magnet Systems in Recent Time

Tore Supra is no longer the only tokamak with superconducting magnets. In 2006, the first fully superconducting tokamak with NbTi magnets, EAST[53] with a radius of 1.8 m, produced its first plasmas in China, then, in 2008 the Korean tokamak KSTAR with a radius of 1.8 m with both NbTi and Nb_3Sn magnets with forced flow conductors in the manner of ITER was put into operation. It was a big success for industrial fabrication. It is remarkable that KSTAR[54] is so far the only machine where no cold testing of the magnets took place before onsite installation, Figure 12.29 Another tokamak, SST1 in India, with NbTi superconducting coils is expected to be commissioned in the near future.

[52] J.L. Duchateau et al., *Fusion Sci. and Technol.* 56 (2009) 1092

[53] S. Wu and EAST Team, *Fusion Engineering and Design* 82 (2007) 463

[54] Y.C. Oh et al., *Fusion Engineering and Design* 84 (2009) 334

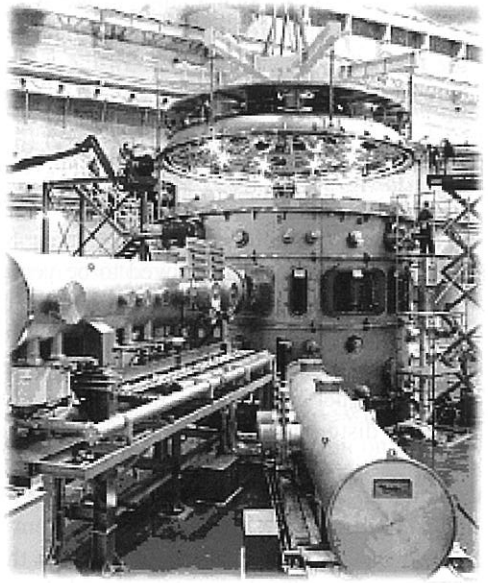

FIGURE 12.29: The KSTAR tokamak at KAERI in Korea[54]. (Courtesy KAERI, Korea.)

12.4.6 ITER as a Worldwide Collaboration Project in Thermonuclear Fusion

General

The ITER adventure was initiated in November 1985 when Ronald Reagan and Mikhail Gorbachev met at Geneva and encouraged the formation of an international collaboration with the goal of finally mastering fusion energy. However, it was only in 1991 that four entities, Europe, Russia, Japan and the US finally began a 6-year funded program with a dedicated project team: the ITER project was born. The ITER project has now been extended to 3 other countries, India, Korea and China; the construction of the machine was officially started in 2006 on the Cadarache site in France. To prove the feasibility of thermonuclear fusion as a potential source of energy for humanity, ITER is departing in a major way from the currently active fusion machines, the JT60 in Japan and the JET in Europe. JET has a major radius of 3 meters, while for ITER in its selected configuration a major radius of 6.2 meters is necessary, the major radius being the radius of the plasma torus. This geometry is necessary to sustain stable plasma discharges for as long as 500s resulting in a fusion power of 500 MW with an amplification of energy Q of 10, the ratio of the output power to the input power.

If the extrapolation from JET, based on plasma physics scaling laws, is considered to be adequate, ITER will also have to handle additional numerous technological challenges. These challenges include, for example, the plasma facing components, that is the inner blanket, the high power plasma heating sources and the very large size of the components.

Of these, the superconducting magnet system is probably the most remarkable one, as it is the real backbone of the machine. In practice, deeply buried in the very heart of the tokamak, repairs are hardly feasible except for a few protruding components like joints for instance, leading to a rigorous no-fault strategy in design, construction, assembly and test. The magnet system represents about 30% of the investment cost of the device.

In the case of ITER, for which a 500 second plasma discharge duration is planned, and probably longer in the later operational stages, a solution with resistive magnets is no longer possible and

the magnet system must be superconducting. The electrical power associated with the refrigerator to compensate for all losses at cryogenic temperatures is estimated to be about 20 MW, a value to be compared to the 2 GW that would be needed for an equivalent resistive system. In machine design, the factor of merit $\xi = R^2 \times B_t^3$ is a key driver of the machine performance with respect to the fusion power and the amplification factor Q. Here R is the major radius of the tokamak and B_t is the magnetic field at the plasma center. The selection of the two parameters R and B_t has to be made in close consideration of questions involving cost, available technology and accessibility to the plasma through the ports. To satisfy the objectives of ITER, the two parameters were set at $R = 6.2$ m and $B_t = 5.3$ T. Due to the toroidal shape, the magnetic field from the center of the plasma to the conductor on the magnet system is increased by a factor of more than 2, which clearly mandates the use of Nb_3Sn for the superconducting material of the toroidal field magnet system system.

The Cable-in-Conduit-Conductor

For the ITER coils, the requirements for high currents in the 70–80 kA range and for very high voltages in operation, 10 to 20 kV to ground for the poloidal field and central solenoid systems inherent in the size of the magnetic systems, led to the selection of the cable-in-conduit-conductor as the best choice for the conductors in the present state of the superconducting technology. Moreover this type of conductor is well adapted to support fast heat deposition. The principle of the CICC is not recent: M. Hoenig at MIT (US) introduced it in 1975 and a number of coils have been made with this type material, mainly in the US and in Japan as we have noted before. The coil with the largest size to use this concept to date was the Westinghouse coil in the Large Coil Task described above, where Nb_3Sn was the superconductor. The maximum performance of that magnet was unfortunately limited by some spreading out of a resistive phase in the magnet.

A modern CICC is basically made in several stages by cabling superconducting and copper strands and then by compacting the cable inside a conduit generally made of stainless steel. A CICC such as the one for ITER is composed of several components, superconducting strands, copper strands, steel bandages, one or more helium channels and the steel encasing conduit, as shown in Figure 12.30. In a project like ITER, the optimum composition of the conductor components is defined by the system design criteria.

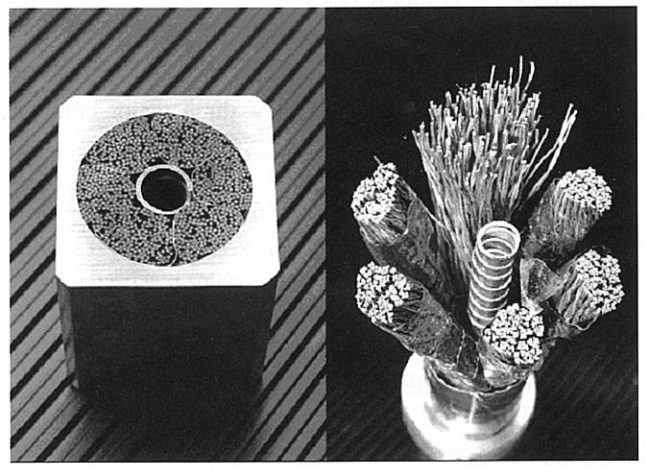

FIGURE 12.30: Conductors of the two ITER model coils. On the left CS model coil (51 mm × 51 mm, 40 kA) on the right an exploded view of the TF model coil (diameter 40.7 mm, 80 kA). (Courtesy ITER.)

The CICC was invented to benefit from the very high volumetric heat capacity of helium, about 500 times the volumetric heat capacity of metallic materials, thereby limiting the temperature excursions in the case of fast energy deposition. This occurs in tokamaks after a very fast decrease to zero of the plasma current when plasma disruption occurs. In this case, a fast magnetic field variation of the order of 100 ms affects the whole coil over lengths well over several meters, creating losses in the superconducting strands. This is rather similar to the kind of event which can occur in high field test facilities where the outer superconducting magnet of a hybrid magnet is affected when the central copper magnet disrupts. The cable in conduit offers an adequate solution to this problem by providing:

- a local helium reservoir,
- a very long wetted perimeter. The diameter of the ITER TF cable is 39.7 mm. It is made of 900 superconducting strands 0.82 mm in diameter with a void fraction in the cable of 30%. This fine subdivision of the strands can be translated into a total of 2.3 meters of wetted perimeter in the cable section facilitating a large heat transfer to the helium reservoir,
- small ac losses for the conductor by controlling its time constant through the contact resistance between strands.

Thanks to the high wetted perimeter, a large heat flux from the conductor to helium takes place during the transients, characterized by the thermal time constant of the CICC which is in the range of 50 ms, of the same order of magnitude as the time constant of the magnetic field variation caused by the disruption. The temperature excursion in the conductor is therefore limited and the conductor ability to withstand the transient is enhanced. During operation, the helium mass flow circulating in the conductor limits the temperature increase due to the residual nuclear heating and to the ac losses generated by the varying magnetic fields during a plasma discharge. The central channel helps to keep the pressure drop at an acceptable level. To date, the community of CICC users is rather small but the number of applications is increasing, each, with somewhat limited associated practical experience as an operational system. There are only four big systems currently in operation in the world: the poloidal field system of the 1999 Japanese Large Helical Device, the winding of the hybrid system at the National High Magnetic Field Laboratory in the US, and the conductors of two superconducting tokamaks: EAST and KSTAR.

The ITER Magnet System

The ITER magnetic field system[55] is composed of three major components shown in Figure 12.31.

- Toroidal Field system (TF)
- Central Solenoid (CS)
- Poloidal Field system (PF) and some correction coils (CC)

The TF system is made up of 18 coils. It provides the main magnetic field to confine the plasma charged particles. The 6 CS coils provide the inductive flux to ramp the plasma current and shape the plasma current.

The main characteristics of these systems are presented in Table 12.2.

The PF system is responsible for the stabilization and positioning of the plasma current. The TF system is a dc system while the PF and the CS systems are pulsed coils. Due to the moderate magnetic field of the PF system, the superconducting material selected for this system is NbTi. The

[55] N. Mitchell et al., *Fusion Engineering and Design* 84 (2009) 113

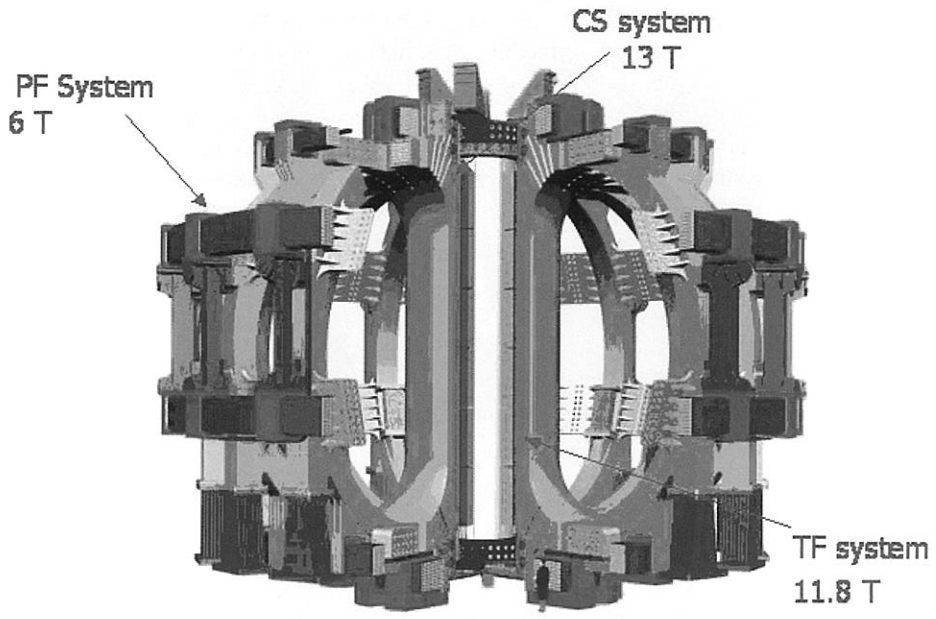

FIGURE 12.31: ITER superconducting systems. (Courtesy ITER.)

TABLE 12.2: Main Characteristics of the ITER Superconducting Systems

System	Energy (GJ)	Peak Field (T)	Total Ampere-Turns (MA)	Conductor Length (km)	Total Weight (t) (strand)
Toroidal Field, TF	41	11.8	164	82.2 Nb_3Sn	6540 (396)
Central Solenoid, CS	6.4	13	147	35.6 Nb_3Sn	974 (118)
Poloidal Field, PF	4	6	58.2	61.4 NbTi	2163 (224)
Correction Coils, CC		4.2	3.6	8.2 NbTi	85

multifilamentary composite is made of very fine filaments, 6 μm in diameter. Due to the high magnetic field (12-13 T), Nb_3Sn has been selected for the CS and the TF system. The total production of 514 tons of Nb_3Sn for ITER will mark the beginning of the industrialization of this superconducting material, the present production being in the range of a few tons per year. It should be emphasized that a very important internationally led project resulted in two model coils during the preparation phase of ITER (1997-2002). The two coils were designed, manufactured and tested as follows:

- A model coil of the central solenoid which was manufactured by the US and Japan and tested at the JAERI facility in Japan. This is illustrated in Figure 12.32. Japan, US and Europe shared the fabrication of the conductor.
- A model coil of the toroidal field system manufactured in Europe and tested at the FZK facility is shown in Figure 12.33.

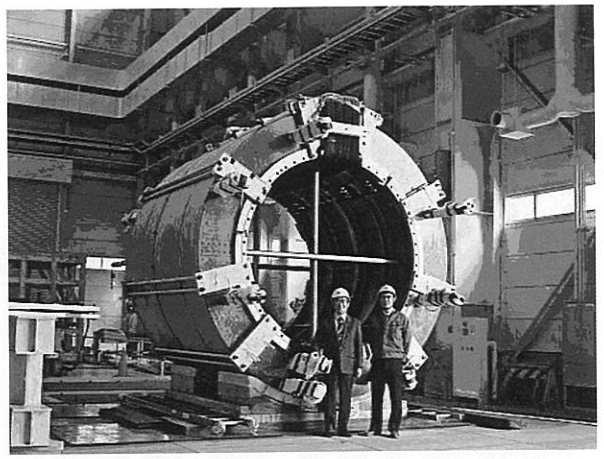

FIGURE 12.32: The outer module CS model coil of ITER at JAERI. (Courtesy ITER and JAERI, Japan.)

These model coil experiments during 2000 through 2002 were crucial in testing the behavior of large Nb_3Sn CICCs with actual dimensions and with the relevant lengths. Some unexpected degradation in the critical performance was found to be due to the great strain sensitivity of the Nb_3Sn strands. The strain is mainly due to the differential thermal contraction between the steel conduit and Nb_3Sn caused by the extreme temperature range between the reaction temperature of 650 °C at which Nb_3Sn is formed, and the cryogenic operating temperature. Some extra strain including bending strain was also indicated during the model coil experiments. This extra strain can be related to the Lorenz force loading the strands at the nominal current, very important findings leading to extensive discussions in the international community. The design of the ITER CICCs was later corrected to take these effects into account.

The CS model coil with a stored energy of 600 MJ was the first very large coil to be tested in a fast varying field related to the ITER operational conditions by discharging the magnet at the rate of 0.6 T/s without quenching. This high rate was made possible by the limited ac losses of the conductor. The successful series of tests effectively constitute a real milestone in applied superconductivity, confirming that the CICC is an appropriate choice for the ITER magnets.

The Construction of ITER

The organization responsible for the construction of ITER is objective and task specific. While the specifications of the various components are prepared by the central ITER organization, the individual components are ordered and constructed under the supervisions of the so-called domestic agencies, which are the seven ITER participants. The budgetary responsibilities of the seven parties to the project are in the form of in-kind contribution. Thus Europe is responsible for bringing contributions representing about 50% of the ITER cost investment. Six partners with the exception of India are involved in the delivery of conductors and magnets where the CICCs represent almost 50% of the magnet investment cost. The challenge is now in the hands of the companies and of the project teams: for example most contracts involving the conductors have already been placed. There is no doubt that quality assurance with all the controls and the acceptance tests will play a major role, it will have to be carried out at a global level, which in itself is another challenge. Again, this task is coordinated by the ITER organization.

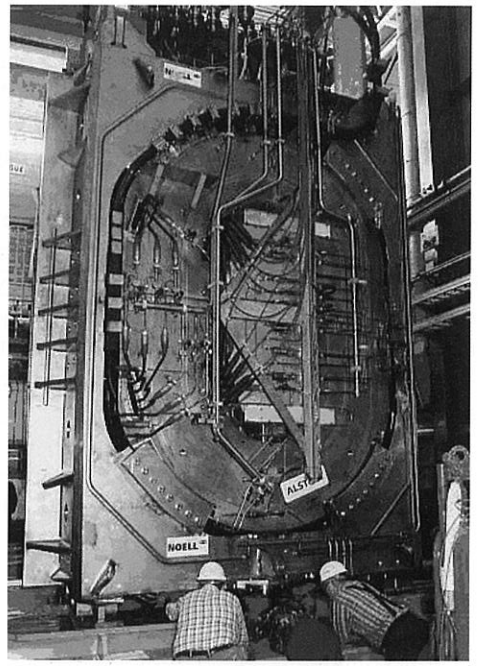

FIGURE 12.33: The TF model coil at the FZK test facility. (Courtesy Fz Karlsrake.)

Introducing DEMO

The next step after ITER will be DEMO[56], a fusion reactor that should provide 1000 MW of dc electrical power. Once ITER has delivered significant results, its anticipated construction could start, 20 years hence. Whether the DEMO magnet system will be an extrapolation of the ITER magnet system or whether a technological revolution will be needed, for example will the conventional NbTi and Nb_3Sn CICCs of ITER, operating at 5 K, be able to satisfy the technological specifications of the DEMO magnet systems or will it be necessary to use new, emerging superconducting materials operating at higher temperatures in the 20 to 50 K range are questions which will have to be answered through development programs yet to be defined. Necessarily the answers are not restricted to the applied superconductivity community only. The dimensioning of such a reactor and its optimization has to be found, in a manner similar to that of ITER, through a collaborative action involving scientists from all the disciplines. For an industrial plant on the scale of DEMO, the utilities will have to play a very strong participatory role in defining the constraints pertinent to dimensioning, construction, operation and maintenance.

JT-60SA Tokamak

Apart from the decisions related to the construction of ITER, an additional agreement between Europe and Japan was established, the so-called Broader Approach for Fusion Energy. This consists of 3 satellite facilities: IFERC, a computation center, a materials research facility, the IFMIF–EVEDA; and a superconducting tokamak JT-60SA[57], replacing the existing Japanese copper coil

[56] P. Komarek, *Fusion Engineering and Design* 81 (2006) 2287

[57] M. Mutsukawa et al., *Fusion Engineering and Design* 83 (2008) 795

tokamak operating in the short pulse, 5 s mode. This new machine will be installed in the existing tokamak hall at Naka in Japan. With a major radius of 2.95 m and a plasma current of 5.5 MA, its dimensions and plasma current are similar to those of JET but JT-60SA will not be a nuclear machine, that is it will not allow the injection of deuterium or tritium. By virtue of the superconducting magnets, the machine will be the largest superconducting tokamak capable of providing plasma discharges as long as 100 s. It is scheduled to operate in 2016. The JT-60SA program aims at supporting the ITER program and to complement ITER towards DEMO, the steady state demonstration reactor mentioned above. Europe will contribute to its construction to the tune of about 50% of the investment cost. Europe will supply an important part of the magnet system: the cryostat, the TF magnets, the power supplies, the HTS current leads and the cryogenic system for the whole magnet system. This activity is coordinated by Fusion For Energy, the cognizant European agency.

A comparison of the plasma dimensions of tokamaks under construction with those of existing installations is shown in Figure 12.34.

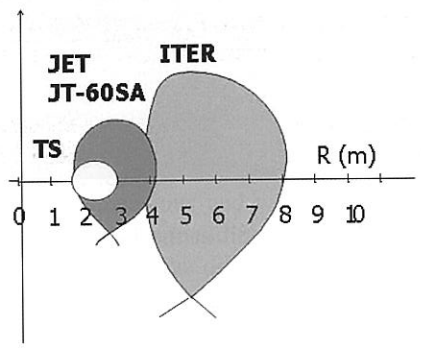

FIGURE 12.34: Plasma dimensions of superconducting tokamaks under construction, ITER, and JT-60SA compared with JET and Tore Supra (TS). (Courtesy ITER.)

Since 2006, much work has been devoted to the optimization of the toroidal field system, which is as always, the most important magnet component of the tokamak. This effort has resulted in important changes from the initial design of the conductor and of the magnet as well. The main characteristics of the JT-60SA TF system are summarized in Table 12.3.

The conductor of the TF system is also a CICC with no central channel and a moderate copper to NbTi ratio of about 2 in the superconducting strands. The winding pack is made of 6 double pancakes, each with 6 turns. A wedge-shaped inboard structure was adopted to allow space for segmentation of the central solenoid into several modules for better control of the plasma shape.

The expected behavior of the TF system has been analyzed in detail assuming normal operation taking into account the nuclear losses and the conductor ac losses. A substantial temperature margin of the conductor, 1.4 K at the end of burn, is a guarantee for safe operation and is adequate to prevent a disruption of the plasma at full current from quenching the coils. Before being shipped to Japan, the 18 coils of the TF magnet system will be tested in a cryogenic test facility, the construction of which has started at CEA, Cadarache.

TABLE 12.3: Main Characteristics of the JT-60SA TF Superconducting System

System	Energy (GJ)	Peak Field (T)	Conductor Current (kA)	Conductor Length (km)	Total Weight (t) (strand)
Toroidal Field TF	1.06	5.65	25.7	24.4 NbTi	280 (33.4)

12.4.7 Superconducting Magnets for Stellarator-Type Fusion Devices

The Large Helical Device

The National Institute for Fusion Science (NIFS) in Toki, Japan, has been working for many years on torsatron-type stellarators. In 1998 a sophisticated large machine, the Large Helical Device with a radius of 3.7 m and superconducting NbTi-coils became operational[58]. While the magnetic field strength is moderate, the construction of the helical coil was a major challenge for industry. It had to be done on site with the plasma vessel already in position, which required a specially designed winding machine. The different ring coils (several meters in diameter) were made with a forced flow cooled CCIC conductor. A view of the LHD during installation is shown in Figure 12.35.

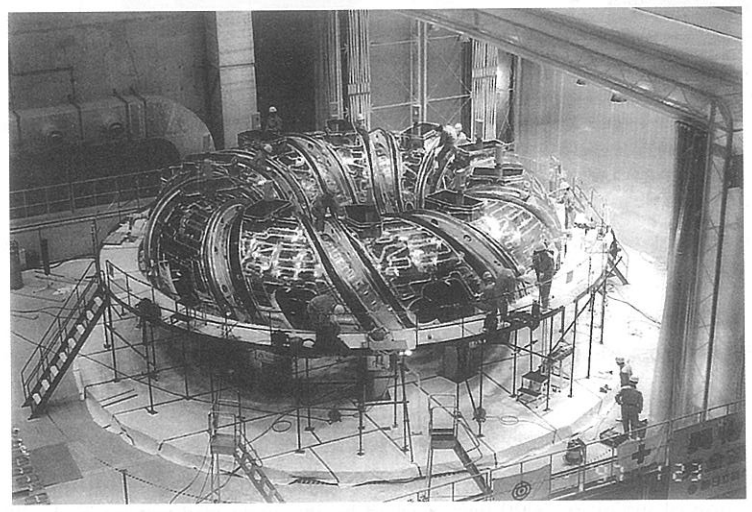

FIGURE 12.35: View of the LHD helical coil during installation at NIFS in Toki, Japan. (Courtesy of the National Institute for Fusion Science.)

[58] T. Satow et al., *IEEE Trans. Appl. Supercond.* 10 (2000) 600

The Modular Stellarator W7-X

A large modular stellarator with superconducting coils, W7-X, is under construction at the Greifswald branch of the Max Planck Institute for Plasmaphysics (IPP)[59]. This modular stellarator experiment of about JET size is a follow-up to the first modular system with copper coils, W7-AS, successfully operated at IPP in Garching in the 1980s. A set of nonplanar coils provide both the toroidal and poloidal field components to achieve the necessary twist of the magnetic field lines. The size of the machine and the potential of the stellarator in general for steady-state operation called for a superconducting confinement magnet system. In an extended development effort, the appropriate superconductor, the coil manufacture and the complicated cryostat were designed and engineered in the 1990s.

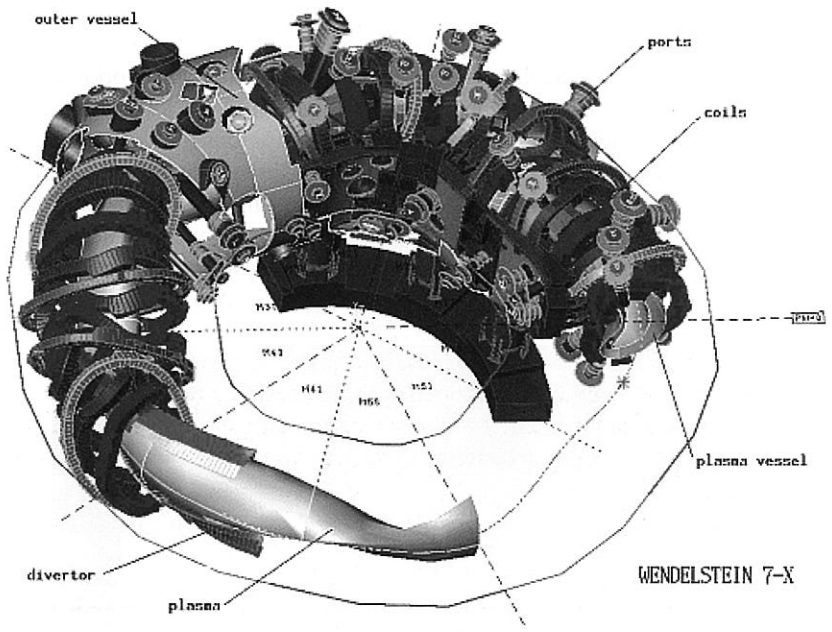

FIGURE 12.36: A representation of the W7-X coil system. (Courtesy of the Max Planck Institute.)

The ultimate goal of this program was the construction and testing of a full size demonstration coil, the completion of which in 1999 was marked by its successful testing in the TOSKA facility at KIT. The main parameters of the W7-X magnet system, illustrated in Figure 12.36, are a plasma major radius of 5.5 m and a magnetic field up to 6.7 T at the winding yielding a central field of 3 T on the plasma axis. This means that NbTi as superconductor is adequate. A set of five different types of nonplanar coils are periodically arranged in the torus. In addition, 20 superconducting planar coils are placed around the torus to follow the variation of the rotational transform of the plasma between the values 5/6 and 5/4 by modifying the main B field. Each nonplanar coil has a height of about 3.3 m, a width of 2.5 m and a depth of 1.5 m.

The superconductor is of the cable in conduit type with NbTi-strands. Due to the need to bend the superconductor through two axes the conduit material is a specially developed 6063 aluminum

[59] L. Wegener, *Fusion Engineering and Design* 84 (2009) 106

FIGURE 12.37: The W7-X coil system during installation at IPP in Greifswald. (Courtesy of the Max Planck Institute.)

alloy which is soft enough after co-extrusion with the bundle of strands to facilitate the winding work, but will be hardened afterward during the curing of the winding pack with its resin at about 1000 C and thereby achieve the necessary stiffness. Its dimensions are 16 x 16mm with 243 strands 0.58 mm in diameter with helium flowing through the voids between the strands. The rated current is 17.6 kA. The construction status in 2010 is well advanced, all coils have been manufactured and pre-tested at CEA Saclay by subcontract and installation in Greifswald is proceeding, as shown in Figure 12.37.

12.5 Electric Power Applications of Superconductivity

William Hassenzahl and Osami Tsukamoto

12.5.1 Introduction

The development of superconducting applications for the electric grid is driven by their promise of improved efficiency, smaller size, and reduced weight as compared to existing technologies, and by the possibility of new applications based on the unique characteristics of superconducting materials. Superconducting power components can also contribute to improved power quality and increased system reliability. This chapter addresses historical developments and technology status of five superconducting power applications: fault-current limiters, superconducting magnetic energy storage (SMES), rotating machinery, power cables, and transformers.

It is instructive to provide a simple description of an electric power system before exploring how superconductivity might contribute to its performance. Though there are several important exceptions, electricity is produced by a "generator", converted to an appropriately high voltage by a transformer, carried by a transmission line over long distances, transformed to a voltage that is appropriate for local distribution systems, carried to a local load by a distribution line or cable,

and finally used for a variety of purposes. Along the path, there are various elements, controls, and feedback systems that ensure the near-continuous operation of the power grid, even under upset conditions that may be short- or long-lived. Note: not all power applications involve a major utility grid: communities in remote areas operate power systems without ties to an extended power grid, large ships have significant electric power systems and may be driven by electric motors that connect directly to the propulsion system.

As mentioned above, there are exceptions that need mentioning. The "generator" is taken here to be a device that converts energy of some form into electric power. It can be a windmill, a gas or steam turbine, a solar cell, etc. These generators can produce ac or dc electricity. In addition, power may be transmitted either as ac or dc electricity, depending on a variety of factors. Transformers only operate on ac power and thus the use of dc requires modification of the process of taking power from the source to the user. Usually the choice of form of electricity used in any situation and any part of the grid is based on ease and efficiency of use and, ultimately, cost.

In principle, most of the conventional components of an electric power system could be replaced by a superconducting equivalent. However, the tremendous developments of conventional technology that have occurred over the past century—as a large fraction of the world has been electrified–have led to standard components that are effective, economical, and simple. These attributes combined with large-scale production deliver capabilities at low costs and provide a significant challenge to the introduction of any new technology.

As with most new concepts, when superconductivity was discovered in 1911, there was a rush by scientists to understand it—and an even greater rush by the power industry, by practical engineers, and by hucksters to capitalize on it. The early euphoria for practical applications was to be repeated over and over with each new breakthrough as the phenomenon was better understood and as materials with properties that seemed better or at least more practical were discovered. Though newspaper headlines at various times from 1911 through the 1950s suggested that superconductivity might have practical applications in the electric power arena, there was no real progress until the early 1960s. That was when practical Type II superconducting materials such as Nb-Ti and Nb_3Sn were discovered. Power applications such as motors, generators, and power cables were suggested early on. New concepts with no conventional equivalent, such as flux pumps for converting power and charging high current magnets, superconducting magnets for energy storage, and fault current limiters were soon to follow. However, developing superconducting systems with the same capability as existing conventional systems turned out to be a significant challenge. In addition, it was not until the last decade, that superconducting materials that could be used in practical devices had characteristics that allowed them to operate effectively above the temperature of liquid helium.

We mentioned above that the ability to carry large currents in the presence of magnetic fields is important for superconductors to be effective in most power applications. In fact, there are several characteristics that can make a superconductor an effective material. Most power applications have large alternating currents, the ability to carry these currents with low losses is critical because the losses occur at the operating temperature and must be removed by a refrigeration system that has a net efficiency of 1 to 10%. That is, the effective room temperature power loss is 10 to 100 times higher than the loss within the conductor itself. Perhaps the most important characteristic of large-scale power equipment is the need to operate at voltages of 100 kV or higher. These two enabling technologies, cryogenic refrigeration and cryogenic dielectrics have also seen rapid development in recent years.

However, considerable development and many full scale demonstrations will be needed before superconducting devices can be integrated into the utility environment. To date, most of these efforts are directly funded by government entities or have a great deal of government support. Initial commercial installations will be for niche applications and will be where space is limited, where power demands are increasing, and/or where initial development costs can be offset by enhanced performance.

Electricity as we use it is not available in a natural form. It must be converted from some other

source. By tracing the path of the energy, it is clear that only a fraction of the initial energy consumed is converted to electricity and that an even smaller fraction is delivered to the consumer. Most electricity is produced by converting heat to rotary mechanical motion that powers a three-phase electrical generator. Generators are typically 95% efficient or better in carrying out this conversion. However, the systems that convert thermal energy to mechanical energy are subject to thermodynamic limits, referred to as Carnot efficiency[60], and which is determined by the upper and lower temperatures of the process. Generally the efficiency of gas and steam turbines is in the range of 30 to 50%. Hydroelectric power generation is 85 to 90% efficient, so it is no surprise that Europe and the US use almost all the water resources available to produce electricity. In addition, many developing countries are building dams for power production. Wind and solar will eventually become important sources of electricity but, in the near term, they continue to have their own sets of barriers to large-scale implementation.

Once electrical energy is produced, it is converted to high voltage for transmission and then converted back to a voltage appropriate for the end user. About 10% of the electrical energy from the generator is lost in transformers and the transmission and distribution systems. Though this may seem to be a small fraction of the total, it is an enormous quantity of energy. Future technical improvements, including superconductivity, can hope to save only a portion of this 10%. There are, however, other drivers for new technologies. One is the ever increasing electricity use in urban settings, which, when combined with environmental and other requirements, requires greater power flow through existing right of ways. Another is the increased electrification of the planet earth. As we begin the 21st century, there are 6 billion people on the earth of which fully one-third do not have electric power. Electric systems are being expanded and new infrastructure will be developed to deliver power to a much larger fraction of humanity as the century progresses. Perhaps the most intriguing aspect of electric power systems vis-á-vis new technologies is the need for the assured delivery of high-quality power. For example, industrial processes such as the manufacture of silicon chips take several days to complete. Loss of power for a fraction of a second can result in the loss of one or more days of preparation and work.

The applications in which superconductivity has the potential to be effective in an electric power system can be separated into two general classes. The first class includes cables, motors, generators and transformers where superconductors replace resistive conductors. The second class includes technologies that will be enabled by superconductivity and that have little or at most limited capability if conventional materials are used. Examples are superconducting magnetic energy storage (SMES), fault current limiters (FCLs), and fault current controllers (FCCs). These technologies are addressed here, but other technologies, such as a superconducting substation[61,62] and an integrated power system in which liquid hydrogen is piped as a fuel and simultaneously functions as a coolant for superconducting cables,[63] are not discussed.

Rather than going into the rationale for use of superconducting applications in the power grid, we note that several earlier documents addressed the potential advantages of superconducting power equipment. Two articles[64,65] in the October, 2004 issue of the *Proceedings of the IEEE* described several power technologies. In 2000, several articles on power applications of superconductors were published in the May, June and August issues of the *Power Engineering Review* (*PER*), at the time the official journal of the IEEE Power Engineering Society. Prior to that time, an issue of the *IEEE Spectrum* (July, 1997) was dedicated to developments of HTS applications for electric power systems.

---

60 M. J. Moran and H. J. Shapiro, *Fundamentals of Engineering Thermodynamics* 5th ed., Wiley Text Books, (2003)
61 GuoMin Zhang et al., (Accepted for publication) *Proc. 2010 Appl. Supercond. Conf.*
62 W. V. Hassenzahl, EPRI Technical Report TR-1000915 (2000)
63 J. R. Bartlit et al., *Proc. Int. Cryogenic Eng. Conf.* (1972) 176
64 W. V. Hassenzahl et al., *Proc. IEEE* 92 (2004) 1655
65 S.S. Kalsi et al., ibid.

12.5.2 Fault-Current Limiters

Faults in transmission and distribution networks cause short-circuit currents that typically reach 10 to 50 times the rated current. These faults may be a temporary short between phases of a three-phase system, a short between one phase and ground, a lightning strike induced short, etc. They may be very short in duration, up to a few cycles, or of much longer duration. No matter the source or duration of the fault, each component of the grid must be designed to withstand the mechanical and thermal loads of the high current during the fault condition. As electrification expands, the number of power stations, other grid components, and interconnections on the existing system increase. The result is a reduction of the effective system impedance and generally greater power flow. Since the voltage is fixed, however, the lower impedance induces larger fault currents. It is not reasonable (nor economical) to replace older network elements just to deal with higher fault currents; thus, some method of limiting short-circuit currents is needed. In principle, an increase of the internal impedance of each element or inserting impedance in series with each element might accomplish this end. There are, however, two undesirable side effects of this type of solution. First, higher impedances usually cause increased energy loss, and second, fluctuating loads would cause greater feedback to control systems, which would decrease overall grid stability.

Today, the electric utilities either limit fault currents, typically by the use of inductors in low-voltage systems, or interrupt the fault current with special switchgear in high-voltage, high power systems. Nevertheless, all grid components are designed to accommodate the forces produced by the maximum current reached. The switchgear that is available on the high-voltage transmission grid is effective today. However, ever-increasing fault currents are pushing the limits of existing switchgear, which are near their theoretical maximum. A device having a small impedance during normal operation and the ability to develop a considerably higher impedance within a very short time (less than a quarter of an AC cycle) when a fault occurs could limit the short-circuit current to a reasonable value. Ideally, such a fault current limiter (FCL) would operate passively and would return to its normal operational mode immediately after the fault clears.

Several FCL development projects are underway, some of which are based on superconductivity, and others use silicon based switches. A discussion of the various locations where an FCL can be installed on a utility are discussed below, and then some of the existing programs are covered. It is of note that of all the superconducting power technologies, only one device has been purchased directly by a utility from a vendor with no government support. That device is a superconducting fault current limiter (SCFCL) fabricated by Nexans and installed at a substation in Boxberg, Germany.

Applications of Fault Current Limiters

In general, FCLs can be used at all voltage levels in utility grids, industrial systems, and isolated power systems such as large ships. The electric utilities have determined that there are several locations within the power grid where fault current limiters could be effective[64]. Eleven of these are shown in Figure 12.38. Specifications such as voltage, current, power, and response time, etc., depend on the location of the device in the network.

Some of the technical and economic benefits are listed in Table 12.4. They depend very much on the application itself, the structure of the FCL and the specific situation in the power system. As a general rule, the installation of SCFCLs seems most attractive in grids and power systems with rapidly increasing power demand, in heavy load areas, in highly meshed systems, and in locations where new generator units have to be introduced. Irrespective of the voltage level, the two main applications may be classified as coupling (3, 4, 5 and 11 in Figure 12.38) and feeder locations (1, 2, 6, 7, 8 and 10 in Figure 12.38). The main advantage of a coupling location is that the network impedance and the required short-circuit capability are reduced. The feeder location enables the reduction of short-circuit currents in the sources.

TABLE 12.4: Summary of Technical and Economic Benefits of SCFCLs

Technical benefits
- Reduction of high short-circuit currents during fault conditions
- Greater short-circuit capacity during normal operation
- Use of lower impedance (lower loss) transformers
- Improved power quality
- Increases steady-state and transient stability
- Greater flexibility in locating generation
Economic benefits
- Use of more compact devices of installations and devices
- Postponement of component upgrades
- Reduced network losses
- Increased availability
- Replacement of conventional devices

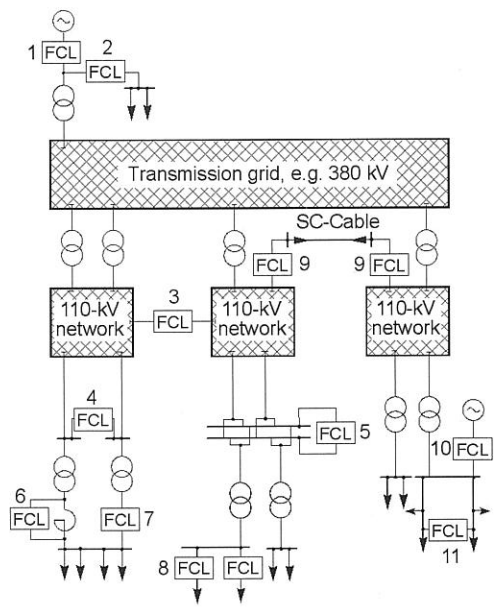

FIGURE 12.38: Locations for FCLs in power systems. (Figure from M. Noe, and P. Komarek.)

Types of SFCLs

Electric utilities, entrepreneurs, and research scientists are investigating a number of technologies in their search for a functional fault current limiter. Perhaps the most promising involve superconductivity because it can offer such a function by changing from "zero" resistivity to a high normal resistivity when either critical current, critical temperature, and/or critical field are exceeded. Several types of Superconducting Fault Current Limiters were proposed long before HTS materials

were discovered[66,67,68]. Some of those concepts have been developed further with HTS materials, while other concepts have come forward and appear to be effective at higher operating temperatures. There are several conceptually different types of FCLs[69,70,71,72,73,74,75]. Four concepts are summarized in Table 12.5 and are described briefly below. In addition, hundreds of patents exist for the technology.

TABLE 12.5: General Characteristics of Superconducting Fault Current Limiter Technologies

Technology	Losses	Triggering	Recovery	Size/Weight	Distortion
Resistive SFCL	Hysteretic (depends on HTS materials)	Passive	HTS conductor must be re-cooled	Potential to be small, because HTS performs limiting action	Only during first cycle
Hybrid Resistive SFCL	Hysteretic (depends on HTS materials)	Passive or Active	Faster than the resistive FCL because less energy is deposited in the HTS	Potential to be small, but additional components may increase size	Only during first cycle
Shielded-Core SFCL	Hysteretic (amount depends on HTS materials)	Passive	Faster than resistive, but re-cooling required	Large and heavy due to iron core and windings	Only during first cycle
Saturable-Core SFCL	Power to DC that saturates the iron core, Joule heating in copper coils	Passive	Immediate	Large and heavy due to iron core and conventional windings	Some; cause by nonlinear magnetic characteristics

Resistive and Hybrid SCFCLs

Figure 12.39 shows the principle of the resistive SCFCL and defines the quantities used here. The current limiting element has an appropriate quantity of superconducting wire, tape or bulk material, which is in parallel with a normal resistor R_p (e.g., a thin conductive sheet on the surface of the superconductor). The superconductor must be rapidly driven normal over its whole length by the fault current to avoid hot spots and for stability reasons. When the superconductor is normal, the

[66] R. T. Kampwirth and K. E. Gray, *IEEE Trans. Magn.* 17 (1981) 565
[67] J. D. Rogers et al., *IEEE Trans. Magn.* 19 (1983) 1051
[68] H. J. Boenig and D. A. Paice,*IEEE Trans. Magn.* 19 (1983) 1054
[69] W. V. Hassenzahl et al., *Proc. IEEE* 92 (2004) 1655
[70] L. Salasoo et al., *IEEE Trans. Appl. Supercond.* 5 (1995) 1079
[71] M. Noe and K.P. Jüngst, *Nachrichten des Forschungszentrums Karlsruhe* 31 (1999) 309
[72] M. Noe and B.R. Oswald, IEEE Trans. Appl. Supercond. 9 (1999) 1347
[73] M. Noe and M. Steurer, *Supercond. Sci. Technol.* 20 (2007) R15
[74] K. Hongesombut et al., *IEEE Trans Appl. Supercond.* 13 (2003) 1828
[75] Masaki Nagata et al., *IEEE Trans Appl. Supercond.* 11 (2001) 2489

parallel normal resistance causes a reduction of the superconductor current $i_{SC}(t)$ as

$$i_{sc}(t) = i_{initial}(t)\frac{R_p}{R_p + R_{SC}(t)} \tag{12.7}$$

The passive transition and current sharing with the normal resistor protects the power grid. Opening the conventional switch, S, after a time t is required to protect the SCFCL itself and to eventually restore grid operation.

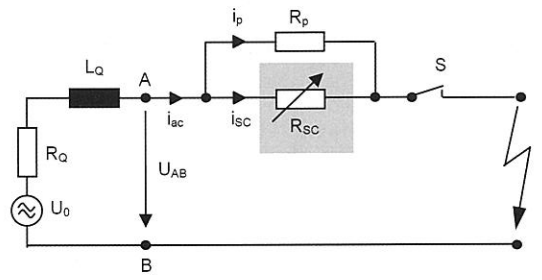

FIGURE 12.39: Schematic of a resistive SFFCL showing the superconductor as a variable resistance. There are several variations on this design that have been used by various manufacturers.

The hybrid resistive SFCLs include a separate, fast switch in series with the superconducting element. This switch quickly isolates the superconductor after most of the current has transitioned to the shunt element, thereby allowing the superconducting element to begin the recovery cycle while the limiting action is sustained by the shunt.

Inductive SCFCL

There are several types of inductive SCFCLs. The two most often considered are the "shielded core" design and the "saturable core" design. In the "shielded core" FCL, a superconducting coil and a conventional copper coil are wrapped around an iron yoke. During normal operation, transformer action causes the current in the superconductor to oppose the current in the copper coil. The flux from these two coils cancel and the iron yoke is essentially out of the circuit. When a fault occurs, the current in the superconductor increases and may exceed the critical current. The resistance of the superconductor causes its current to decrease so that it no longer shields the iron core. The impedance of the copper coil is now determined by the iron yoke. To be effective, this transition must occur in about a millisecond and, once the fault has cleared, the superconductor must recover while the FCL is under normal load.

Unlike resistive and shielded-core SFCLs, which rely on the quenching of superconductors to achieve increased impedance, saturable-core SFCLs utilize the dynamic behavior of the magnetic properties of iron to change the inductive reactance on the AC line. The concept utilizes an iron core, that is normally saturated by a DC superconducting coil, and an AC winding made of a conventional conductor. The conventional conductors are wrapped around the core and together form an impedance in series with the AC line. The system is designed so that at normal current levels, the iron is completely saturated and the conventional coil appears as a low-impedance air core reactor. When the current in the AC coils increase during a fault, the iron goes out of saturation, which increases the FCL's impedance. This change occurs in microseconds so that the core goes in and out of saturation twice during each cycle. The superconductor in this type of FCL does not quench so that there is no issue of recovery after a fault.

State of the Art SCFCL

There is ongoing development of several types of SCFCL. Tables 12.6 and 12.7 give a snapshot of many of the existing SCFCL projects.

TABLE 12.6: HTS SFCL Projects in the United States and Asia

Project	Avanti	AEP-TIDD	Puji	Korea
Location	Los Angeles, CA	Ohio	Kunming, China	Gochang, Junbuk Province
Site	Shandin Substation	TIDD Subtation	Puji Substation	Gochang Power Testing Center
Status	Operating at 13 kV	To be installed May 2011	Operating	Operation tests
Developer	Zenergy Power	Zenergy Power	Innopower	Consortium[76]
Utility/ Host	Southern California Edison (SCE)	AEP	Yunnan Electric Power Grid	KEPCO
Start Date	January 2009	July 2011	December 2007	TBD[3]
End Date	October 2010	October 2012	TBD	TBD
Type	Saturable Core	Saturable Core	Saturable Core	Hybrid Resistive
Phases	3	3	3	3

TABLE 12.7: SFCL Projects in Europe

Project	Nexans	Nexans	ATA
Location	Lancashire, UK	Boxberg, Germany	North Italy
Site	Bamber Bridge	Local Power Plant	San Dionigi Substation (MI)
Status	Operating	Operating	Fabrication of first prototype
Developer	Nexans	Nexans	ERSE Spa
Utility/ Host	Consortium[1]	Vattenfall Europe Generation AG	A2A Reti Elettriche Spa Group
Start Date	Fall 2009	Fall 2009	Early 2010
End Date	Mid 2010	Late 2010	End of 2011
Type	Resistive	Resistive	Resistive
Phases	3	3	3

Several SCFCLs have been installed on utility systems. Perhaps the most impressive is the resistive SFCL shown in Figure 12.40. It was constructed by Nexans and installed at a substation in Boxberg, Germany. Another FCL that saw nearly two years of operation on a utility grid is shown in Figure 12.41. It was constructed by Zenergy Corporation and was installed at the Avanti substation in California.

[76] Gochang Power Consortium

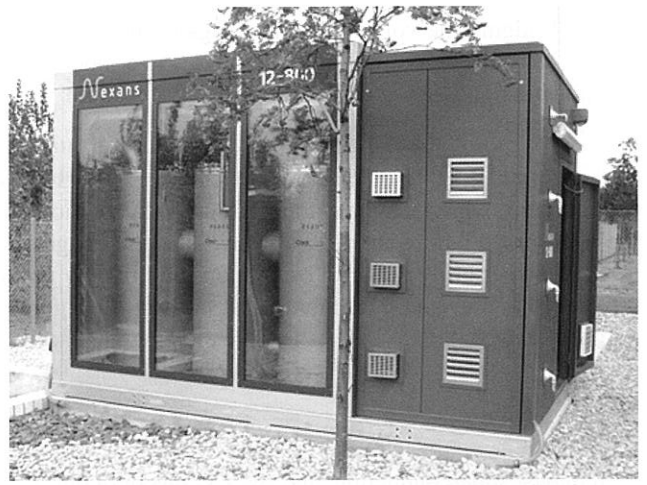

FIGURE 12.40: A resistive SCFCL constructed by Nexans and installed at the Boxberg substation. (Courtesy Nexans-Boxberg.)

FIGURE 12.41: A saturated core SCFCL constructed by Zenergy and installed at the Avanti substation. (Courtesy Zenergy Corporation.)

12.5.3 SMES

Efficient and reliable electric energy storage technologies have become more and more important in the past few decades. Superconducting magnetic energy storage (SMES) has the potential of becoming the most efficient of all energy storage systems, including the various kinds of batteries, flywheel energy storage, pumped-hydro, and capacitors. Furthermore, SMES has long calendar life, long cycle life, and a rapid response to power demands. Therefore, from a technical sense, SMES is an ideal storage system for electric utilities. SMES may be used by a utility in several application areas.

- Load leveling or arbitrage: for efficient use of power generation systems coping with diurnal demand fluctuations and also the non-dispatchable power generation of renewable energy systems such as solar and wind. Today, the most often used large-scale storage technology is pumped hydro. However, its efficiency is only 70–80%, whereas the efficiency of SMES is expected to be more than 90%. In addition, most of the effective sites for pumped hydro are already in use.

- Power quality (PQ): bridging the voltage dips and sags in the power grid. A voltage dip of only a few ac cycles can cause multimillion dollar losses to a modern factory, such as those that make semiconductors and electronic systems. PQ systems are very effective and often have short payback periods.

- System stability and spinning reserve: large-and extended power grids occasionally exhibit low frequency oscillations, which may lead to instabilities. In addition, loss of critical generation can induce widespread failure and lead to black outs. A storage system such as SMES can help stabilize the power grid to control oscillations and rapidly provide a reserve of energy "spinning reserve" to prevent a black out. Most large grids require power generators to maintain a certain percentage of capacity in the form of spinning reserve.

SMES System Design

Figure 12.42 is a simplified schematic of a SMES system. Key components are a superconducting magnet, a switch, which maybe superconducting, and AC/DC inverter/converter.

The magnet and the switch are maintained at an appropriate operating temperature. The energy stored in a magnet is given by:

$$W = \frac{LI^2}{2} \tag{12.8}$$

$$= \oint_V \frac{B^2}{2\mu_0} \mathrm{dV} \tag{12.9}$$

where the energy W is in Joules, the inductance L is in Henry s, current I is in amperes, the field B is in Tesla, and μ_0 is the permeability of free space. One can look at the first of these two formulations and conclude that there is a trade-off between inductance (or number of turns) and the current carried by the SMES coil. Looking at the second formulation, it is clear that for a given size and geometry, the higher the magnetic field, the greater the stored energy.

The magnet is charged and discharged from and to the AC power line, respectively, through the AC/DC inverter/converter, which is often referred to as a power conditioning system (PCS). If the switch is superconducting rather than a normal conductor, the device is more efficient. However, the response time of the system is much longer than is acceptable for either PQ or stability applications.

In other energy storage systems such as batteries, flywheels, and pumped-hydro, the electric energy is converted to chemical, kinetic and potential energy, respectively, and the conversion of the energy inevitably involves losses. In SMES, electric energy is stored directly in the form of electricity in the superconducting magnet, which has very low loss. Intrinsically, SMES is quite efficient and has the ability to respond within less than an AC cycle to demands from a power controller.

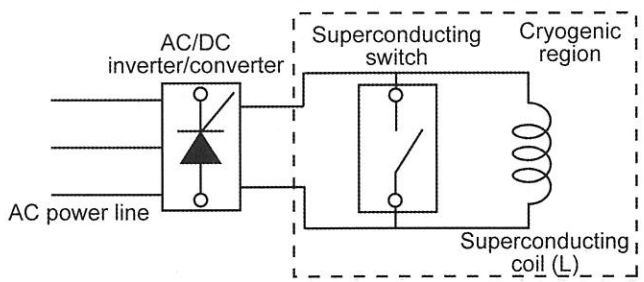

FIGURE 12.42: Simplified SMES schematic.

History of SMES

The concept of using SMES on a utility grid to level diurnal power demand variations was proposed in France in 1969 [77]. Feasibility studies of a large-scale SMES as an alternative to pumped-hydro were conducted in the early 1970s by several institutions[78,79]. These designs were based on large-scale superconducting magnet and semiconductor switching device technologies that saw great strides in 1960–1970.

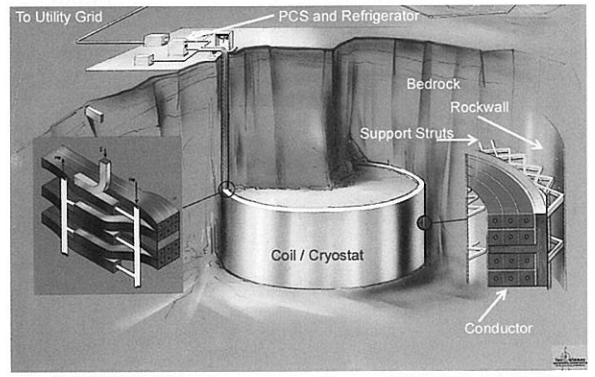

FIGURE 12.43: Large-scale SMES plant constructed underground. (Courtesy Los Alamos Laboratory.)

Figure 12.43 shows one concept of a large SMES plant constructed underground. This device stores several thousand MWh of energy. The diameter of the superconducting solenoid magnet depends on the operating field and is ≈200 m. Internal structures to support the electromagnetic force in the magnet are unacceptably costly in a magnet of this size. Therefore, it was determined that bedrock structure was required. The magnet is installed in an underground tunnel and the magnetic force is transmitted to the surface of the rock wall. The magnet is placed more than 100 m below the earth's surface, to use the structural capabilities of hard rock and to reduce the magnetic field at the surface. The technical feasibility of that type of SMES was demonstrated, but, at the time, its cost was determined to be too high for practical development.

A different and more realistic application of SMES was proposed by Los Alamos and the Bonneville Power Administration in 1976 [80]. Its purpose was to stabilize a specific instability that occurred in the 900 mile long Pacific Power Corridor from near Seattle to Southern California. A 30 MJ coil, Figure 12.44, coupled to the grid with a 10 MW PCS, was constructed and installed at the Tacoma substation south of Seattle in the early 1980s [81]. Following this project, some other projects were conducted, mostly in the US and Japan. However, those projects showed that, except in specific niche markets, the economic merits of even medium-scale SMES were very limited. A summary of the status of SMES late in the 1980s is described in Hassenzahl[82].

Near the end of the 1980s, business development and research efforts were started on small or mi-

[77] M. Ferrier, *Low Temperature and Electric Power* (1970) 425
[78] W.V Hassenzahl, *IEEE Trans. Magn.* 11 (1975) 482
[79] R. W. Boom et al., ibid. 475
[80] L Cresap (BPA), W. Hassenzahl (LASL), private communication
[81] E. Hoffman et al., *IEEE Trans. Magn.*, 17 (1981) 521
[82] W. V. Hassenzahl, *IEEE Trans. Magn.* 25 (1989) 750

cro SMES devices that stored up to several MJ for a variety of applications in the PQ area, including compensation of load fluctuations of factories and military applications. Superconductor Inc. (later purchased by American Superconductor Corporation: AMSC) developed micro SMES storing about 1 MJ and coupled to the power system by modern motor drive electronics with a power capacity of 430 kVA. These devices were functional in terms of reducing voltage sags in the power line, particularly those associated with overload power conditions. The complete microSMES system including refrigerator and converter was installed in a transportable semitrailer. The effectiveness of this micro SMES was verified at several sites.

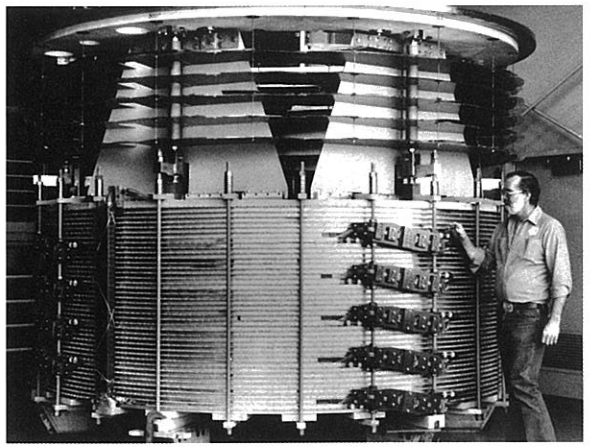

FIGURE 12.44: The 30 MJ coil constructed for installation on the BPA power grid. (Courtesy by Alamos National Laboratory.)

Also in the mid1980s, utilities in Japan became interested in SMES because the diurnal load variation was increasing as overall demand grew rapidly. SMES was expected also in Japan to be promising as a technology to shave the peak demand and stabilize the utility grid. In this situation, the national project of SMES was established by the Ministry of Economy, Trade and Industry (METI) and New Energy Development Organization (NEDO) in 1991. Much of the recent work on SMES has been carried out as Phase I-IV SMES projects. In addition, several small SMES systems have been constructed in Korea, China, Australia, and Europe.

In phase III of the METI and NEDO SMES project (Japanese fiscal years 2004–2008), a multipurpose 20 MVA SMES for utility grid use was developed using Nb-Ti conductors cooled by liquid helium at 4.2 K based on the R&D results of the phase I and II projects. The SMES was installed in a copper refinery that experienced considerable power fluctuations. It interfaced with the refinery and the power grid. In this project, the load fluctuation caused by the refinery was suppressed (note that the 30 MJ BPA SMES was placed adjacent to an aluminum refinery for the same reason, but was never used for that purpose). Chubu Electric Power Company and Toshiba developed and installed a 5 MVA (later increased to 10 MVA) SMES in a modern LED panel factory to compensate voltage dips in the utility grid in 2003[83] (Figure 12.45). The four-pole configuration was used for the SMES coil to reduce stray magnetic flux. This device is still in operation.

The biggest issue at present in SMES technology has to do with the potential impact of HTS materials. The advantage will be operating at temperatures above those available with liquid helium.

[83] S. Nagaya et al., *IEEE Trans. Appl. Supercond.* 14 (2004) 699

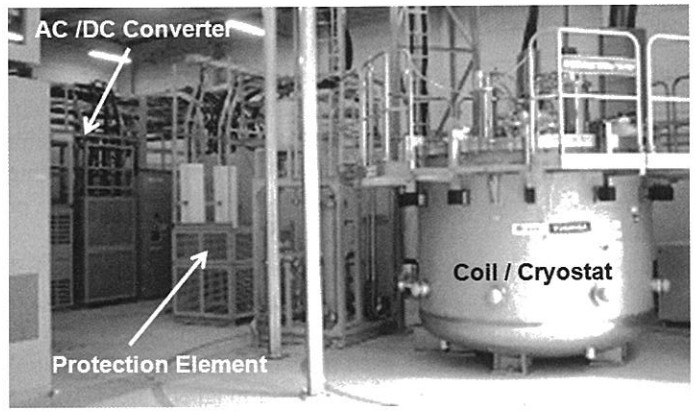

FIGURE 12.45: SMES installed in the LED factory. (Courtesy of Chubu Electric Power Company.)

HTS coated conductors (CCs) technology has progressed remarkably and these materials are now becoming commercially available. In the near future, fabricating a SMES coil wound of CCs will be possible. Critical current density of CCs at 20 K is much higher at fields above 10 T than that of low temperature superconductor wires (LTS wires) made of Nb-Ti and Nb_3Sn at 4.2 K. Because of the backing material, the mechanical strength of CCs is greater than those of LTS wires. As a result, a high field and thus compact coil operated at $\approx$ 20 K can be made using CCs. The disadvantage of CCs today is cost. To be economically competitive in a SMES device, the conductor cost must drop to 10 or 20 \$/kAm at 20 k and 10 T. The likelihood of reaching this target in the near future is small. However, the potential merit of a compact CC based coil is obvious as shown in Figure 12.46. Some effort is underway to build SMES devices with HTS materials.

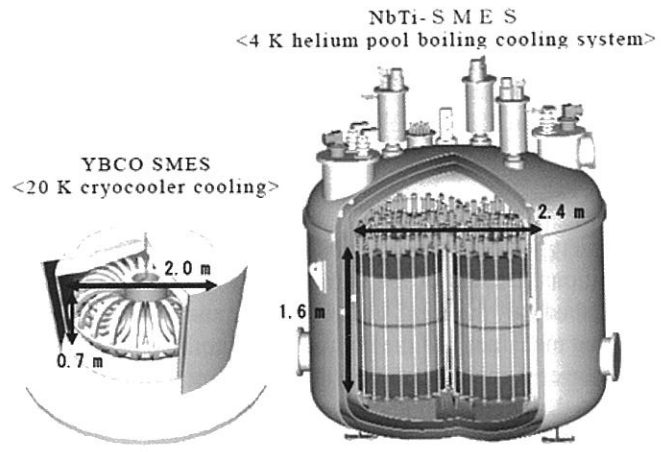

FIGURE 12.46: Comparison of HTS CC coil and NbTi LTS coil for 20 MJ class SMES. (Courtesy Los Alamos National Laboratory.)

12.5.4 Superconducting Rotating Machines

Three types of rotating machines are used in power applications. The two most generally used are generators and motors. In addition, synchronous condensers, which are much like generators in design, are used for a few special applications. The key to the effective implementation of superconducting machines is the very high magnetic flux density delivered by the high current density available in superconductors. Today superconducting motors and generators are progressing rapidly to commercial scale in a variety of areas using HTS materials.

Because superconductors have losses when carrying alternating currents or when exposed to varying magnetic fields, the preponderance of superconducting machines use superconductors in configurations where both current and magnetic field are nearly constant. There are various ways to build generators and motors. By far, the geometry used most often, for both conventional and superconducting machines, has a coil on the rotor that produces a magnetic field. However, this geometry requires cryogenic cooling on the rotor, which presents thermodynamic challenges to the designer.

It was clear early on that the higher magnetic field would, for a given size, increase the available torque between the rotor and stator, and thus allow superconducting machines to be smaller and lighter than conventional machines. Thus, work on superconducting machines began soon after the discovery of Nb-Ti and $Nb3_Sn$ in the early 1960s. All of these early machines were limited by the need to use liquid helium as a coolant. However, the early work on these machines and the lessons learned have contributed greatly to recent machine development using HTS materials. An early observation, which remains true today, was that to be effective and economically competitive a superconducting machine must operate near practical design limits in many areas, which encompass, though not necessarily exclusively, the parameters listed in Table 12.8.

TABLE 12.8: Design Considerations for Superconducting Rotating Machines

Design Requirements	
Magnetic field	Efficiency
Mechanical stress	Electric stress
Internal impedance	Mechanical stiffness
Cryogenic cooling	Normal cooling
Superconductor	Stabilizer

Several different machine types were chosen as likely to be most successful with superconductors for electric power applications. Details of the various early designs and construction of different machines have been published in[84,85,86,87,88]. However, the most effective designs, then and now are the synchronous rotating machines and the homopolar motor. Homopolar generators can also be effective, but rectified ac power in many ways provides a more controllable source of direct current. Some of the early machines that were built and tested are shown in Table 12.9.

During the 1970s the main approach for superconducting generators was to build very large machines that would match the capabilities of anticipated very large nuclear reactors. These would be

[84] H. H. Woodson et al., *IEEE Trans. Power App. Syst.* PAS-85 (1966)
[85] A. Atherton, *Proc 1972 Appl. Supercond. Conf.* (1972) 16
[86] J. L. Smith et al., *IEEE Transa. Magn.*, 11 (1975) 129
[87] H. O. Stevens et al., *IEEE Trans. Magn.* 13 (1977) 269
[88] C. E. Oberly, ibid. 260

TABLE 12.9: Early, Low Temperature Rotating Machines

Description	Power	Group	Date
Homopolar disk solid brushes	50 hp	IRD England	1966
Homopolar liquid brushes	1000 hp	NSRDC USA	1972
Homopolar disk solid brushes	3 MW	Toshiba Japan	1973
AC Synchronous Rotating field	2 MVA	MIT USA	1973
AC Synchronous Rotating field	5 MVA	Westinghouse	1973
AC Synchronous Rotating field	1 MVA	Leningrad USSR	1973

in the 1GW range, which, if conventional, would often exceed the capacity of rail and road transportation systems in the US. The apparent advantages of superconducting generators in the GW range were lower weight and smaller footprint, which allowed for easier transportation and a slight increase in efficiency. Several programs addressed the design of these large generators, the most interesting of these in the US were carried out by Westinghouse, General Electric, and MIT, all under the support of the Electric Power Research Institute[89]. These programs continued for several years and led to the development of conceptual designs and prototypes. However, the effort on these generators ended when large nuclear power plants went out of favor. The development of homopolar motors and generators continued through the early 1980s [90]. In 1980, the US Navy installed a 300 kW superconducting homopolar generator and a 400 hp superconducting homopolar motor on the naval ship Jupiter II, making it the first naval vessel to be propelled completely by superconductivity. In 1983 the Jupiter II drive system was upgraded by installing a conventional ac generator and a rectifier, which powered a 3000 hp homopolar motor[91]. This ship was stationed at the Baltimore harbor for viewing during the 1986 Applied Superconductivity Conference.

In 1987 Japan began a program to build a superconducting generator in the 200 MW range with a possible extension to 600 MW. The intention was to have modular generators that would in combination exceed 1 GVA, but which could also be used with smaller nuclear plants, and possibly with conventional thermal plants. Besides the advantages discussed earlier, superconducting generators intrinsically have a small internal synchronous reactance, which is effective for control of system voltages. They can also be designed to have more rapid response to demands than conventional generators because of the reduced inertia. The Japanese program was called "Super-GM project", and was reorganized by NEDO in 1991 and supported by MITI as a part of Japan's New Sunshine Project. Several rotors were constructed with LTS field windings and were tested in a grid environment. A 70 MW class model generator was operated for more than 1500 h in the Osaka power station. A thorough description of the results of the Super-GM project is described in 9 papers in the 2002 issue of Cryogenics. Nitta[92] is the first paper of the set. Figure 12.47 shows the field test installation of one of the Super-GM generators.

With the discovery of high-temperature superconductors in 1986, several programs were initiated to use these new materials in rotating machines. A great deal of effort has gone into HTS materials development over the past 25 years. One result of that work is that today these materials have the capabilities that will allow the development of commercially viable superconducting rotating machines. However, the key breakthrough is the ability to design and build high power density, highly efficient machines that can operate at 30–40 K. These machines use conduction cooled coils

[89] Mario Rabinowitz, ibid. 255
[90] A. Arkkio et al., *IEEE Trans. Magn.* 17 (1981) 900
[91] M. Superczynski, *IEEE Tran. Magn.*23 (1987) 348
[92] Tanzo Nitta, *Cryogenics* 42 (2002) 151

FIGURE 12.47: A Super-GM 70 MVA generator under field test at the Osaka Power Station. (Courtesy OEPCO.)

and can operate with standard Gifford-McMahon cryocoolers. A summary of the state of the art of rotating electrical machines in 2004 and some of the details and history noted above are available in Kalsi et al.[93]

One of the most widely used superconducting rotating machine topologies is an air-core topology illustrated schematically in Figure 12.48. The field winding is mounted on a metallic rotor that is nonmagnetic (hence the term "air core") and consists of several coils (poles) that are conduction-cooled through the support structure.

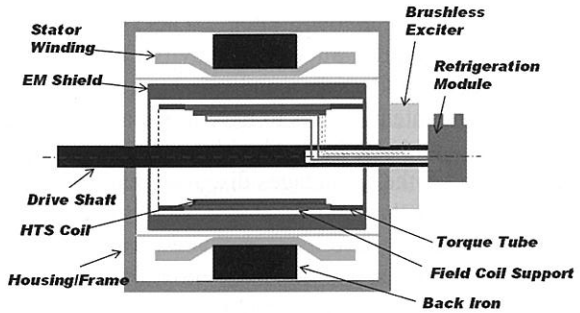

FIGURE 12.48: Air-core electric machine topology.

The primary components of the rotor assembly are as follows:

- HTS field winding operating at 30–40 K
- Rotor support structure
- Cooling loop
- External cryocooler module connected to the motor's cooling loop at the non-drive end of the shaft through a rotating coupling
- Room-temperature electromagnetic shield

[93] S.S. Kalsi et al., *Proce. IEEE* 92 (2004) 1675

- Torque tube for transferring torque from the "cold" (cryogenically-cooled) environment to the "warm" shaft ends.

The superconducting field winding is an assembly containing multiple polesets, each fabricated using wire that is designed to withstand the magnetic and mechanical forces experienced in the rotor. The polesets are attached to a metallic support structure on the rotor which provides support against centrifugal and torsional loading. The flux pattern is shown in Figure 12.49.

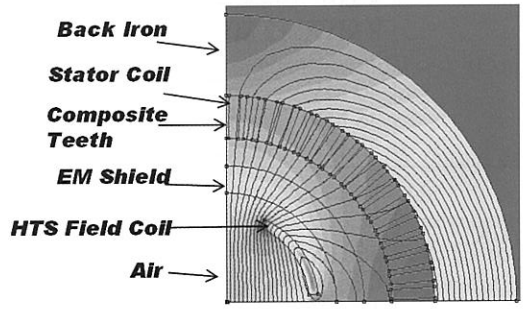

FIGURE 12.49: Flux distribution in an "air-core" electric machine topology; note the use of non-magnetic teeth in the stator.

The polesets and support structure are enclosed in a vacuum-sealed cryostat that minimizes radiant heat input and provides the insulated operating environment required by the HTS field coils. An electromagnetic (EM) shield, which is located at the outside surface of the cryostat, reduces losses in the field winding by attenuating field variations caused by the stator winding. It also carries a high transient torque during a fault, and provides damping for low-frequency torsional oscillations, negative sequence currents and any other harmonic currents generated by a variable-frequency drive.

An alternative design, Figure 12.50, uses an iron core in the rotor and magnetic teeth in the stator. Though fully saturated, the iron core nevertheless increases the flux density at the stator, and thus contributes to some additional reduction in footprint.

In addition to the synchronous machines, work continues on homopolar motors. They have somewhat limited interest because of need for brush contacts that must carry very high currents.

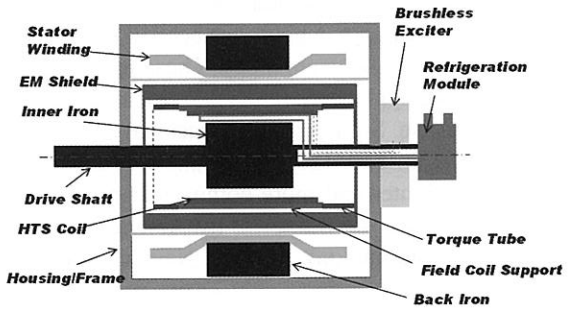

FIGURE 12.50: Machine topology with rotor iron.

An impressive array of superconducting machines has been constructed and demonstrated during the last decade, as summarized in Table 12.10. As a result, they appear to be one of the most promising applications of superconductivity.

TABLE 12.10: Recent HTS Machine Developments

Manufacturer	Machine	Timeline
AMSC (US)	5 MW demonstration motor	2004
	8 MVA, 12 MVA synchronous condenser	2005/2006
	40 MVA generator design study	2006
	36 MW ship propulsion motor	2008
	8 MW wind generator design study	2010
Converteam (UK)	200 kW demonstrator	2006
	1.25 MVA hydro generator	2008
	500 kW demo-generator	2008
	8 MW wind generator design study	2010
Dooson, KERI (Korea)	1 MVA demonstration generator	2007
	5 MW motor (homopolar)	2010
GE (US)	100 MVA utility generator	2006 (discontinued)
	5 MVA homopolar induction motor	2008
LEI (US)	5 MVA high speed generator	2006
Reliance Electric (US)	10.5 MVA generator design study	2008
IHI Marine, SEI (JP)	265 kW ship propeller motor	2010
	2.5 MW ship propeller motor	2010
Siemens (Germany)	400 kW demonstration motor	2001
	4 MVA industrial generator	2005
	4 MW ship propeller motor	2000

Several programs around the world are addressing HTS motors. A 1 MW HTS motor by KERI and Doosan Heavy Industries has been developed under the Korean DAPAS program. In addition to radial flux type HTS machines, a Japanese team including Sumitomo Electric and IHI finished the development of a 365 kW axial flux type HTS motor cooled by liquid nitrogen.

Perhaps the greatest progress in rotating machines has been in the area of ship propulsion motors using HTS based, air-core synchronous AC technology. These motors offer significant benefits for both naval and commercial shipping applications[93,94,95,96], including high power density, high efficiency and low structure-borne noise. Significant advances have been supported by the US Navy in the area of propulsion motors with 120–150 revolutions/min and ratings above 30 MW. HTS technology can be 2.5 to 5 times lighter and more compact than conventional technology in this size range. After a series of early motor development by American Superconductor (AMSC) and Reliance Electric (later Rockwell Automation), the U.S. Navy's Office of Naval Research (ONR)

[94] Kalsi S et al., Naval Symposium on Electric Machines, Philadelphia, PA (2000)

[95] Eckels P and Snitcher G, Naval Symposium on Electric Machines, Philadelphia, PA (2004)

[96] Weeber K K et al., *IEEE 2003 Power Engineering Society Annual Meeting*, Emerging Technologies Panel Session, Toronto, ON, (2003)

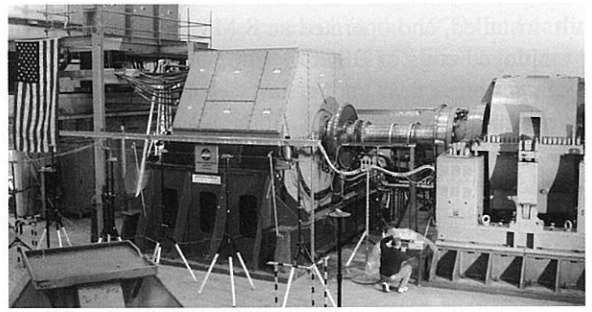

FIGURE 12.51: A 36 MVA, HTS synchronous motor under test. (Courtesy US Navy, ONR.)

funded AMSC and Alstom (now Converteam) to build a 5 MW output power, 230 r/min propulsion motor to validate technologies for larger ship propulsion motors.

Based on this success, the ONR funded a full-scale 36 MVA advanced technology demonstrator, a successful program now representing the state-of-the-art in HTS rotating machinery; see Figure 12.51. The motor has an output shaft speed of 120 rpm and generates over 2.9 million Newton-meters (2.2 million ft-lbs) of torque. The development team was led by American Superconductor (AMSC) as prime contractor, with Northrop Grumman, Electric Machinery, Inc., BMT-Syntek, and CAPS. The motor's design characteristics were achieved or exceeded as shown in Table 12.11.

TABLE 12.11: Characteristics of 36 MVA Motor Developed for the US Navy

Parameter	Design	Measured
Design Power	37.2 MW	> 37.2 MW
Voltage	5.8 kV	6.6 kV
Current	1.275 kA	1.28 kA
Efficiency	97 %	97 %

Siemens has designed, manufactured and tested a series of HTS synchronous machines, including, a generator for marine application rated 4 MVA at 60 Hz and 3600 rpm. The company carried out the first-ever synchronization of an HTS generator onto the grid in 2005. The rotor consisted of HTS pancake coils manufactured from 1G HTS wire from what is now Bruker HTS. Zenergy Power and Converteam have announced a project to build a 1.25 MW hydrogenerator.

Another significant development is the recognition that compact, lightweight HTS generators can enable 10 MW-class generators for offshore wind turbines. Programs towards this goal have been launched by Converteam, AMSC in collaboration with TECO-Westinghouse, and by the Danish Technical University in collaboration with Denmark's Riso National Laboratory.

A different design concept is used for a development carried out by General Electric for a 5 MW high rotational speed generator supported by the US Air Force. Here, a homopolar design concept uses a stationary HTS winding that excites the machine's rotor iron. KERI and Doosan Heavy Industries have also announced plans to explore this idea.

As mentioned early in this section, another application of rotating machine technology is the synchronous condenser, which is essentially a generator without a power source. It provides reactive, out-of-phase power (MVAR) rather than real, in-phase power (MVA). AMSC and Tennessee Valley

Authority designed, built, installed, and operated an 8 MVAR 13.8 kV dynamic synchronous condenser[97]. The machine employed coils of BSCCO wire, an inner iron topology, and a liquid neon cooling loop. The unit was installed near an arc furnace of the Hoeganaes steel plant in Gallatin, Tennessee. It began grid operation on October 10, 2004, was brought into regular operation in January 2005 and operated until November 2005. In practice, it reduced voltage flicker in the area that was caused by the arc furnace.

At the Hoeganaes site, transient disturbance+489s occurred during the 30 minutes to 1 hour melt cycles in the arc furnace at 1 hour intervals. With active changes in reactance during each melt cycle, the unit experienced an enormous number of reactive events—of order 5 million—during the year. While certain peripheral equipment required maintenance during this period, the rotating machine itself performed very successfully in what must be considered one of the most rigorous in-site tests of HTS equipment to date. In spite of this success, utility needs are for much larger, 50 MVAR machines; so further development is required for a commercial entry point. In summary, although superconductor rotating machinery has not yet entered the commercial realm, the technology based on HTS wire is well developed, and the prospects look bright for commercialization in a variety of applications.

12.5.5 Superconducting Cables

Power transmission and distribution by cables as compared to overhead lines has developed for a variety of reasons. The most important are right-of-way and environmental considerations. Power use per square meter in high population areas where there is limited space, such as city centers, and where there is need for vehicle and pedestrian access is providing an ever-increasing demand for underground power cables. The key to the effectiveness of cables compared to lines in air is that the voltage breakdown capability (V/m) of the insulators used for cables is 100 to 1000 times better than air. Thus, the power flow along underground cables in a restricted corridor can be considerably greater than is possible with overhead lines. In addition, as designed, the stray electric field from an underground cable is negligible. The rationale for various conventional cable designs and the development thereof are described in detail in the EPRI publication referred to as the Green Book[98]. Superconducting cables appear to provide an even greater power density than conventional cables. Thus, just as conventional cables have been used to increase power flow in specific corridors and right-of-ways, in the not-too-distant future, superconducting cables will replace both overhead lines and conventional cables.

As with other applications, superconducting power cables were considered for development with each new development. At present, both ac and dc superconducting power cables appear promising for future installations. Below, after a brief description of the history of the various efforts on superconducting cables, some of the existing programs will be described.

Serious development on superconducting cables began in the late 1960s after Nb-Ti and Nb_3Sn became available on a near commercial scale. Early work using low temperature superconductors began in Europe[99,100,101] and later in the US[102,103,104] and Russia[105]. Significant development programs existed for ac and dc superconducting cables. These programs addressed the significant issues

[97] S. S. Kalsi et al., *IEEE Trans. Appl. Supercond.* 15 (2005) 2146
[98] *Underground Transmission Systems Reference Book*, EPRI product number 1012334 (2006)
[99] P. Klaudy, *Adv. Cryogenic Eng.* 11 (1967) 684
[100] P. Klaudy et al., *IEEE Trans. Magn.* 17 (1981) 153
[101] F. Moisson and J. M. Leroux, *J. Appl. Phys.* 42 (1971) 154
[102] H. M. Long and J. Nottaro, ibid. 155
[103] E.B. Forsyth and R.A. Thomas, *Cryogenics* 26 (1986) 599
[104] H. L. Laquer et al., *IEEE Trans. Magn. Mag*-17 (1977) 182
[105] P. I. Dolgosheyev et al., *IEEE Trans. Magn. Mag*-15 (1979) 150

of superconducting cable technology and the research in the 1970s and early 1980s is generally applicable to many of the technical issues associated with HTS power cables today.

Perhaps the largest LTS power cable effort was in the US, which included the ac cable program at BNL[103] and the dc cable program at LASL[104]. These programs addressed very different issues associated with electric power. The ac cable effort explored a variety of issues associated with relatively short, multi-kilometer systems, while the dc cable effort was directed to very high power, long distance transmission systems. The latter had been proposed by Garwin and Matisoo[106] in 1967 as a means to transmit power from collections of massive electricity generators, e.g., nuclear power farms or hydroelectric dams to distant load centers.

These LTS cable projects were abandoned, for several reasons.

- In 1973, OPEC established an oil embargo that led to greater conservation efforts and the growth rate of electric power decreased to almost zero for several years.
- Nuclear plants went into disfavor and their costs and construction time, with environmental add-ons, made their profitability less certain.
- The operating temperature of LTS systems is so low that refrigerator size and efficiency impact the overall economics, limiting their attractiveness to only the very highest power capacities.
- The diameter of the cryostat for LTS cables is significantly larger than the existing ducts in use for many conventional cables, so they could not be simple retrofits that upgraded power flow at many sites.

The discovery of high-temperature superconductors in 1986 sparked renewed interest in superconducting power cables. HTS based power cables have significantly lower refrigeration requirements than LTS based cables. Thus, capital and operating costs for this component are less. However, today, and for the foreseeable future, the cost for HTS conductors is significantly higher than that of LTS conductors, which offsets the refrigeration advantages. In addition, today, HTS materials are more difficult to make in a form suitable for power cables. On the other hand, since the energy required to power the refrigeration equipment affects the overall efficiency of the system, HTS cables, both ac and dc, are more efficient than either an LTS or a conventional cable. In the near term, it appears that HTS ac cables can be effective at relatively low power levels, 10 to 100s of megawatts that are needed in urban and suburban environments. HTS dc cables appear to be more likely for very high power, long distance power transmission.

Power cables and transmission lines are designed to operate at a fixed voltage while instantaneous power flow is determined by the dc or rms-ac current. Because superconductors can carry orders of magnitude more current than conventional conductors of the same cross section, in a given envelope (or existing duct) HTS superconducting cables can carry several times more power than a conventional cable.

A number of HTS cable designs have been developed to take advantage of the benefits of superconductivity, while minimizing the additional capital and operating costs that result from the material refrigeration and vacuum insulation requirements. Different cable architectures have important effects in terms of efficiency, radiated stray electromagnetic fields, and reactive power requirements. There are several types of HTS power cable under development. One ac cable design is based on a single conductor, with HTS wires stranded around a flexible core in a channel filled with liquid nitrogen coolant as depicted in Figure 12.52.

This design is referred to as a "warm dielectric design" because it employs an outer dielectric insulation layer at room temperature. Of the various superconducting ac cables, it uses the least

[106] R. L. Garwin and J. Matisoo, *Proc. IEEE.* 55 (1967) 538

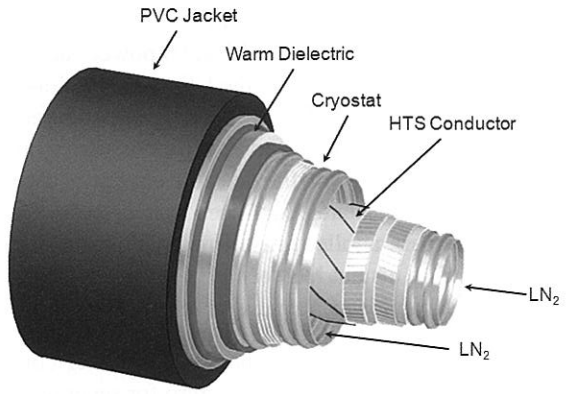

FIGURE 12.52: Single-phase warm dielectric cable. (Courtesy Nexans Corporation.)

amount of HTS wire for a given level of power transfer, but it has a high inductance and has an external magnetic field. Because the three phases of the system are close together, the magnetic field produced by one phase induces losses in the other phases. An advantage of this cable design is its use of insulation developed for conventional cables. The second ac cable design employs two concentric layers of HTS wire separated by a cold dielectric as shown in Figure 12.53.

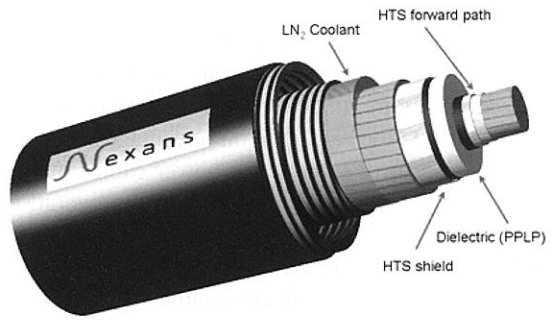

FIGURE 12.53: Single phase cold dielectric cable. (Courtesy Nexans Corporation.)

It is commonly referred to as a "cold dielectric design". Liquid nitrogen coolant may contact avoiding both cooling and dielectric insulation between the center conductor layer and the outer shield layer. Compared to the warm dielectric design, it has a lower inductance, a higher current carrying capacity, reduced ac losses, and very low stray magnetic fields. It also uses more superconductor than either of the other designs.

The third ac cable design is a concentric triplex, or three-conductor, design as shown in Figure 12.54. This design appears to be optimum at low to medium voltage levels. It has a very low inductance, and it uses less superconducting material than the coaxial design.

HTS dc cables are being considered for long distance, high power transmission, *vis-á-vis* [106] and the present interest in renewable energy sources such as wind and solar. They are also under consideration for shorter power transmission for the interconnection of large ac power systems that do not operate synchronously. Most of the HTS ac cables built to date use multiple cryostats that

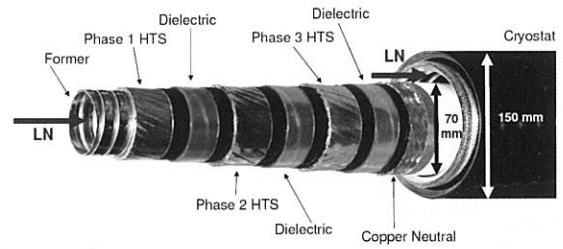

FIGURE 12.54: Triaxial three phase cable installed by Southwire at AEP's Bixby substation. (Courtesy Southwire Corporation.)

have lengths of about 100 m and are permanently evacuated. For power transmission of 1000s of kilometers, the risk associated with failure of one or a few of these cryostats requires a different solution. Figure 12.55 shows a concept of a superconducting dc cable that can carry up to 10 GW [107].

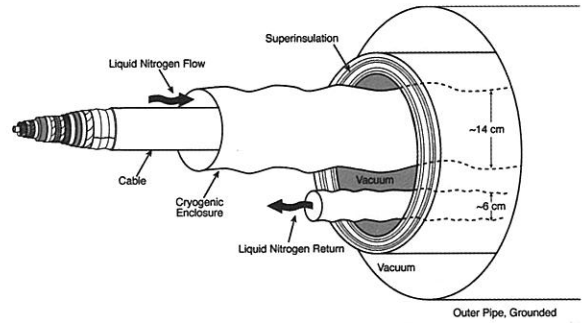

FIGURE 12.55: A superconducting dc cable designed to carry 10 GW over distances greater than 500 km. (Courtesy EPRI.)

This design has a long outer pipe, such as those used for gas pipelines, which contains two cryostat pipes, one for the power cable and the other for coolant return. The size of the outer pipe is determined by the vacuum requirements including the installation of pumps every kilometer or so and refrigeration stations separated by 10 to 20 kilometers. Besides the obvious increase of power density, the cold dielectric designs have inductances that are roughly about one-sixth those of conventional cables and 1/20th of that of overhead lines in the same voltage class[108]. Just as electrical current flows through the path of least resistance, power flow selects the lowest impedance path. As a result, coupled with the high current capacities of HTS cables, this quality provides superconducting cables with the potential to relieve transmission bottlenecks. Several evaluations of their lower impedance in a utility environment support this conclusion. Assessments of the Italian power grid[109] and of specific bottlenecks in the Chicago area[110] showed significant improvements

[107] W. Hassenzahl et al., *EPRI report* 1020458 (2009)
[108] N. Kelley et al., *Proc. IEEE/PES, Trans. and Dist. Conf.* 2 (2001) 871
[109] A. Mansoldo et al., *Proc. IEEE/PES Winter Meeting*, New York (2002) 142
[110] R. Silberglitt et al., RAND Corporation Science and Technology Policy Institute Report (2002)

TABLE 12.12: Superconducting Cables that Have been Installed and Operated at Utility Voltages

Lead Manufacturer	Use / Location	Voltage	Current	Installed	Removed
Southwire	In Plant, Grid Connected, USA	12.4 kV	1.25 kA	2000	2005
Sumitomo	In Plant, Japan	67 kV	1.0 kA	2001	2002
nkt Cables	On Grid, Sweden	30 kV	2.0 kA	2001	2003
Sumitomo/ Superpower*	National Grid, USA NY	34.5 kV	0.8 kA	2006	2008
Southwire	On Grid AEP Ohio USA	13.2 kV	3.0 kA	2006	Present
AMSC/Nexans	LIPA/ Long Island, USA NY	138 kV	2.5 kA	2007	Present
Keri/LS-Cable	South Korea Test Center	22.9 kV	1.5 kA	2006	2009
Changtong Cable	Baiyin, China	10.5 kV	1.5 kA	2004	2007

* After operating for a year with BSCCO tape, a 30 m section was removed and replaced with a coated conductor based section. Thus it was the first superconducting cable on a power grid with Gen II HTS material.

in power flow.

The downside of the lower impedance of superconductive cables is the potential for increased fault current. During a fault, a cable carrying 5 kA may see as much as 100 kA for short periods. Superconducting cables can be protected against such currents by using a conventional conductor such as copper in intimate contact with the superconductor. The HTS conductors would transition to the normal state when their critical current is exceeded and the stabilizer would carry the bulk of the current until the fault is cleared. On the flip side, when designed properly, the superconducting cables nonlinear impedance can be an advantage as it can assist in limiting the fault current[111].

Several HTS power cables have been installed and operated for extended periods of time. Some of these installations are listed in Table 12.12. Other projects that are under development are also listed in the table. Rather than describe the details of some of these projects, we include Figures 12.56 to 12.58, which are representative of the various installations. Descriptions of the various figures explain significant details

12.5.6 Superconducting Transformers

Issues associated with superconducting transformers were initially addressed in the mid 1960s[112], with the conclusion that, to be effective, 50 to 60 Hz power transformers would require a warm steel yoke and special low-loss superconductors. It was realized that cryogenics was a critical enabling technology and the need for thermal insulation, which added several centimeters to the coil dimensions, meant that at a 4 K operating temperature, only transformers having power ratings above 100 MW had a chance of becoming economically competitive. An additional barrier to LTS based transformers was the drive to improve conventional transformers. This effort increased the overall efficiency of power transformers from $\approx 99\%$ to $\approx 99.5\%$ from 1960 to 2000 [113].

There were some efforts to design low-loss Nb-Ti superconductors with fine filaments (< 0.1 micron) for transformer use, but the complication and expense of refrigeration at 4 K were of tantamount importance and, through the mid-1990s, only a few small experimental LTS devices were

[111] Pat Duggan, Consolidated Edison, private communication (2009)
[112] S. H. Minnich, *Proc. 1996 Appl. Supercond. Conf.* (1967) 32
[113] B. W. McConnell, *IEEE Power Eng.Rev.* 18 (1998) 8

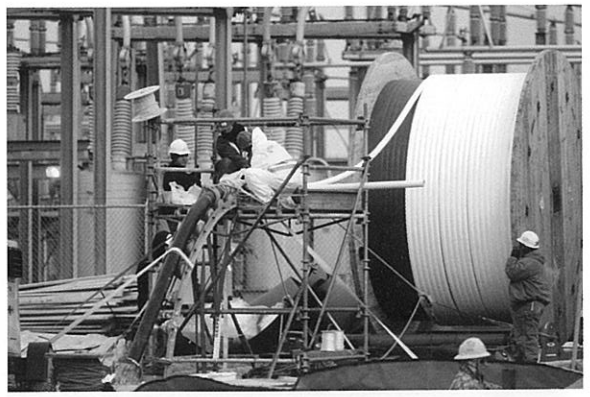

FIGURE 12.56: Pulling Southwire's triaxial cable into a cable duct at AEP's Bixby substation near Columbus, Ohio. (Courtesy Southwire Corporation.)

FIGURE 12.57: Installation of the Changtong warm dielectric HTS cable at the Changtong cable plant in Baiyin, China. (Courtesy Changtong Inc., China.)

ever made. The major work in this area was in Europe by Alsthom and ABB, in Japan by Toshiba, and at several universities as described in a review article in 2004 [69].

Although transformers for ac power applications had not advanced to a practical stage with LTS materials, special "dc transformers" use LTS materials and are effective elements in test facilities for certifying very high current conductors. In a typical dc transformer, the secondary and the specimen to be measured are both maintained at the operating temperature. Thus, the only resistance in the circuit is due to the joints between the conductors of the transformer secondary and the specimen. This allows high currents to be maintained for periods of minutes. Several of these dc transformers were designed and built by various laboratories around the world from the 1970s to the present. The most spectacular of these systems was built for tests of a 300 kA conductor[114] for a 5000 MWh SMES system that was under development in the US in the late 1980s. The special transformer for this test consisted of a single-strand, 200-turn primary and a two-turn, 30-strand secondary. The system operated in a bath of superfluid helium at 1.8 K and included a superconducting dipole

[114] D. L. Walker et al., *IEEE Trans. Magn.* 25 (1989) 1596

FIGURE 12.58: Terminations for the three phases of the LIPA cable produced by Nexans and AMSC. (Courtesy Nexans Corporation)

that could produce a background field up to 7.5 T. The highest current reached in the tests was an impressive 280 kA at a field of 5.8 T [115]. More recently this technique has been applied to tests of 50 kA conductors for ITER[116].

12.5.7 Conventional Transformer Characteristics

Large, conventional power transformers use oil as a coolant and as a component of the electrical insulation. The specialized practices of designing and building these transformers are described in many articles and several books[117]. The electric power grid uses several types of conventional transformers. Each generator has step-up transformer to convert its high-current low-voltage (typically 20 kV to 30 kV) electric power to an appropriate voltage (129 kV to 500 kV) for the transmission grid. These units have limited flexibility and operate at near capacity most of the time. They are designed to have efficiencies of 99.5 to 99.8%, which is considerably greater than the other transformers in the grid.

The step-down transformers at substations and in distribution centers are designed to be more flexible and to allow different voltages as the load changes. About half of them have tap changers, which operate either automatically under load or manually during a brief out-of-service period. The addition of this feature to a transformer makes it heavier, more expensive, and considerable more complicated.

Transformers and cables must meet several insulation tests. The first is the "basic insulation level" or "basic impulse level" referred to as "bil". The bil requirement of conventional transformers and cables is based on the anticipated voltage that they may experience during a lightning strike or other short period fault event. The bil levels for 69 kV and 345 kV transformers are 350 kV and 1300 kV respectively. The bil impulse test has a specific waveform and lasts about 50 μs [98,117].

Another dielectric issue for transformers and cables is a phenomenon referred to as "partial discharge". Even if the insulation is capable of withstanding the bil tests, all insulation has occasional imperfections, e.g., voids or particles with significantly different dielectric constants. These lead to local increases in electric fields at the operating voltage and may cause internal discharges with currents measured in picocoulombs. The energy associated with these partial discharges can damage insulation and decrease transformer and cable life[98].

[115] J. Zeigler et al., *IEEE Trans. Magn.* 27 (1991) 2395

[116] Y. Shi et al., *IEEE Trans. Appl. Supercond.* 20 (2010) 1155

[117] J. Harlow, ed. *Electric Power Transformer Engineering*, 2nd Edition, 2007 CRC Press Florida

To be effective in the power grid, HTS based transformers must mimic conventional transformers in performance and durability. However, operation at cryogenic temperatures imposes several major constraints on the design and operation. Although the first thought might be that the superconductor and its losses are the critical issue, in fact, a combination of cooling and insulation provides the real challenge. There are two design approaches to accommodate this combination in the transformer. The first is to replicate conventional transformer design by using liquid nitrogen as a replacement for the oil. The second is to use a solid insulation and indirect cooling. Both approaches have advantages and disadvantages. The use of liquid nitrogen and near conventional design provides a ready solution to the insulation issue, but conductor performance is so low at temperatures available with this solution, i.e., above 65 K, that a great deal of material is required. Existing HTS materials operate best below 50 K or so, at which temperature they can better meet the demands of field and current in a transformer. However, solid, low-temperature insulation that can be effective in physically large devices is not proven. Several programs are in process to develop some of these materials[118,119]. In the future, transformers using HTS materials may offer a variety of benefits to the electric utility. These include:

1. enhanced efficiency (because losses in superconductors are less than losses in conventional conductors at 300 K, and because losses at 50 K to 70 K are not so important as at 4 K),
2. the ability to run in an overloaded condition without impacting insulation life,
3. a reduced footprint (both weight and size are less),
4. the potential for lower leakage reactance,
5. ease of siting because oil is not used, and
6. the ability to limit fault currents.

These advantages and a discussion of the economic benefits and many significant developments of HTS transformers are described in several background articles[120,121,122,123,69].

The advantages of superconducting transformers are generally derived from the higher current density available and, in those that are intended as fault current limiters, the ability of the conductor to transition to a resistive state. The higher current density leads to a reduced dimension for the windings. In this regard, an additional advantage of the fact that the conduction cooled superconducting transformers do not use oil is that they are much lighter and smaller than any other type of transformer. There are other impacts of the use of superconductors. For example, there is a lower leakage reactance due to the higher magnetic fields within the HTS windings. Detailed analyses looking at the various tradeoffs are required to determine the optimum coil geometry.

Roughly half of the losses in a conventional transformer are in the iron core (hysteresis) and half in the conductor. However, if the iron losses were to occur at the cryogenic operating temperature, it would cause the efficiency to be so low that the transformer would not be competitive. Thus, the iron core must be thermally isolated from the coils and the cryogenic refrigeration system so that none of its hysteresis losses appear as a cryogenic load. Though there are no resistive losses in the

[118] M. Hara and H. Okubo, *Cryogenics* 38 (1998) 1083

[119] J. H. Choi et al., *IEEE Trans. Appl. Supercond* 19 (2009) 1972

[120] S. Mehta et al., *IEEE Spectr.* (1997) 44

[121] J. Laumond, *Handbook of Applied Superconductivity* 2 Institute of Physics Pub. (1998) 1613

[122] V. R. Ramanan et al., *47th Int. Wire and Cable Symp.* (1998)

[123] G. Donnier-Valentin et al., *IEEE Trans. Appl. Supercond.* 11 (2001) 1498

superconducting coils, there are, however, ac losses and heat flow from the surroundings that must be removed by a cryogenic refrigerator.

Fault currents are one of the most significant issues with all transformers. In the superconducting transformer, these currents can be accommodated by the use of co-wound normal conductors that carry the fault current for a few cycles. A powerful feature of an HTS transformer can be operational characteristics under long-duration overload conditions. By designing the HTS windings and the refrigeration system so that the transformer can carry two or more times the design current without transitioning to the normal state, one can avoid redundant installations and thus reduce system costs. The ac losses, some of which are proportional to the square of the current, will be considerably greater at higher currents so the refrigeration requirements during overload become a critical part of transformer design. Conventional transformers are designed to operate under such overload conditions, but high temperatures damage the insulation and result in loss of transformer life.

For widespread adoption, HTS transformers must meet or surpass the performance characteristics of today's conventional transformers, provide some of the added benefits mentioned above, and be economically competitive. These requirements provide a huge challenge to future development. Nevertheless, today, there are several HTS transformer development programs underway worldwide.

Many programs groups began developing superconducting transformers in the late 1990s. A few small model devices were constructed early on and a few near utility scale transformers were constructed and tested. The early work at universities and laboratories has continued on and off over the past decade, but most of the larger projects reached a test phase and ended either with successful tests or a variety of failures. No superconducting power transformers have been operated for long periods. In addition, because of lack of availability of appropriate superconducting wires, none of the existing devices use materials that will be needed for a commercially competitive transformer in the future. Nevertheless, there have been several successful tests of superconducting transformers. A group in Japan[124,125]—including Fuji Electric, Kyushu Transformer, Taiyo Toyo Sanso Co. Kyushu University, and Kyushu Electric Power—developed, tested, and connected to the grid a 1MVA, 22/6.9kV single-phase, liquid nitrogen bath-cooled transformer. The transformer withstood a 100 kV bil test. The group has carried out some development work on a similar 3MVA 3-phase system. A group in the US—including Waukesha Electric Systems, SuperPower, Oak Ridge National Lab, and Rochester Gas & Electric—built and tested a cryo-cooled 1MVA, 13.8/6.9kV single-phase transformer. The same team has completed construction and some preliminary testing of a 5/10 MVA, 24.9/4.6kV 3 phase prototype transformer. The testing was ended by the observation of considerable partial discharge. A group, including ABB, American Superconductor, Los Alamos National Laboratory, and Southern California Edison, worked on the design of a 10 MVA, three-phase liquid nitrogen bath cooled transformer until it became clear that the cost of BSCCO material would not allow the development of a competitive device. They did test a 630 kVA, 18.7 kV/420 V three-phase liquid nitrogen bath cooled transformer with Electricitè de France. This transformer was successfully connected to the grid in Geneva, Switzerland[126]. More recently[127], there have been several studies as to the incorporation of tap changing systems into a superconducting transformer. In slightly different arena, Siemens[128] built and tested a 1 MVA liquid nitrogen bath cooled HTS transformer for railway applications, where reduction in weight is dominant and the system must operate under a somewhat different set of performance and design criteria. More recently, a group in Japan[129] tested a 4 MVA transformer designed for use on the Shinkansen.

[124] K. Funaki et al., *Cryogenics* 38 (1998) 211
[125] K. Funaki et al., *IEEE Trans. Appl. Supercond.* 11 (2001) 1578
[126] H. Zueger, *Cryogenics* 38 (1998) 1169
[127] S. W. Kim et al., *IEEE Trans. Appl. Supercond.* 17 (2007) 1939
[128] R. Schlosser, *IEEE Trans. Appl. Supercond.* 13 (2003) 2325
[129] H. Kamijo et al., *IEEE Trans. Appl. Supercond.* 17 (2007) 1927

12.6 Magnetic Separation

Christopher Rey

12.6.1 Introduction

Commercial applications using the principles of magnetic separation have been around for more than one hundred years. Magnetic separators have been used since the time of Joseph Henry, when electromagnets were used to remove nails from horses' feed[130,131]. Principles of magnetic separation are widely used in commercial applications today. Typical uses range from the simple removal of coarse tramp iron and steel from garbage, to the more sophisticated separations, such as the removal of weakly magnetic mineral contaminants from paper-coating clays. Technical advancements in magnetic separator design have led to the commercial use of high gradient magnetic separators (HGMS). These devices are capable of removing weakly magnetic particles and process tons of material per hour. This continued progress has greatly broadened and enhanced the commercial magnetic separations market. For example, it is estimated that the introduction of HGMS into the purification of kaolin clay has nearly doubled the worldwide useful reserves[132] by making lower grade ores economically attractive. Until the development of HGMS, magnetic separation techniques had been confined to manipulating mixtures that contained one or more of the three strongly magnetic (ferromagnetic) elements: iron, nickel, and cobalt. HGMS is potentially applicable to many more elements, mixtures, and compounds. For example, there are over 56 weakly magnetic elements (diamagnetic and paramagnetic) contained within the periodic table. Perhaps of even greater potential benefit is the possibility of manipulating *non-magnetic* substances (the term *non-magnetic* is typically reserved for materials that display extremely weak paramagnetic or diamagnetic properties), e.g. pollutants in water, using appropriate magnetic "seeding" techniques. Recently HGMS, fabricated with superconducting coils, have been introduced into the kaolin industry. Superconducting HGMS devices can produce even higher magnetic fields and operate with less than one fifth the total power consumption of conventional resistive units. Higher magnetic fields translate to better particulate selectivity and increased productivity by processing more material per unit canister volume. For a more complete description of the history and development of high gradient magnetic separation, see reference[133].

12.6.2 Principles of Magnetic Separation

Magnetic Phenomena

All materials possess magnetic properties to some extent. The relative strength of these magnetic properties varies widely among different materials. Materials are typically classified into four categories based upon the strength of their magnetic properties: (1) ferromagnetic, (2) strongly magnetic, (3) weakly magnetic and (4) non-magnetic. With the exception of ferromagnetic, the boundary defining the difference between strongly magnetic, weakly magnetic, and non-magnetic is arbitrary and typically application dependent. Any particle introduced to a magnetic field will

[130] F. Knoll, *Perry's Chemical Engineers' Handbook*, 17th ed., ed. by D. Green and J. Maloney, New York: Mcgraw-Hill, (1997) 19–40
[131] C. M. Rey, *Engineering Superconductivity*, ed. By P. Lee, New York, John Wiley & Sons, (2001) 448
[132] J. Iannicelli, *Ultrafine Grinding and Separation of Industrial Minerals*, ed. by S. Malghan, New York: American Institute of Mining, Metallurgical and Petroleum Engineers Inc. (1983) 105
[133] H. Kolm, J. Oberteuffer, and D. Kelland, *Scientific American* 233 (1975) 46

become magnetized. The magnetic moment of an atom results from the electron spins, their orbital angular momentum and the change induced in the orbital angular momentum[134].

Materials that exhibit a positive magnetization when placed in an external magnetic field are described as paramagnetic. Materials that exhibit a negative magnetization are described as diamagnetic. All materials will display some degree of diamagnetism due to the moment induced by an applied magnetic field; however, this type of diamagnetism is relatively weak and can be negligible if other forms of magnetic properties are present, e.g., paramagnetism or ferromagnetism. Paramagnetism results from the electron spins and their orbital angular momentum. Atoms with unpaired electrons typically exhibit paramagnetism. Paramagnetic materials are further classified as strongly or weakly paramagnetic depending upon the strength of the magnetization, the magnetic moment per unit volume, when placed in an external magnetic field. A large number of elements and their compounds exhibit paramagnetism. Some common examples are hematite (Fe_2O_3) and pyrite (FeS_2). Table 12.13 lists the magnetic susceptibility of some common elements and minerals. When domains of paramagnetism are created in some materials such that long-range order is established, the magnetization can be quite large and the materials are described as ferromagnetic. These elements include iron, nickel, and cobalt and a relatively small number of compounds of these elements. An example of a ferromagnetic ore is magnetite (Fe_3O_4).

TABLE 12.13: Magnetic Susceptibility of Some Common Elements and Minerals

Substance	Susceptibility (10^{-6} cgs)	Substance	Susceptibility (10^{-6} cgs)
Aluminum	+10.5	Ferberite	+39.3
Al_2O_3	-37	Galena	-0.4
Apatite	+1.0 to +18.0	Garnierite	+30.7
Aragonite	-0.4	Gold	-28.0
Asbolan	+150.0	Ilmenite	+15.45 to +70.0
Azurite	+12.2 to +19.0	Lead	-23
Anatase	+0.96 to +5.60	Malachite	+10.5 to +14.5
Beryl	+0.4	Millerite	+0.21 to +3.9
Braunite	+35.0 to +150.0	Molybdenite	+4.9 to +7.1
Biotite	+40.0	Molybdenum	+89.0
Barite (pure)	-71.3	Rutile	+0.85 to +4.78
Brannerite	+3.5	Scheelite	+0.13 to +0.27
Chromium	+180.0	Siderite	+65.2 to +103.8
Chromite	+125.6 to +450.0	Titanium	+150.0
Cobalt	Ferromagnetic	Tungsten	+59.0
Cobaltine	+2.0	Uranium	+395.0
Cobaltite	+0.34 to +0.64	Vanadium	+255.0
Columbite	+32.6 to +37.2	Vanadinite	-0.2 to +0.27
Copper	-0.1	Wolframite	+42.2

[134] R. M. Bozorth, *Ferromagnetism*, New York: IEEE Press, re-issued 1993

12.6.3 Magnetic Separation Dynamics

Magnetic Forces

Several magnetic separation concepts have been proposed throughout the years, but they all rely on the same electromagnetic principle: a particle exposed to an external spatially varying magnetic field, i.e., a magnetic field gradient, will experience a force in newtons (N) equal to:

$$\mathbf{F}_M = V\,\mathbf{M}(\mathbf{B})\cdot \mathrm{grad}\mathbf{B} \tag{12.10}$$

where V is the volume of the particle in cubic meters (m^3), $\mathbf{M}(\mathbf{B})$ is the magnetic field-dependent magnetization (in amperes/meter) of the particle and grad$\mathbf{B}$ is the gradient of the magnetic induction (in tesla/meter)[134]. The magnetic force acting on a particle can be rewritten in terms of the magnetic susceptibility where $\mathbf{M}(\mathbf{B}) = \chi_m(\mathbf{B})\mathbf{H}$ such that:

$$\mathbf{F}_M = \chi_m(\mathbf{B})V\,\mathbf{H}\cdot \mathrm{grad}\mathbf{B}. \tag{12.11}$$

The implications of Equation (12.11) are that in order to have large magnetic separation forces, it is not only the particles magnetic susceptibility that is important, but also a combination of both high magnetic field intensity and magnetic field gradient that determine the magnitude of the magnetic force.

Fluid Dynamic Effects

For many magnetic separation processing techniques (i.e., wet processing), the particles are often mixed within an aqueous fluid (slurry) which moves past the high gradient collector. Typically, the high gradient collector is a mesh fabricated from thin ribbons or wires of highly permeable stainless steel, which concentrates the magnetic field lines. In general magnetic field gradients are large near sharp edges or corners. Thus, the magnetic force, given in Equations (12.10) and (12.11), acting on the particle can be quite large. The mesh acts as a filtering mechanism by trapping magnetic particles attracted to the wire and allowing non-magnetic particle to pass freely. While traveling within this fluid, however, there are several other competing forces acting on each mixture of particle, which include

F_M = magnetic force, F_D = fluid viscous drag force
F_G = gravitational force, F_B = fluid buoyant force.

Neglecting the buoyant force of the particle, Newton's law for the equation of motion for this particle in a fluid is given by Equation (12.12):

$$\rho V(d^2r/dt^2) = F_M + F_D + F_G, \tag{12.12}$$

where ρ is the particle density in kg/m^3, V is the particle volume in m^3, r is the position coordinate in meters, t is the time in seconds, and the magnetic force has been defined previously in Equation (12.10) and (12.11). To a first order approximation, the viscous drag force is given by

$$F_D = 3\pi\eta v a, \tag{12.13}$$

where ρ = particle density (kg/m^3), v = fluid velocity (m/s), a = particle diameter (m), and η = fluid viscosity (N-s/m^2). Figure 12.59 illustrates the various magnetic forces acting on a magnetic particle described in Equations (12.10) and (12.11). For a magnetic particle to be collected at the surface of the wire within the magnetized volume of the separator, the following condition must be met:

$$F_M \geq F_D + F_G. \tag{12.14}$$

In the analysis above, both the density and particle size (diameter) are extremely important in the magnitude of the magnetic and viscous drag force. The magnetic force varies as the cube of

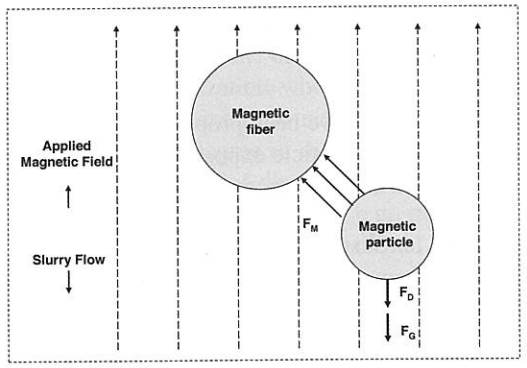

FIGURE 12.59: Schematic representation of a magnetic fiber in a high gradient magnetic separator and the forces acting on a magnetic particle.

the particle diameter, a^3. The viscous drag force varies linearly with the particle diameter. This implies that separations between particles with similar magnetic susceptibilities are possible only when significant size and density difference exists.

12.6.4 Open Gradient Magnet Systems

The large magnetic field gradients used in separation devices are typically created using two different methods. The first method is known as the open gradient magnet system (OGMS). The second method is the matrix/filter. Open gradient devices separate particles with different magnetic susceptibilities by preferentially directing them in open spaces using magnetic forces. In the open gradient technique, the conductor geometry or suitably designed pole pieces generate magnetic field gradients and hence the magnetic forces on the particles. The magnetic forces are often in competition with other forces such as gravity, electrostatics, drag, and buoyancy. A significant shortcoming of open gradient systems is that the magnetic field gradients that can be generated are typically less than 2 T/cm. Typically, these low magnetic field gradients limit the use of OGMS devices to the separation of strongly magnetic minerals and metal scrap.

Open gradient systems have the advantage in high-volume processing. No magnetic matrix or filter is required to trap the magnetic particle mechanically. In standard operation, the particle stream is passed down the bore and magnetic particles are either pushed radially inward or outward depending on whether they are diamagnetic or paramagnetic. The particles can then be physically separated further down stream.

12.6.5 Matrix/Filter Systems

The second method most often used to generate magnetic field gradients in separation devices is the use of a magnetic matrix or filter. Frantz patented the conceptual basis for the modern ferromagnetic filament-type collector matrix[135] in 1937. The Frantz magnetic filter (Frantz Ferrofilter®) utilized a matrix of ferromagnetic type 430 stainless steel screens fabricated from thin sharp ribbons. In general, magnetic field gradients are large near sharp edges or corners. The introduction of a large number of spheroids, wires, or a mesh of wires will similarly create regions of high gradients near the wires. The magnetic field gradient near the vicinity of the wire can be as high as 10,000 T/cm. A magnetic particle traveling past the wire will experience two magnetic fields: one from the

[135] S.G. Frantz, U.S. Patent 2,074,085, March 16, 1937

background ambient field B_0 of the magnet and the other from the collector wire B_c, where the total magnetic field is the vector sum of the two contributions, namely, $B_t = B_0 + B_c$. A more detailed analysis on the shape effects of the matrix on the capture cross section of the particle can be found elsewhere[136].

A significant disadvantage of the matrix/filter system is the problem of build-up of magnetic particles. A magnetic separation device that utilizes a matrix/filter to mechanically trap magnetic particles must be periodically cleaned in order to prevent clogging. This means that during the cleaning of the matrix/filter, the magnetic field must be reduced to zero (or near zero) in order to minimize the magnetic trapping force. Periodically cycling the magnetic field in order to clean the matrix/filter reduces processing efficiency.

12.6.6 Characteristics of High Gradient Magnetic Separation

The efficiency of a magnetic separation device is typically expressed in two ways[137]. First, it may be characterized by the so-called "Grade". The Grade is defined as the percentage ratio of the desired component in mass relative to the total mass of the magnetic fraction (Mags). Second, the separation efficiency can be characterized by the so-called "Recovery". The Recovery is defined as the percentage ratio of the amount of magnetic material recovered relative to the total amount of magnetic material in the "Feed". The two measures are independent quantities and together determine the efficiency of the separation. For most separation devices, there is a relation between the grade and the recovery of the processed material. By adjusting the operating parameters of the separator, the grade can be increased at the expense of the recovery, and vice versa. For example, Figure 12.60 shows processing data for the magnetically trapped product of a taconite ore.

The percent Recovery and Grade is plotted as a function of the slurry flow rate at a constant applied field of 2 T. As the Recovery of the magnetically trapped product decreases with increasing flow rate, the Grade correspondingly increases.

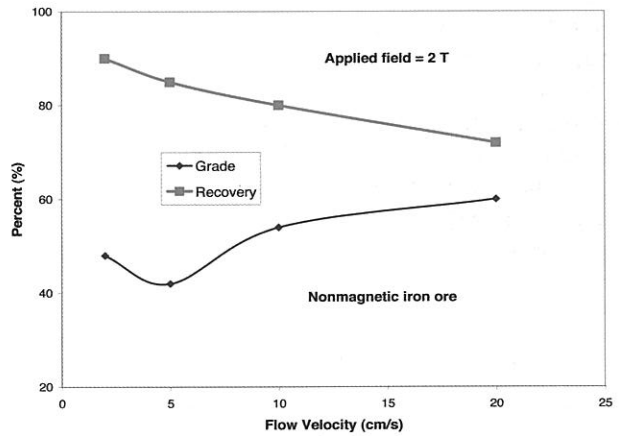

FIGURE 12.60: Grade and Recovery of a non-magnetic iron ore (non-mags) vs. slurry flow velocity at a constant applied field of 2 T.

[136] Z. J. Stekly and J. V. Minervini, *IEEE Trans. Magn.* 12 (1976)

[137] S. Foner and B. Schwartz (ed.), *Superconducting Machines and Devices*, New York, Plenum Press, (1974) 581

12.6.7 Magnetic Separation Equipment

There are several terms that are often used to characterize magnetic separation devices, such as permanent magnet, electromagnet, high gradient, open gradient, etc., but the devices themselves basically fall into two separate categories: (1) batch-type and (2) continuous-type. Table 12.14 summarizes some common types of magnetic separators and their ranges of potential applications. The following information concerning commercial magnetic separations units can be found in more detail in Knoll[130] and Rey[131].

Batch-type

Batch-type separators are most useful when the unprocessed feed materials contain a relatively small amount of magnetic material to be trapped in the collection volume. This allows for a convenient duty cycle for the device. Batch-type separation devices are most often fabricated using iron bound solenoid electromagnets surrounding a cylindrical canister. The cross section of the canister is circular in order to minimize the amount of conductor used to magnetize the collection volume. Utilizing a long coil where the height of the coil exceeds the canister height further maximizes the efficiency of a batch-type solenoid electromagnet. Iron pole pieces of the magnet are then designed to extend into the top and bottom of the solenoid. Batch-type separators operate on the principle of cycling the magnetic field from a maximum value down to zero applied field. It is important to have a magnetically soft material with a low remnant field as the collection matrix, so that when the applied field is reduced to zero the force acting on the magnetic particles is minimized. In normal operation, typical duty cycles for mineral separations vary between 10% and 80%.

Resistive Solenoid Electromagnets

In March 1973, the first large-scale HGMS was installed at the Freeport Kaolin Co. in Gordon, Georgia[130,131]. The separator was a 2.1 m diameter resistive electromagnet fabricated by Pacific Electric Motor Co. The separator could generate magnetic fields up to 2 T and process nearly 3800 liters of slurry per minute or 60 metric tons per hour (dry basis). The central magnetic field was 2 T, with an electrical power consumption of nearly 500 kW. The conductor consisted of 16 hollow water-cooled copper coils surrounded by a vault like steel enclosure that was 3.65 m × 3.65 m × 2.44 m [138,139]. For its day, this magnet represented a thirteen-fold increase in process capacity over the largest previous commercial magnetic separator. Continued improvements in magnet design have led to similarly sized units operating at 2 T with less than 300 kW of electrical power consumption. In 1982, the first 3 m diameter resistive electromagnetic separator went into operation[140]. This enormous unit could process 130 tons per hour of kaolin with about 400 kW of electrical power consumption. To date, there have been twenty-nine resistive electromagnets, 2.1 m and 3 m in diameter, installed in the US and eight others in the rest of the world for the purification of kaolin clay[140].

Low Temperature Superconducting Solenoid Electromagnets

In a low temperature superconducting (LTS) magnet, the magnetic field is generated in exactly the same way as in a conventional resistive electromagnet. The only real difference between the two is that the conductor in the LTS magnet must be maintained at a suitably low temperature in order to remain in its superconducting state. The key benefits offered by superconducting magnets

[138] J. Iannicelli, paper presented at the AIME/SME Meeting in Atlanta, GA, March 6-10, 1983. Reprinted by Aquafine Corporation Brunswick, GA.

[139] J. Iannicelli, Clays and *Clay Minerals*, 20, Great Britain: Pergamon Press, (1976) 64

[140] Aquafine Corporation, Products Catalog, Brunswick, GA, 1996

are (1) very low power consumption, resulting from zero resistance in the conductor windings (see section below) and (2) much higher magnetic fields resulting in better selectivity of particles and higher separation efficiency. However, the zero resistance property of a superconductor is only true for direct current (dc). For applications where the electromagnetic field is changing in time (ac), a superconducting material no longer operates with zero electrical resistance. Therefore, for batch-type magnetic separators, which periodically cycle the magnetic field, there is a practical limitation on the maximum allowable magnetic field ramp rate for these devices.

Several LTS materials have been studied, but the most prominent in terms of conductor fabrication and commercial implementation is an alloy of niobium and titanium (NbTi). In order to enhance electric and thermal stability of the superconductor, the NbTi is typically embedded in a normal metal matrix of copper or aluminum. This allows for greater heat transfer through thermal conduction and also provides a low resistance electrical path in the event that the superconductor comes out of its superconducting state. One disadvantage of the normal metal matrix is in ac applications. In ac applications, additional Joule heating is caused by the generation of induced currents in the normal metal matrix. To fabricate these composite superconductors, fine filaments of NbTi are either drawn or extruded with the aluminum or copper. The filament size of the NbTi can vary between about 5 and 30 microns depending upon the application. Copper and aluminum clad superconducting windings using NbTi conductor are now common place in the research community and have been used in applications such as motors, generators, transformers, and magnets.

An important aspect of the design of an LTS magnet is the choice of refrigeration or cryogenic cooling system that will be used to cool the conductor windings. There are two basic refrigeration routes that have been used successfully. The first and most prevalent route is the use of liquid or gaseous cryogens. The NbTi conductor windings are typically cooled by either immersion in a bath of liquid helium or by forcing cold, two-phase, helium gas around the conductor. Helium gas will liquefy at 4.2 K at atmospheric pressure. The helium gas that is boiled-off or heated by ac-loss is recirculated through a liquefier, cooled and recondensed into liquid or a two-phase mixture. The second method used to cool superconducting windings is through indirect cooling using a refrigerator. These refrigerators are commonly referred to as cryocoolers. Cryocoolers, based on various thermodynamic cycles, allow cooling to extremely low temperatures. One such device commonly used in the cryogenic industry is the Gifford-McMahon cryocooler. Recent advances in Gifford-McMahon cryocooler technology permit these units to generate temperatures of 4 K or lower. The units enable superconducting windings to be cooled indirectly and without the presence of liquid or gaseous cryogens and are particularly advantageous in small-scale systems where the cost of a liquefier cannot be justified. The two major drawbacks to these systems are (1) the constant supply of electrical power that is essential for reliable operation and (2) the relatively small cooling capacity of cryocoolers, typically a few watts, at 4 K. In 1996, the first successful demonstration of kaolin benefaction using a high temperature superconducting (HTS) magnetic separator was reported[141]. In this report, five different types of kaolin clays representing major worldwide deposits were processed in a 5 cm diameter warm bore HTS magnet in fields up to 2.5 T. However, because of the higher cost of the HTS wire per ampere-meter compared to its LTS counterpart, it is unclear at this time if the economic benefits from increased refrigeration efficiency will outweigh the additional capital cost of the HTS wire.

Energy Efficiency

One of the major drawbacks of conventional resistive type magnetic separators using water cooled copper conductor windings, is the high operating cost due to the large electrical power consumption. The power consumption in a conventional copper magnetic separator can be as high as 400 kW in a 3 m diameter unit. In a superconducting unit, the primary source of power consumption is the

[141] Eriez Magnetics, Products Catalog, Erie, PA, 1997

refrigeration unit. An equivalent 3 m diameter LTS unit is rated at about 50 kW. In production environments these units operate approximately 8000 hours per year with an expected lifetime between five and ten years. In the southern US, where most of the processing plants are located, the present average price of electricity is approximately $0.05/kWh. This translates to an annual cost saving of about $140,000 (dollars) per year with a lifetime saving of $1.4 million (dollars) for a superconducting magnet over its resistive counterpart. For processing plants located in non-industrialzed countries, the savings in annual operating cost is even more substantial as price and availability of electrical power is at a premium.

Installed Systems

The first large-scale LTS magnetic separator went into operation in 1986. The device had a 2.1 m diameter bore and was fabricated by Eriez Magnetics of Erie, Pennsylvania[142]. The device was installed at the J. M. Huber Company in Georgia and used for the benefaction of kaolin clay. The installed cost of this device was around 2 million dollars. To date, twelve batch-type LTS magnetic separation systems have been installed in the US. Eight of the twelve LTS systems installed have been retrofits, where the existing resistive electromagnets have been replaced with superconducting windings. Worldwide, five other batch-type LTS magnetic separation systems have been installed for the benefaction of kaolin clay in Australia, Brazil, China, England, and Germany. LTS magnetic separation systems appear to be displacing their conventional resistive counterparts.

Continuous-type

One of the primary shortcomings of the batch-type separator is processing efficiency. Batch-type separators operate on a duty cycle, so there is a period of time when material is not being processed. Continuous-type separation devices are designed to maximize the duty cycle and minimize the processing time. Continuous-type separators are advantageous when the magnetic fraction of the unprocessed feed material is relatively high.

Drum and Pulley Magnets

In the earliest magnetic separators, and in many that are still applicable for attracting strongly magnetic materials, permanent magnets were used in an open single surface device. These devices consisted of suspended magnets, pulleys, conveyors, or drums. These devices produced fields in the neighborhood 0.06 T and gradients of the order of 0.05 T/cm. Drum and pulley magnetic separation equipment has been used since the time of Thomas Edison, where he used a magnetic pulley for the concentration of nickel ore. These are among the most common types of magnetic separators in the world today. They can be made from either permanent or electromagnets and process either wet or dry feeds. Dry magnetic drums can be designed to perform as lifting magnets or pulleys. Magnetic drum devices have stationary magnets while pulley drums rotate. Schematics for a drum-type separator are shown in Figure 12.61.

Wet Drum Magnetic Separators

Wet drum separators are used exclusively for the processing of wet feed material for the separation of strongly magnetic coarse particles. The key processing variable that determines the size and processing capacity of the device are slurry volume, percent magnets and solids in the slurry, and

[142] Z. J. Stekly, *IEEE Trans. Magn.* 11 (1975) 1594

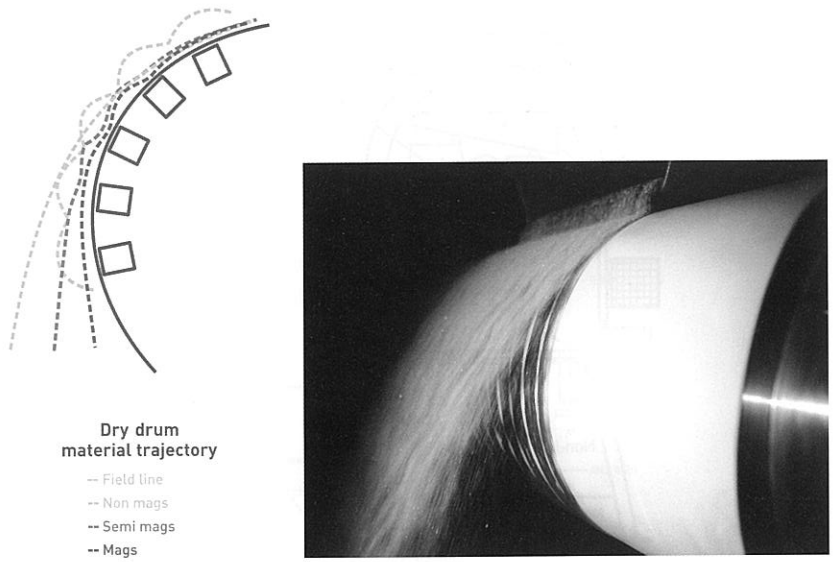

FIGURE 12.61: (a) The principle behind a rare-earth permanent magnet drum-type separator. (b) Rare-earth drum-type separator in operation. (Courtesy Outotec Inc.)

the required recovery and concentration of magnetic particles. Several vendors manufacture these devices. Typical drum sizes vary from 0.023 m to 1.2 m in diameter with heights up to 3 m. An example of a wet drum magnetic separator is shown in Figure 12.62. Unprocessed feed material is introduced into the first drum, which is used to remove the strongly magnetic coarse particles. The processed material is then fed into the second drum for the removal of finer magnetic particles. Units with single drums can process slurry with magnetics up to 20% by weight and units with two drums can process slurry up to 45% magnetics by weight. Recommended maximum particle size is 6 mm. Concurrent devices can process finer particles down to about 0.8 mm (20 mesh) with an optimum solids content of about 30% by weight. Wet drum separators have the advantage of being able to process material with a wide variation in particle size and throughput. The installed cost of a single wet drum-type separator can vary between $25,000 and $75,000 per meter of magnet width. Multiple drum cost increase in direct proportion to the number of drums required.

LTS Reciprocating Magnet System

As early as 1975, studies were carried out on a new type of magnetic separator design that benefits from the zero resistance property of superconducting coils[143]. In 1989, Carpco (now Outotec) introduced the first commercial reciprocating magnetic separator. Unlike its LTS batch-type predecessor that cycles its magnetic field, this magnet maintains the field at a constant level and instead cycles the matrix/filter canister in and out of the active magnetic field region. This design allows for semicontinuous processing and reduces ac losses by not cycling the magnetic field. The magnet operates in what is known as the "persistent mode". Below the superconducting transition temperature, a superconducting magnet can be energized and then disconnected from the power supply, and current will continue to flow without additional power input. The basic processing cycle for the reciprocating magnetic separator is shown in Figure 12.63. The key feature is that while one matrix

[143] Z. J. Stekly, *IEEE Trans. Magn.* 11 (1975) 1594

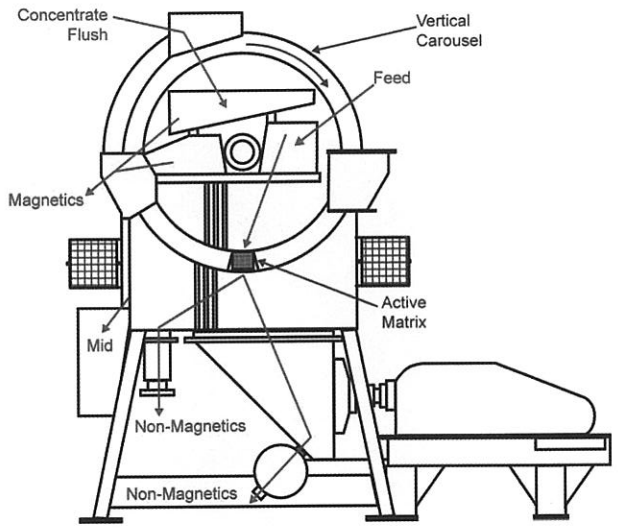

FIGURE 12.62: Wet drum magnetic separator arrangements. (Courtesy Outotec Inc.)

canister is processing material in the central magnetic field region, the other matrix canister is being cleaned/flushed in the low field region[144].

Installed System

In 1989, the first LTS reciprocating magnetic separations unit used in the purification of kaolin clay went into operation in Cornwall in the United Kingdom. This unit consists of a NbTi conductor winding operating in a bath of liquid helium. It has a warm bore diameter of about 0.28 m with a maximum central field of 4 T and can process between 2 and 5 tons of kaolin per hour. In 1992, the second LTS reciprocating magnet system was installed in southern Germany for the purification of kaolin clay. This unit has a 0.26 m warm bore diameter with a maximum central field of 5 T and can process up to 5 tons of kaolin per hour. To date (July 2010), twenty-six more industrial scale LTS reciprocating magnetic separators have been installed worldwide. Reciprocating systems with warm bore diameters up to 1 meter and central fields of 5 T are presently in operation, see Figure 12.64. Ten smaller diameter LTS reciprocating units, operating in research laboratories and pilot scale production lines, have also been installed. One might expect that the complexity of superconducting technology would restrict the commercial viability of these units to developed and industrialized areas. In reality, the simplicity and reliability of the low-loss cryogen technology coupled with the reciprocating canister principle has enabled operation of these units in Munguba and Rio Caprim[144], which are remote areas of the Amazon rain forest.

12.6.8 Applications of Magnetic Separation

There are several commercially available mineral separation technologies utilizing specific gravity, magnetic separation, electrostatic separation, column flotation, etc. All of these techniques exploit various discernible properties among mixtures of minerals. A comparison of different separation methods as a function of particle size range is shown in Figure 12.65.

[144] Carpco (now Outotec), Products Catalog, Jacksonville, FL, 1998 or see www.Outotec.com

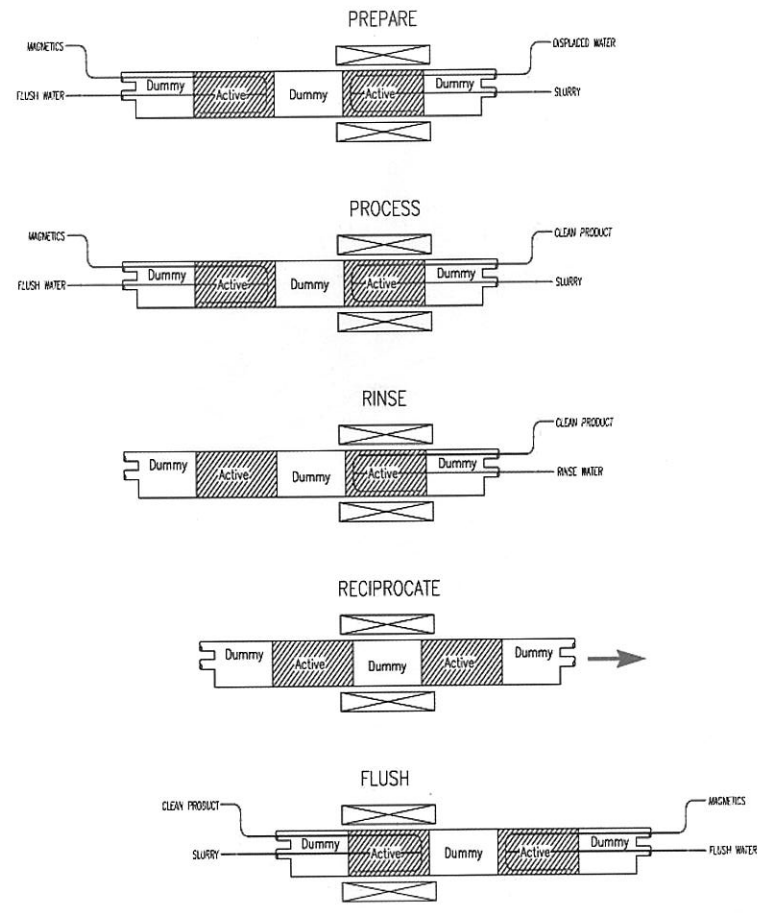

FIGURE 12.63: A schematic representation of a Reciprocating-type operating cycle. (Courtesy Outotec Inc.)

Each separation technology has its own particular strength; however, it is typically a combination of techniques that provides the best industrial minerals separation processes. Commercial magnetic separators come in a variety of shapes and sizes depending upon the required application. To select the most appropriate magnetic separator for a specific application requires an evaluation of several variables including type of material being processed, wet or dry processing, particle-size, magnetic characteristics, and processing rate. Table 12.14. summarizes some of these defining parameters.

There are several commercial/industrial applications which utilize magnetic separation or in which magnetic separation could play a role in the future e.g., kaolin clay purification, titanium dioxide purification, waste water remediation, waste soil remediation[145], coal purification[146] chem-

[145] L. A. World, F. C. Prenger, D. D. Hill, D. D. Padilla, to be published in *Emerging Technologies in Hazardous Waste Management*, Proceedings of the 16th American Chemical Society Conference, Boston MA, August, 1998

[146] J. Iannicelli and T. Webster, Electric Power Research Institute Grant No. NP- 3273, research project S106-1, 1983

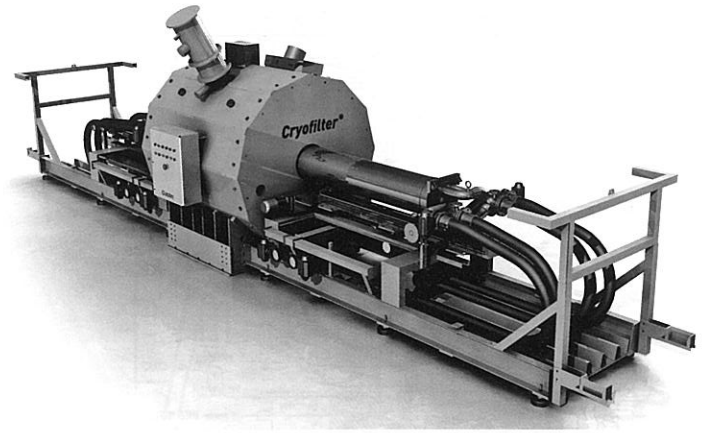

FIGURE 12.64: A 5 T low temperature superconducting reciprocating magnet with a 0.5 m bore, installed in Georgia. This magnet can process 20 tons of kaolin clay per hour. (Courtesy Outotec Inc.)

TABLE 12.14: Potential Applications of Magnetic Separators

Device	Magnet	Maximum Field (T)	Matrix	Maximum Gradient (T/cm)	Required Susceptibility	Particle Size (mm)
Grate	Permanent	0.05	Rods	0.05	Ferromagnetic	< 12
Pulley	Permanent	0.02	–	0.01 - 0.1	Ferromagnetic	< 50
Drum	Permanent	0.05 - 0.1	–	0.05 - 0.1	Ferromagnetic	0.02 - 20
Belt	Electromagnet	0.01 - 0.1	–	0.01 - 0.1	Ferromagnetic	0.15 - 30
Induced roll	Electromagnet	2	–	20	Paramagnetic	0.03 - 3
Carpco	Electromagnet	2	Steel balls	4.5	Paramagnetic	0.01 - 1
C-frame; Jones	Electromagnet	2	Grooved Plates	20	Paramagnetic	0.01 - 2
Marston Sala	Electromagnet superconducting	2 - 5 T	Steel wool	2500	Paramagnetic weak	0.0001 - 2

ical processing[147,148,149], and solid-liquid separation[150]. For brevity purposes, only kaolin clay and titanium dioxide are presented in more detail.

Kaolin Processing

Kaolin is a naturally occurring white clay consisting of microscopic platelets of aluminum silicate. The U.S. is the largest producer and exporter of kaolin in the world, with over 10 million tons valued at over 1.3 billion dollars produced in 1993. Georgia generates 80% of the tonnage and 90% of the value of kaolin in the U.S[138,139]. Kaolin is used in the manufacture of fine porcelain and as a base filler in the manufacture of high-grade paper. One of the most widely recognized industrial

[147] H. J. Schneider-Muntau (ed.), *High Magnetic Fields*, New Jersey: World Scientific, (1997) 31

[148] S. Dale, S. Wolf, and T. Schnieder, *Energy Applications of High-Temperature Superconductivity*, 2, 1976

[149] R. Mitchell and D. Allen, *Industrial Applications of Magnetic Separation*, IEEE Catalog No. 78CH1447-2, p.142, 1979

[150] C. M. Rey, K. Keller, and B. Fuchs, *Magnetic Processing in Magnetic Fields*, NewJersey: World Scientific, 2004

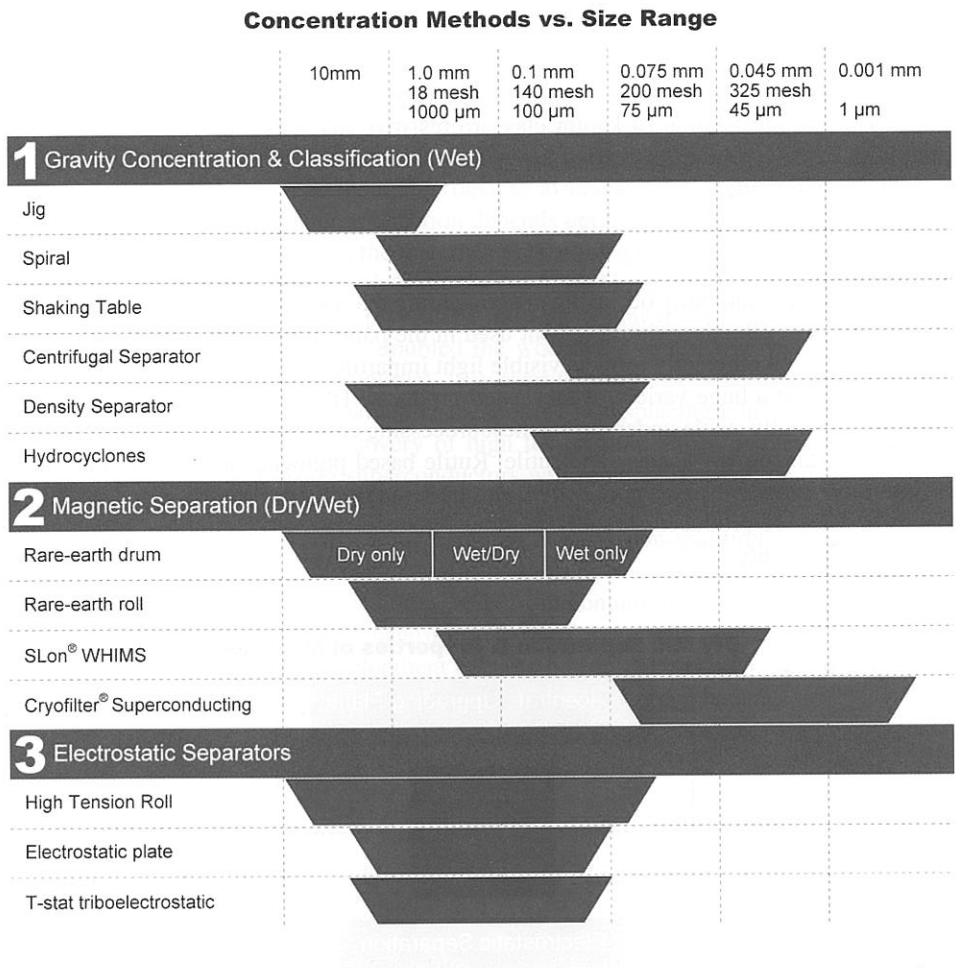

FIGURE 12.65: A comparison of separation methods as a function of particle size. (Courtesy Outotec Inc.)

applications of high gradient magnetic separation is in the purification of kaolin clay. Magnetic separation has been used in the kaolin industry for over 25 years. The primary benefit is increased whiteness or brightness of the kaolin product for paper or ceramic applications. Magnetic separation has offered additional benefits to kaolin processing such as improved viscosity or rheology. Magnetic separation is used primarily to remove small paramagnetic impurities of titanium and iron compounds that discolor the clay. The impurities' content typically comprise between 2 and 5% of the weight of kaolin. The quality of the processed clay is determined by the resulting brightness. The industrial association that establishes the brightness standards for the kaolin industry is the Technical Association of the Pulp and Paper Industry (TAPPI). Brightness is typically measured using a reflectance technique and results compared with industry standards, e.g., TAPPI T 646 om-94 for pulverized material with 45°/0° geometry[151]. The improvement in brightness after magnetic separation depends upon many processing variables such as the initial quality of the unprocessed clay, magnetic field strength, mesh size and density, retention time, etc. Typical improvement between 1 and five brightness units can be expected as a result of processing kaolin in a magnetic field. Es-

[151] *TAPPI Test Methods*, Atlanta: TAPPI Press, 1997

sentially all kaolin is processed through magnetic separators. The most common separator size in current use can process kaolin slurry at typically 70 to 120 m^3/h, which translates to a production rate of approximately 23 to 45 metric tons per hour (dry basis). Most of the magnetic separation devices used in the purification of kaolin clay are resistive magnets that operate in batch mode. However, both batch-type and reciprocating-type superconducting magnets are quickly displacing their resistive counterparts.

Titanium Dioxide

Rutile or anatase is a naturally occurring ore containing microscopic particles of titanium dioxide (TiO_2). It is the most effective white pigment used in the paint, paper, and plastics industries. It is widely used because it efficiently refracts visible light imparting whiteness, brightness, and opacity when incorporated in a huge variety of fabricated products. Titanium dioxide is chemically inert, insoluble, and thermally stable under the harshest processing conditions. TiO_e is produced commercially in two crystal forms—anatase and rutile. Rutile based pigments are preferred because they refract light more efficiently, are more stable, and less photoreactive. Worldwide, over 2.2 million metric tons of TiO_2 are produced annually. A typical method for the separation of titanium dioxide is shown in Figure 12.66.

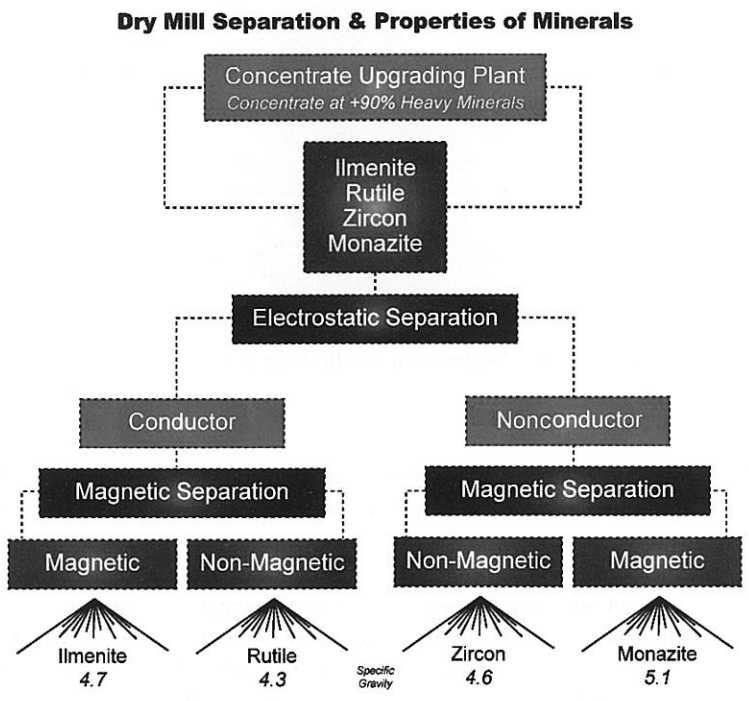

FIGURE 12.66: Dry mill separation process of rutile and ilmenite. (Courtesy Outotec Inc.)

Magnetic separation is used in both the front end screening process as well as the final processing of the "fines" of the product. As shown in Figure 12.66, both ilmenite ($FeTiO_3$) and rutile (TiO_2) are electrically conductive, but, successful separation is possible because ilmenite is strongly paramagnetic and rutile is very weakly paramagnetic.

12.6.9 Summary

Magnetic separation has been used in the processing of materials for more than one hundred years. Magnetic separation has a variety of modern uses ranging from the simple removal of tramp iron to the highly sophisticated removal of weakly paramagnetic minerals from clays. There are several different types of magnetic separation devices available. The choice and type of magnetic separator best suited for a particular application depends upon several variables such as wet or dry processing, magnetic susceptibility of the materials present, magnetic fraction of the feed materials, particle-size, and processing rate. The introduction of High Gradient Magnetic Separation greatly expanded the role that these devices play in the mining of minerals. It has been estimated that the introduction of HGMS has nearly doubled the worldwide useful reserves of kaolin clay, by allowing the mining of lower grade material. It is clear that in large-scale high gradient magnetic separators, low temperature superconducting technology is displacing conventional water-cooled copper magnets. With the recent discovery of high temperature superconductivity, it remains to be seen if these new ceramic-oxide superconductors will replace the traditional intermetallic low temperature superconductors.

Magnetic separation techniques are being explored in many non-traditional applications such as wastewater cleanup, the removal of pyritic sulfur and ash from pulverized coal, chemical processing, and the removal of uranium oxide compounds from contaminated soil. The use of "magnetic seeding" techniques on non-magnetic materials may open an entirely new area of benefits and applications. As more research and development is being performed, magnetic separation techniques continue to find new areas of potential environmental and commercial benefit.

12.7 Superconducting Induction Heating of Nonferrous Metals

Niklas Magnusson and Larry Masur

12.7.1 Conventional Aluminum, Copper and Brass Induction Heating

Electromagnetic induction is widely applied for industrial heating of metals. The process is fast, clean, and in most cases very energy efficient[152]. However, when heating non-magnetic materials with low electrical resistivity such as aluminum, copper and brass, the efficiency becomes low. In aluminum extrusion plants, 50/60 Hz induction heaters are used to preheat billets, large cylinders, about 0.2 m in diameter and up to or above 1 m in length, from room temperature to around 500 °C to soften the metal before the billet is pressed through the extruder.

In conventional billet heaters, AC currents are passed through copper coils to generate a strong time-varying magnetic field. The aluminum billet is placed in this field, and the resistive losses due to the electric currents being induced in the billet generate heat, Figure 12.67. The efficiency of the process depends to a large extent on the losses in the induction coil. The current density of the windings of the induction coil is extremely high, typically around 20 A/mm^2, and, consequently, modern aluminum billet heaters operate with efficiencies in the 50% range, being one of the large-scale electrotechnical components with absolutely the poorest energy efficiency.

Large heaters have power ratings exceeding 1 MW of which 500 kW are losses dissipated in the hollow, water-cooled copper conductors and then converted into useless cooling water at temperatures around 40 °C. With 4000 operating hours per year and an energy cost of $0.05/kWh, the

[152] N. Magnusson and M.Runde, Proc. Eighth Int. Extrusion. Tech. Seminar, Orlando, FL, USA, (2004) 389

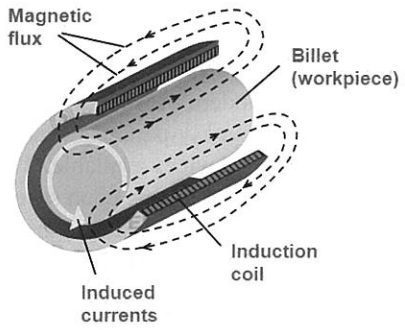

FIGURE 12.67: Principle of conventional induction heating[153].

annual value of the energy losses becomes $ 100,000 for one unit.

12.7.2 AC Superconducting Induction Heating

To increase the efficiency, the losses in the induction coil have to be reduced. One approach is to introduce windings consisting of superconducting material. In 2002 a small-scale (10 kW) superconducting AC induction heater shown in Figure 12.68, was designed, built and tested. The aluminum billet to be heated was placed in the center and was enclosed by high-temperature thermal insulation. The BSCCO/Ag HTS coil was built up of 24 double pancake coils. At the coil ends flux-diverters were inserted in the form of transformer sheets to straighten the magnetic field and hence to reduce the radial magnetic field, which otherwise would result in unacceptably high losses. The HTS coil was immersed in liquid nitrogen.

The energy efficiency of the small-scale AC superconducting induction heater was 47%, which is about the same as for conventional heaters. However, studies showed that scale up advantages and the use of an AC optimized superconductor could increase the efficiency to 80-90%. Hence, by replacing the copper windings of the AC induction coil with windings of HTS tapes, there is a potential for increasing the efficiency beyond 80%. However, the investment costs for such a solution (especially for the cooling device) are rather high and it requires the development of an AC optimized HTS tape.

12.7.3 DC Superconducting Induction Heating

The AC superconducting induction heater was, although clearly energy saving, not economically viable. At this point it was necessary to go back to the electromagnetic basics and reconsider the concept[154].

From Lenz's law we know that currents are induced in a loop when the magnetic flux enclosed by the loop is subjected to a change. For the conventional induction heater, this change is obtained by applying an AC magnetic field to the material to be heated. An alternative solution to obtain the change in magnetic flux is to rotate the material in a static magnetic field. When the loop is rotated with constant speed in the DC magnetic field, the enclosed flux varies sinusoidally in the same way as a static loop in a sinusoidal magnetic field, Figure 12.69.

To accomplish the change in enclosed flux in the aluminum billet, the topology of the rotating

[153] Reprinted with permission from the *Proceedings of the Eighth International Aluminum Extrusion Technology Seminar*, published by the Extrusion Technology for Aluminum Profiles Foundation.

[154] N. Magnusson, *Proc. Int. Symp. Heat Electromag. Sourc.*, Padua, Italy, (June 2007) 497

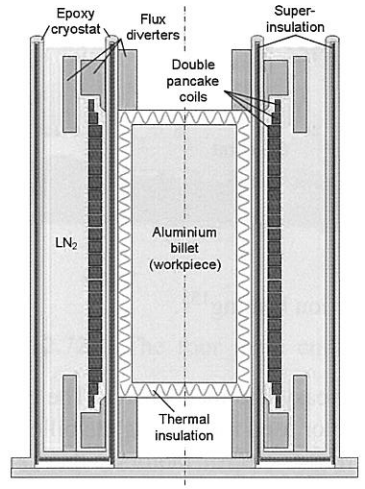

(a)

(b)

FIGURE 12.68: Schematic drawing of the AC induction heater (a) and the superconducting induction coil (b)[153].

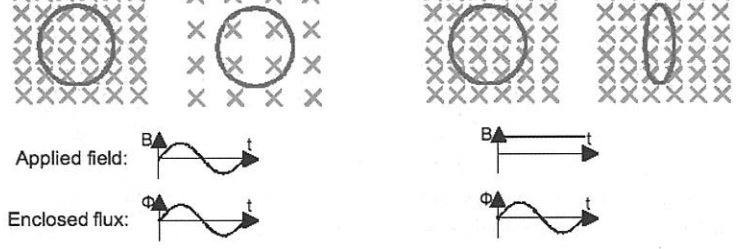

FIGURE 12.69: Applied magnetic field and enclosed magnetic flux in a loop for a time-varying field and a static loop (left) and a static field and rotating loop (right)[155].

billet heater becomes different from the one of a conventional heater. With the magnetic field oriented in parallel with the billet axis, the enclosed flux is not changed as the billet is rotated around its axis. Instead, the magnetic field should be applied perpendicular to the billet axis. Consider the schematic drawing in Figure 12.70. A DC current in a coil generates a DC magnetic field oriented perpendicular to the axis of the aluminum billet. The aluminum billet is rotated around its axis. For any given loop in a plane parallel to the rotational axis, the magnetic flux enclosed by the loop will change as the billet is rotated and hence currents are induced and these induced currents cause resistive heating in the billet. As the billet is rotated by a motor, mechanical energy from the motor is converted into heat in the billet.

The DC currents generating the DC magnetic field are passed losslessly through the coil by the

[155] Reprinted with permission from the *Proceedings of the 2007 Heating by Electromagnetic Sources Symposium.*

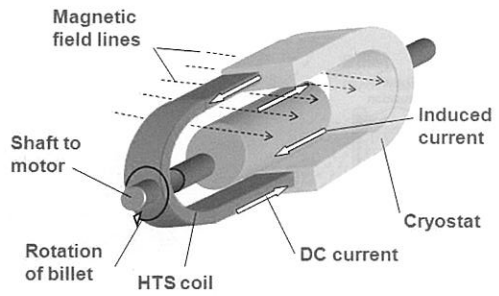

FIGURE 12.70: Principle of DC superconducting induction heating[153].

use of superconducting wires or tapes making the cooling easy and inexpensive. The efficiency of the system becomes determined by the efficiency of the motor used for rotating the billet and by the need of cooling power and the cooling efficiency. Asynchronous electric motors in the 500 kW class typically operate with efficiencies well above 90% yielding an overall efficiency of up to 90% when also the efficiency of the cooling system is considered.

12.7.4 Commercial Deployment

The first magnetic billet heater was put into commercial operation at the German aluminum extrusion works Weseralu GmbH & Co KG, in July 2008. Weseralu extrudes approximately 14,000 t of aluminum profiles per year for an annual turnover of about €50 million. Weseralu's market focus is on highly demanding profiles for the automotive and engineering sectors; hence high technical achievement in billet heating is an important part of the manufacturing strategy.

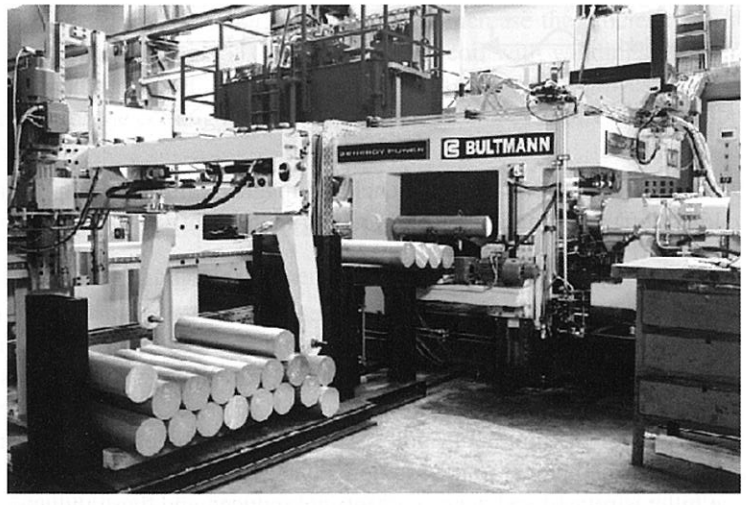

FIGURE 12.71: Photograph of magnetic billet heater operating at Weseralu aluminum profile extrusion plant[156].

[156]Reprinted with permission from *Light Metal Age Magazine* 67:2 (2009)

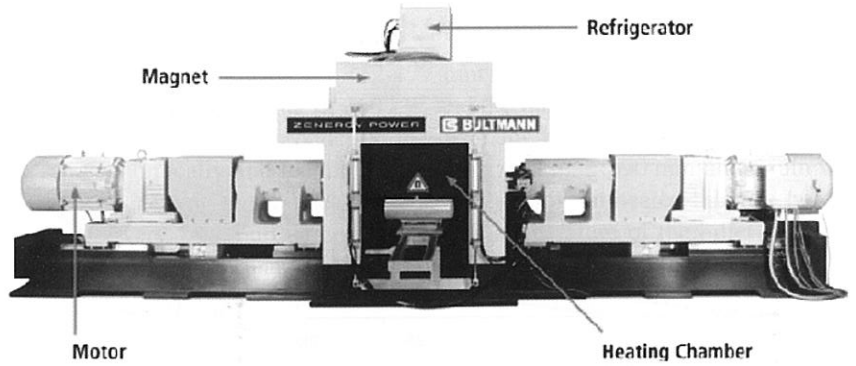

FIGURE 12.72: The four main components of the magnetic induction heater for aluminum billets[156].

This magnetic heater which has been in commercial operation at Weseralu is equipped with a DC-powered superconductive magnetic coil. Due to the uninhibited flow of electricity the coil delivers a sufficiently strong magnetic field for induction heating with a power input of merely 10 W. As described above, the rotation of the billet induces eddy currents, which work to oppose the rotation and create a strong braking torque. This is overcome by industrial electric motors of a size of 100 kW-500 kW. The energy consumed by the motors is directly converted into heat within the rotating billet. The power supply of the motors involves standard frequency converters which cause electric losses on the order of 2–3% of the total power consumption of the magnetic heater. The cooling system and the power supply of the magnet consume about 13 kW. The total energy efficiency of a magnetic heater including all losses caused by peripheral technical devices is greater than 80%. A photograph of the plant is shown in Figure 12.71.

12.7.5 Simple Technical Design

As shown in Figure 12.72, the central component of a magnetic heater is a superconducting magnet. A refrigeration system consisting of commercial off-the-shelf components keeps it at its operating temperature. The magnet generates a magnetic field which penetrates into two thermally insulated heating chambers in which the billets rotate. Electric motors on either side provide the rotational energy. The motors can slide in and out to accommodate different billet lengths and a hydraulic system locks the billets to the drive systems. The machine focuses the heating effect exclusively on the rotating billets. In contrast to AC induction heaters, no critical component in the magnetic heater is subjected to significant temperature increase, vibrations or any other mechanical stress factors.

12.7.6 Low Frequency Billet Heating

A magnetic heater reduces the power consumption of heating aluminum billets to an average 150 kWh/t and at the same time improves the quality of the heating process. AC induction heaters operating at normal power grid frequencies of 50–60 Hz induce eddy currents mostly close to the surface of billets. In contrast, lower frequencies and a more powerful magnetic field lead to a deeper penetration of heating energy. For magnetic heating it has proved favorable to rotate billets within the magnetic field at speeds between 240 rpm and 750 rpm. This corresponds to frequencies of 4–12.5 Hz. Figure 12.73 illustrates the difference in penetration depth between an AC induction heater operating at 60 Hz and a magnetic heater operating at 4 Hz. The x-axis shows the position along the

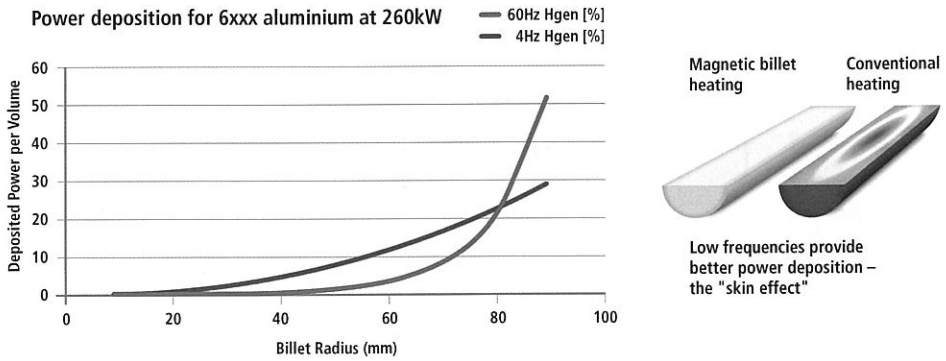

(a) (b)

FIGURE 12.73: Comparison of deposited heat per volume as a function of distance from billet center between 60 Hz and 4 Hz magnetic induction frequencies for aluminum[156].

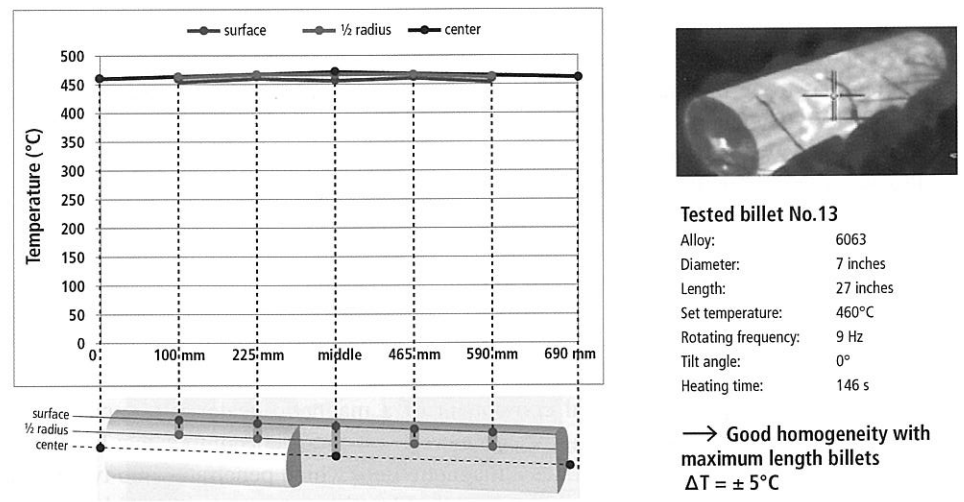

Tested billet No.13

Alloy:	6063
Diameter:	7 inches
Length:	27 inches
Set temperature:	460°C
Rotating frequency:	9 Hz
Tilt angle:	0°
Heating time:	146 s

⟶ Good homogeneity with maximum length billets
ΔT = ± 5°C

(a) (b)

FIGURE 12.74: Comparison of temperature along the length and at the center and surface of an aluminum billet after heating. Note the negligible temperature gradient[156].

radius of the billet while the y-axis gives the heating power. Even though the total power delivered to the billet is the same in both cases, the 60 Hz curve is delivering higher power at the surface of the billet and then falling to less than 20% within about 15 mm of the surface. On the other hand, at 4 Hz the power input is much more uniform, penetrating about 50 mm before falling to 20%. With a magnetic heater the energy penetration is three times as deep as with an ac induction heater. This leads to a much more uniform heating, Figure 12.74, which provides better preconditions for the subsequent extrusion. Moreover, the heating process can be run faster and does not involve a risk of locally melting the material.

12.7.7 A Field Report: Experiences with Operation

This magnetic heater is optimized for 152-177 mm diameter billets with a length of 690 mm. Its electric drives have a power output of 360 kW and the machine has a capacity of 2.2 t/hr when heating aluminum. In commercial production the magnetic billet heater has been found to be advantageous both economically and technically. Heating 152 mm×690 mm aluminum billets takes only 140 s per billet; heating two billets simultaneously allows a heated billet to be delivered to the extrusion press every 70 s. Furthermore, the target temperature of the billet could be lowered by more than 30 °C due to the enhanced temperature homogeneity throughout the billet. The lower billet temperature in turn enabled improvements in extrusion, especially with complex and highly precise aluminum profiles. Moreover the quality of surface finishes has been improved. At Weseralu GmbH & Co KG, the increase of productivity directly attributable to the deployment of the magnetic billet heater has been found to amount to an average of 25% across a variety of profiles. Achieving these results did not involve any significant additional expense; the results occurred as a consequence of optimizing the billet temperature and extrusion speed. At the same time the cost of heating aluminum billets was reduced by 50% compared with conventional induction heating. The combined economic effect of energy savings and productivity improvements resulted in a payback period of less than two years for the magnetic billet heater.

12.8 Superconducting Magnets for NMR

Gerhard Roth

12.8.1 Introduction

When Edward Purcell in 1945 and Felix Bloch in 1946 independently recorded the first Nuclear Magnetic Resonance (NMR) signal[157,158], for many years no one thought that NMR would ever develop into such a large field of diverse applications, a field of research which today is giving us deep insight into the chemical structure of molecules, biomolecules and since 1978 even into living bodies. Very much like the phenomenon of superconductivity, NMR started as a physics discovery leading to the Nobel Prize for a number of researchers who first described the new effect[159,160,161,162] ; the phenomenon then disappeared for many years amid the vast amount of new science, but once the time was propitious, the background technology appeared and industrialization led to its widespread practical use. Even particle physics became involved in the late 1960s when experiments involving dynamic polarization of various nuclei became an essential tool in the study of the structure of matter using the then rapidly increasing access to electron and proton beams from high energy accelerators[163,164].

Today, NMR methods are continuously developing as an advanced analytical tool, expanding

[157] F. Bloch, W. W. Hansen and M. Packard, *Phys. Rev.* 70 (1946) 460
[158] E. M. Purcell, H. C. Torrey and R. V. Pound, *Phys. Rev.* 69, (1945) 37
[159] P. C. Lauterbur, *Nature* 242 (1973) 190
[160] M. K. Stehling, R. Turner, and P. Mansfield, *Science* 254 (1991) 43
[161] A. Kumar, D. Welti and R. R. Ernst, *J. Magn. Res* 18 (1975) 69
[162] G. Otting, E. Liepinsh, B. T. Farmer and K. Wuethrich, *J. Biomol.* NMR 1 (1991) 209
[163] M. Borghini and A. Abragam, *Compt. Rend.* 248 (1959) 1803
[164] H. Desportes and B. Tsai, *Proc. Int. Symp. Magn. Techn.*1965, 509, Stanford Linear Accelerator Center, Stanford University, Stanford, California, Sept. 1965

into new fields of applications in industrial process control, as an analysis and screening tool in food industry, in medicine for the screening of newborns for certain inherited deceases. The growth of NMR is intimately connected with the development of superconducting magnets for the simple reason that the signal-to-noise ratio of the NMR signal increases with the square of the magnetic field strength and the spatial resolution between individual signals increases linearly with the magnetic field strength. This was recognized as early as 1965, and became especially important once the chemical shift was discovered and the relation of this shift to the chemical neighborhood of the observed nucleus.

The limitations of permanent and electromagnets were appreciated in the early 1960s; further progress in NMR techniques became closely connected to progress in superconducting magnet technology, which in turn became the most important and also the most expensive part of an NMR spectrometer[165]. We tend to forget the role which the other, equally important enabling technology, played in the development of the spectroscopy industry, namely the development of the digital computer. Both technologies were responsible for the unprecedented growth of a relatively arcane phenomenon and its intrusion into everyday life, specifically MRI, the offshoot of NMR, both of which today account for the only truly large scale commercial application of superconductivity.

NMR is an important method for structure determination in analytical chemistry and biology as well as in various specialized applications such as, for example, its younger brother, MRI, where it is widely used for diagnostics in medicine. Many building blocks from different areas needed to come together to form today's complex instruments and one key component of these is quite naturally the magnet, the superconducting magnet. In its early days NMR had to do with a permanent or a resistive magnet, limited in performance to the registration of simple signals from elements or proton signals in a few simple molecules. However, for today's largely diversified and demanding applications the use of high field magnets, that is superconducting magnets, is essential.

As an illustration what an early NMR spectrometer looked like, Figure 12.75 is an example of the first commercial NMR spectrometer manufactured in 1962 by the Trüb-Täuber company of Switzerland, equipped with a 25 MHz (0.59 T) permanent magnet.

We should comment here that, as in other branches of science, the terminology of NMR usage had assumed its own course: the magnetic field strength is always expressed in MHz, corresponding to the resonance frequency of protons at that particular field. The "frequency to field" ratio is fixed for each individual nucleus. For hydrogen, this ratio is 42.576 MHz per tesla, thus the magnetic field strength of this first magnet would have been 0.59 T. The necessary spectrometer electronics needed three large cabinets, filled with advanced RF-tube technology of that time. Experimentally it was hard work to get all parameters adjusted in the right and stable way to be able to record a resonance signal. Contrast this with Figure 12.76 which shows a modern 300 MHz (7.05 T) spectrometer with experimental capabilities exceeding by far those implemented in the first 25 MHz system and a 1000 MHz magnet, the latter being the dominant part of a very high field spectrometer. The lowest frequency superconducting NMR system available today is based on a 7 T magnet.

The 1000 MHz spectrometer installation has a 23.49 T magnet, reasonably compact electronics and is a system which offers a huge variety of experimental possibilities. The magnet weighs about 15 t and stores an energy of some 50 MJ. It represents the zenith of both the current thinking in advanced magnet design and the latest superconductor wire technology.

Superconducting magnets for high resolution NMR have certain features, which although not unique to this application do necessitate a somewhat different approach in magnet design than standard precision laboratory magnets. The requirements are demanding and restrictive:

- Stability: very low drift over time with a field decay in the range of $< 1 \times 10^{-8}$ Hz/h.

[165] P. Grivet and M. Sauzade, *Proc. Int. Symp. Magn. Techn.*1965, 517, Stanford Linear Accelerator Center, Stanford University, Stanford, California, Sept. 1965

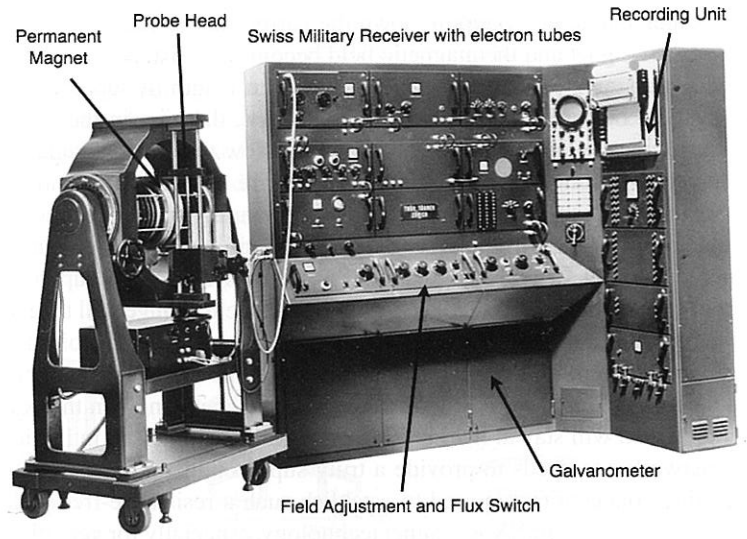

FIGURE 12.75: First commercial 25 MHz (0.57 T) NMR spectrometer in 1962 by Trüb-Täuber. (Courtesy T. Keller, Bruker Biospin.)

FIGURE 12.76: 300 MHz NMR spectrometer, left, 1000 MHz NMR magnet, right. (Courtesy Bruker-Biospin.)

- Homogeneity: in the range of $\sim 1 \times 10^{-10}$ over a sample volume 10 mm in diameter by 30 mm in length.
- Helium consumption: A cryostat system with very low helium consumption to ensure good long term stability and requiring little or no attention.

12.8.2 Stability

To meet the required criterion of very high stability over time the NMR magnet must be operated in the persistent mode, a continuous feed from a power supply simply will not do. In this mode, once the magnet has been ramped up to full field, the magnet windings are connected to a superconducting short circuit which allows the current to circulate in what amounts to a resistance free loop. Once

the closed loop is superconducting, ramping down the current in the current leads to zero will not affect the current in the magnet and the magnetic field becomes persistent.

This is effected with a superconducting switch which is a length of superconducting wire surrounded by an electrical heater. When the heater is activated, the wire in the switch becomes resistive and, when ramping up the magnet, the current will flow through the superconducting path. The resistive voltage drop along this normal conducting wire length corresponds to the inductive voltage drop across the superconducting coil generated by ramping up the magnet. Once full field is reached, the voltage drop across the magnet and the switch will level off after some time. Then the heater of the superconducting switch is switched off and the wire becomes superconducting again. When the current of the power supply is reduced again, the current change will take place only along the resistance-free path and not along the inductive path of the coil. At this point the power supply current can be reduced to zero and the current leads and the power supply can be removed from the magnet. The process is illustrated in Figure 12.77. The magnet is now in the persistent mode, a "persistent" magnet which will stay at field as long as it remains immersed in liquid helium. In this simple electrical network one needs to provide a truly superconducting path for the loop current; these superconducting connections required to establish such a resistance-free path were and still are one of the biggest challenges in NMR magnet technology, especially for very high field magnets. In modern superconducting magnets such switches can be manufactured in an almost perfect way, so that the resulting magnet drift frequently falls below 2 Hz/h which corresponds to a decay time of 30,000 years. Obviously such a decay time would meet the most demanding requirements of any NMR spectroscopist.

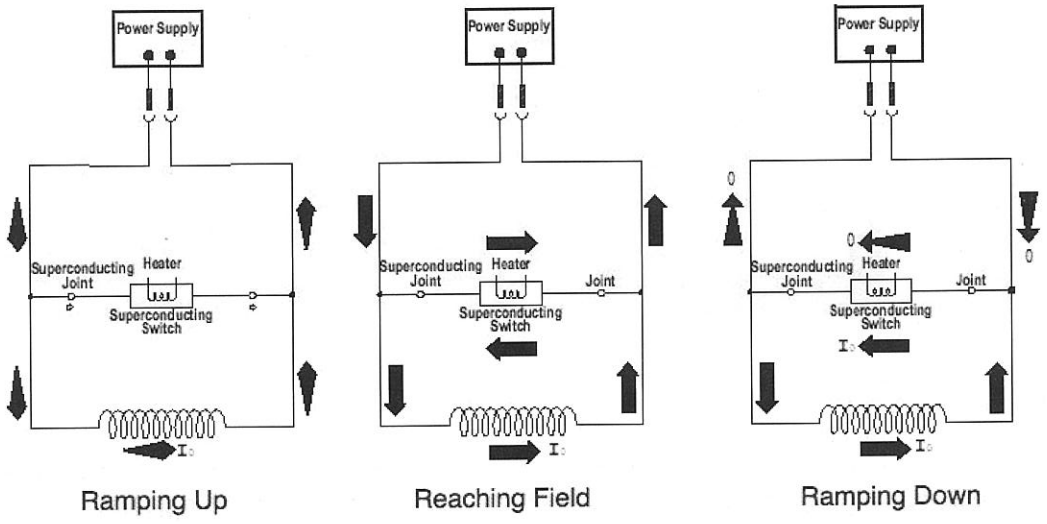

FIGURE 12.77: Making a magnet persistent.

12.8.3 Homogeneity

A magnetic field precision of 10^{-10} implies a frequency resolution of 0.1 Hz at 1 GHz, which corresponds to a high resolution line width. Typically the goal for the superconducting magnet is to reach homogeneity of $\sim 10^{-5}$ over an axial length of ~5 cm, which can be achieved by designing the magnet as a solenoid with correction coils, which compensate for the second, fourth and even-

tually higher order field errors. In addition, such a solenoid is equipped with a set of further small correction coils, the superconducting shim coils which can be adjusted individually. Normally the magnet as manufactured will not reach the calculated homogeneity, as there are always winding errors and imperfect mechanical tolerances, which will introduce unacceptable errors in the field, usually irregular gradients. The usual procedure after fabrication is to survey the existing field gradients by measuring the magnetic field irregularities with NMR probes and then correcting the errors by energizing the compensating superconducting shim coils.

At the outset when the magnetic field strengths were still low, it was sufficient to apply a first order correction in x, y and z only (Figure 12.78).

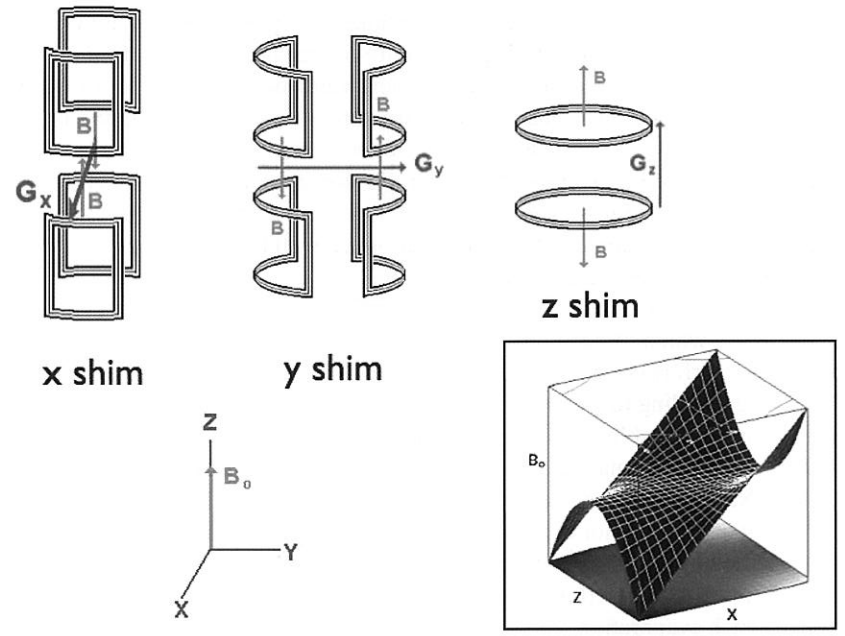

FIGURE 12.78: Three first order x, y, z shims. Insert: xz^2 shim field correction plot.

With increasing field strengths, z^2 needed to be added and for magnets containing Nb_3Sn it became common practice to add second order shim coils as well to correct zx, zy, xy and $x^2 - y^2$ field errors. As the error correction contribution of these shims decreases rapidly with their distance from the magnet center, the correction coils require a very large number of turns in large magnets. This large number of turns cannot be wound perfectly which introduces another effect here: as the influence of the first order shims decreases less rapidly with the distance from the magnetic center, winding errors in the second and higher order shim coils lead to a considerable change in the first order shim settings when the second order shims are applied. When a third order shim is applied the influence on the lower order shims dramatically increases so that for large superconducting shims this can no longer be done.

With an appropriate set of first and second order superconducting shims the basic homogeneity requirements can be satisfied. Once this is achieved, a third set of higher order correction coils is added, consisting of resistive room-temperature shims inserted into the room temperature bore of the complete magnet. In low field magnets these additional room-temperature shim systems usually contained a total of 12 different shims. For 500 MHz devices, this was extended to 20 and later to 32

different shims correcting up to the fifth order. In current high field magnets, the room-temperature shim systems typically contain around 40 different shims, which can be addressed separately and are able to correct gradients up to the eighth order.

12.8.4 Cryostat

The cryostat housing the NMR magnet system is an equally important component defining the long-term stability. NMR devices are sufficiently sensitive that they can monitor changes in the thermal equilibrium conditions in the outer cryostat system, that is changes in cryostat temperature through ambient temperature changes. Ambient pressure changes can also be observed, even the bubbling of evaporating liquid helium and liquid nitrogen when evaporation rates are too high are registered. At lower fields this was not an issue, fortunately cryostat technology improved in step with increasing field strength and increasing sensitivity of the spectrometers. In the early days typical helium hold times were only a few days, but they were soon extended to a month and more. Today hold times are approaching values in the range of up to 1 year, depending on magnet type and even for small cryostats.

Progress was not achieved by simply increasing the storage volume of the helium and nitrogen vessels, but by reducing the helium evaporation rate down to incredibly low levels, to ~ 5 ml/h for the small magnets, so that the annual consumption dropped well below 50 l per year, corresponding to helium costs of typically less than € 500 per year.

Until the early 1990s all magnet cryostats were operated at 4.2 K. By the time NMR frequencies approached 500 MHz, which of necessity would involve Nb_3Sn technology, several attempts were made to improve the performance by taking advantage of the field shift in the critical field of NbTi wires by ~3 T, corresponding to ~130 MHz, by lowering the temperature of the helium bath[166].

In an early attempt to establish a long-term stable helium cooling technique suitable for NMR magnets, a 500 MHz (11.7 T) magnet was successfully designed and built for operation at 2.3 K at the Francis Bitter National Magnet Laboratory at MIT[167] (Figure 12.79). The method to generate temperatures below 4.2 K was not exactly unique as the magnet bath was directly pumped in the usual manner. The helium vessel was in turn surrounded by another 4.2 K vessel, isolated from the magnet bath. Helium was transferred from the 4.2 K vessel through a needle valve into the 2.3 K magnet bath in a "flash evaporation" process while pumping. Although this system was operational for a while, it turned out that this method was not really suitable for a long-term stable NMR magnet with little or no need for customer interference to operate the magnet. Also, with a line width of 1.5 Hz, this was not really a high resolution system, one which would normally require a line-width typically is in the range of 0.2 Hz.

The transition to a long-term stable and disturbance free high resolution NMR magnet took more than another decade, until the first fully sub-cooled magnet using pressurized He II technology was introduced in 1992 to push the highest available field strength to 750 MHz (17.6 T).

A similar direct method of directly pumping on a helium bath was extensively used in high energy physics (HEP) experiments at various accelerator facilities when dynamically oriented and polarized targets were used in numerous nuclear structure investigations[168]. In this NMR application the magnetic fields employed were relatively low, rarely exceeding 6 tesla, but the magnets themselves were unusually complex Helmholtz systems, with sixth to eighth order corrections. Access for detectors was the reason for the open magnet structures, and helium consumption was irrelevant in the presence of large helium recirculating liquefaction plant.

[166] W. D. Coles, G. V. Brown, E. H. Meyn and E. R. Schrader, *J. Appl. Phys.* 40 (1969)

[167] J. E. C. Williams, L. J. Neuringer, E. Bobrov, R. Weggel, D. J. Ruben and W. G. Harrison, *Rev. Sci. Instrum.* 52 (1981) 649

[168] T. Powell, M. Borghini, O. Chamberlain et al., *Phys. Rev. Lett.* (1970) 753

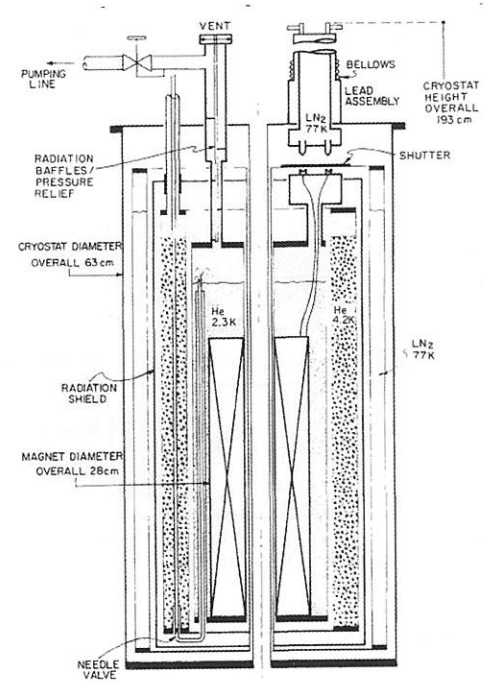

FIGURE 12.79: First NMR magnet operated at ~2.2 K, which was designed and built at MIT in 1979.

12.8.5 Major NMR Magnet Development Steps

The history of this science is relatively long. On occasion, years were needed to solve certain issues before progress could be made, progress which depended not only on the continuous development of superconducting strands but also on new magnet technology; see Figure 12.80.

A good example of this is the long time delay between the 500 MHz and 600 MHz magnets where no new superconducting materials were introduced when compared with the relatively short period for the 750 MHz, 800 MHz and 900 MHz magnets which occurred after the introduction of the new 2 K sub-cooling technology. However NMR did not develop in a technological vacuum; other large scale research applications instigated the intense and detailed research into superconducting materials, as we have observed before, thereby greatly benefiting the advances in related fields using superconducting materials and superconducting magnets. Modern technology is only too familiar with such multi-parameter relationships, not necessarily linear, the growth in size of particle accelerators being an example of technical progress driven by multidisciplinary science needs.

As mentioned before, early NMR spectrometers used permanent or resistive electromagnets which ultimately covered frequencies up to 90 MHz. The first major system involving superconductors was the introduction in 1968 of a 180 MHz (4.2 T) magnet, made with single-core or mono-filamentary NbTi conductor. This frequency was chosen because it was a multiple of 90 MHz, a frequency common to a number of installed spectrometers. The frequency also had the advantage that it simply could be reached by just doubling the existing 90 MHz spectrometer frequency.

Soon a new generation of 200 to 300 MHz (4.7 to 7 T) magnets appeared, which was quickly extended to 360 MHz (8.5 T), the reason being that at this field/frequency the limit for magnets built from mono-filamentary NbTi wire was reached. The widely observed occurrence of flux jumps led to numerous magnet quenches and a number of magnet failures in the production. The problem, as

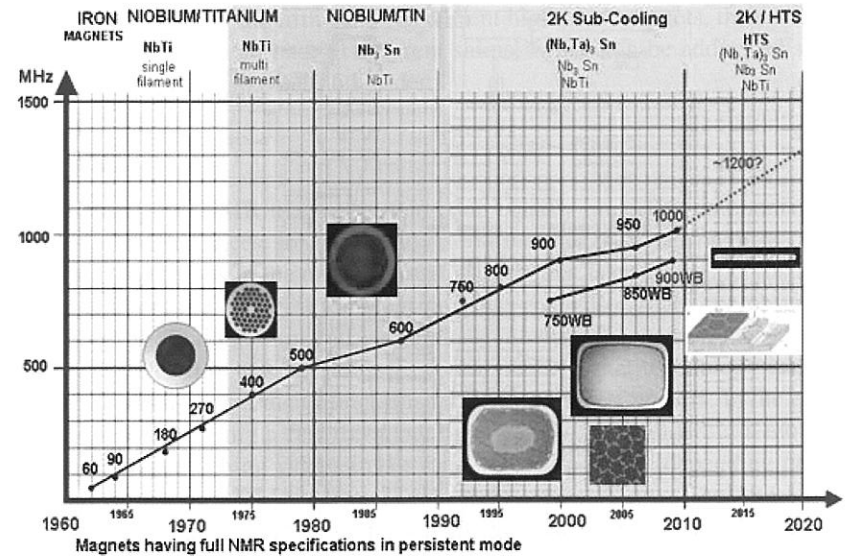

FIGURE 12.80: Progress of the NMR frequencies as a function of time.

always, was caused by too large a filament diameter, somehow violating the then understood stability criteria. During this period the underlying theory of stability was being introduced, conductor manufacturers were beginning to understand the problem and were quickly introducing new multifilamentary conductors with many small filaments to satisfy demand. In spite of new conductors, the magic threshold of 8.5 T, and thus the magnet with the highest field, remained uncrossed for a few more years.

To reach 400 MHz (9.4 T) required more NbTi wire development and NMR spectroscopy at that time but fortunately an unrelated branch of physics, HEP, needed more advanced materials. Not only were large particle detectors being built with superconducting magnets, but the accelerators themselves were assembled from many hundreds of superconducting magnets. This activity demanded not only industrial production of the materials, but also major qualitative improvements. As soon as there was production experience, the necessary process adjustments could be made and reliable materials with substantial critical currents at ~9.5 T could be manufactured reliably. The composition of NbTi was adapted for high field use so that from the early 1980 on, 9.4 T magnets could be built routinely. Ultimately though, in spite of significant improvements in the high field properties of NbTi, the limit was reached at this field.

12.8.6 Nb_3Sn Technology

The next step to reach even higher fields required the use of superconductors, with higher upper critical fields, so that the field range could be extended. There were several promising superconducting compounds; among these were Nb_3Zr, Nb_3Al, Nb_3Sn and Nb_3V. Initially the properties of these diverse compounds were similar, but the industrial production of Nb_3Sn in tape form quickly assured the dominance of this material. However the detrimental properties of tape were soon recognized so that attention reverted to the production of filamentary conductor. Again the demand subsided and such developments which took place focused on understanding the mechanical properties of the material rather than on improving the electrical and magnetic behavior. At this stage, at the beginning of the 1970s, another outside interest began to influence the thinking behind niobium-tin: plasma physics and its demands in connection with fusion reactors. These devices required high magnetic

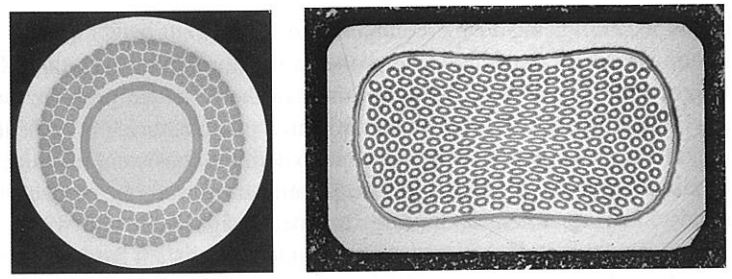

FIGURE 12.81: Examples of Nb_3Sn conductor with inner copper stabilization, (left) and with outer copper stabilization, (right).

fields in large volumes spurring the industry to re-examine its programs vis-à-vis niobium-tin.

In the Large Coil Task Demonstration Program at the Oak Ridge National Laboratory in the US, a sextuplet of large FD-shaped coils manufactured in the US, Europe and Japan, demonstrated that niobium-tin has potential; the project rekindled interest in this material. In the ensuing decade interest in other niobium compounds faded, Nb_3Sn became the material of choice for high field DC applications and its production followed in the footsteps of NbTi in the form of multi-filamentary copper clad conductor. This conductor was produced in every variant demanded by the application, strand, wire, cable, monolith, just like NbTi, but with one very important difference: the magnet with which it was wound needed to be heat treated to form the compound. This heat treatment requirement resulted in a number of different manufacturing processes, each appropriate for its intended application.

The bronze process described below is suitable for DC applications such as NMR where magnetization issues at low fields are less important than for example, in pulsed accelerator magnets. Other manufacturing processes are used for such applications, but we must emphasize that in every application the triad of current, field and temperature must be adjusted to maximize the effectiveness of the device. The left side of Figure 12.81 shows an earlier round type of Nb_3Sn conductor with approximately 6,000 filaments with a diameter of ~4 μm each. The filaments are pure Nb embedded in a 13% CuSn Bronze tube. The boundary of the CuSn bronze is separated by a Ta barrier from the stabilizing Cu in the center. This is necessary as the material needs to be heat treated at 700 °C, to form the superconducting Nb_3Sn phase, a process in which tin diffuses into the niobium filaments in a solid state diffusion process. Without this barrier, tin inevitably would also diffuse into the surrounding stabilizing Cu, this way forming bronze, which would destroy the electrical and stabilizing properties of Cu at low temperatures. The conductor shown on the right in the figure is a modern high performance rectangular Nb_3Sn conductor with an inverted architecture. The stabilizing copper is on the outside of the conductor and the bronze is inside, again separated by a tantalum barrier. Embedded in the bronze are ~50,000 filaments, which may be of pure niobium or may in addition contain some tantalum. The bronze may in addition to Cu and Sn also contain some small amounts of Ti. After heat treatment, this structure will result in a $(NbTaTi)_3Sn$ conductor having the best high-field superconducting properties for bronze type conductors available today.

The new wire types faced some interesting problems in high-field NMR magnets caused by the complexity of the material. The material needed to be heat treated which reduced the ductility of the wire; the conductor became too brittle to be bent into the small radii of ~30 mm or so which would be needed for an NMR magnet. This led to the "wind and react" method mentioned earlier; that is the magnet coil was wound completely with the ductile, unreacted wire and then heat treated. Not only does this process have a rather long learning curve, new joining technologies had to be developed as well for connecting a small number of NbTi filaments with a large number of Nb_3Sn

filaments (~5,000 – ~50,000)) using a superconducting solder[169].

The early niobium-tin NMR magnets were prone to drifting which was initially attributed to malfunctioning joints. However, it turned out that most of the observed problems were due to the superconducting wire itself. Its brittleness, the complicated manufacturing process and the thermal heat treatment, included too many variable parameters to define a consistent manufacturing process. These problems existed for quite a while until the parameters governing bronze quality, filament size, drawing process, heat treatment conditions, magnet design itself and winding details were were fully understood. Early "good" magnets were considerably distant from what we expect good drift performance to be today.

Once the bronze route became established, many 500 MHz (11.7 T) magnets were routinely manufactured beginning in the early 1980s, followed later by 600 MHz (14 T) magnets. The long development time between these two systems was an unwelcome indicator that with existing technology progress towards even higher fields would be very tedious and slow, unless new methods were discovered thereby again speeding up high field development.

In 1985 the Research Center in Karlsruhe (now KIT) and Bruker entered into a basic development program aimed at introducing new technologies and extending the existing 11.7 T field strengths by at least 50%. This was a challenging project and the goal could be reached only by either obtaining superconductors with much higher critical currents at high fields or by increasing the critical current of existing superconductors by lowering the helium bath temperature below the lambda point.

12.8.7 Subcooling Technology

Initially it was believed that the extreme sensitivity of NMR experiments made the operation of high resolution magnets at helium temperatures below 4.2 K unlikely. Pumping on the helium bath was expected to introduce vibrations which would be detrimental to the resolution and the refilling of a low pressure bath would complicate matters. Fortunately in the development cooperation between the Research Center and Bruker in Karlsruhe alluded to before, the pressurized He II cooling method, invented at CEA in Grenoble, proved to be the route through which these magnets could be operated at about 2 K, thereby exploiting the properties of the superconductors used to the fullest.

The Research Center in Karlsruhe had existing experience with pressurized He II technology at that time which had been transferred successfully from the ideas developed and demonstrated at CEA during the TOSKA and Tore Supra programs[170]. The "HOMER" facility in Karlsruhe housed a readily available 19.3 T laboratory magnet[171], the field of which was extended to 20.3 T in 1988, at that time a world record for a pure superconducting solenoid[172]. This magnet had a large helium consumption, somewhere in the range of ~15 l/h, nor was it persistent and and its homogeneity was certainly not in a range that one could think of an NMR experiment.

At Bruker, also located in Karlsruhe, there was lot of experience with low-loss cryostats, with persistent magnets, with high homogeneity NMR magnets, with additional shim coils. Bruker also had the other components, which make an NMR spectrometer, such as probe heads, filters, high-frequency electronics, pulse programs and the necessary spectrometer software. The close vicinity of these two facilities was an excellent opportunity to combine the expertise in high field magnets and the expertise in NMR and start a collaboration with the goal of raising the available spectrometer frequency.

The "HOMER" installation also facilitated the study of the properties of new advanced superconductors at high fields, so that there was no necessity to extrapolate measured data to the desired

[169] C. A. Swenson and W. D. Markiewicz, *IEEE Trans. Appl. Supercond.* 9.2 (1999) 185

[170] G. Claudet et al., *Cryogenics* 26 (1986) 443

[171] P. Turowski and T. Schneider, *Cryogenics*. 27 (1987) 403

[172] P. Turowski and T Schneider, *Physica* B 155 (1989) 87

field strength for the planned magnets. This provided a degree of confidence in magnet design, in addition to the existing high fields expertise, so that the first project was able to reach its goal successfully after only seven years of development. The progress in wire technology did not stop either and with $(NbTa)_3Sn$ capable of higher current densities at high fields, it became possible to design 18 T magnets at 4.2 K. Also the new higher current densities allowed the rapid advance to 800 HHz (18.8 T), a frequency which was previously accessible reliably with sub-cooled magnets only.

The sub-cooling technology for high resolution NMR magnets proved to be one of the more intricate components of the collaboration, as for once the problem was not technological but cultural: how to adapt the physics laboratory technology to NMR customer, who is not interested in operating a complex superconducting magnet, but only in performing analytical experiments. The difficult part here was to make the system reliable and convenient enough, with limited attention by the user. The helium consumption had to be reduced as far as possible and the system was required to exhibit extreme long term stability without supervision. Ultimately the combination of Bruker's low-loss cryostat expertise and the experience of the Research Center Karlsruhe in the design and construction of pressurized He II cryostats resulted in a "100 mW-cryostat". This was a big step forward, as now the helium consumption was reduced by a factor of ~100 in comparison with the performance of other laboratory magnets of similar size. The helium usage of the first systems was 140 ml/h with a liquid hold-time of two months. The sub-cooling method required for long term stability is quite simple: the helium vessel is divided into two parts, isolated thermally but connected hydrostatically. Helium from the upper reservoir is expanded through a J-T valve at about 10 mbar, then passes through a heat exchanger and leaves the cryostat via a narrow bore pumping line. Such a system has the necessary long term thermal stability and requires the minimum of customer attention once it has been properly set up.

The other big issue was to suppress any vibration, which could arise from the pumping system required for the low-temperature operation. Thus from the very beginning the design preconditions required that vibration sources be reduced to the lowest possible level; the pumping line from the magnet to the pumping station was equipped with vibration stops so that no pump vibration effects were observed in the NMR signal.

It is only natural that when vibration issues occurred, as happened from time to time due to external sources such as traffic, building vibrations and so on, it became common practice of the service personnel to blame the pumps and to switch the pumping system off as a first test. It took quite a long time before everybody realized, that the origin of the vibrations was never the pumping system, but invariably some other external source. Once the peripheral issues were settled, the truly sub-cooled high field magnet using pressurized He II technology became a fully usable, commercially viable, high resolution NMR magnet. Figure 12.82 illustrates the new 750 MHz (17.6 T) magnet as well as the sub-cooling technology described.

No sooner was the basic design methodology for very high field magnets established, than it became increasingly obvious that it would be difficult to extend this field to even higher values as the known superconductors were approaching their upper critical field values with rapidly decreasing current densities. Of course the available current densities also improved slowly, and ultimately the NMR frequency could be pushed to the current 1 GHz [173]. In 1996 an actively shielded 600 MHz magnet was introduced as a result of an earlier parallel magnet technology development program for 4.2 K lower field magnets. In this program the focus was shifted from purely increasing the field strength to increasing the customer convenience. The introduction of the first actively shielded 800 MHz magnet set the starting point for the replacement of all high field magnet types with actively shielded magnets. With better and even more advanced superconductors it became possible, by 2004, to actively shield 900 MHz (21 T) systems[174]. Two years later the maximum frequency for

[173] G. Roth, *Bruker SpinReport* 152/153 p. 14

[174] G. Roth, *Bruker SpinReport* 156, p. 33

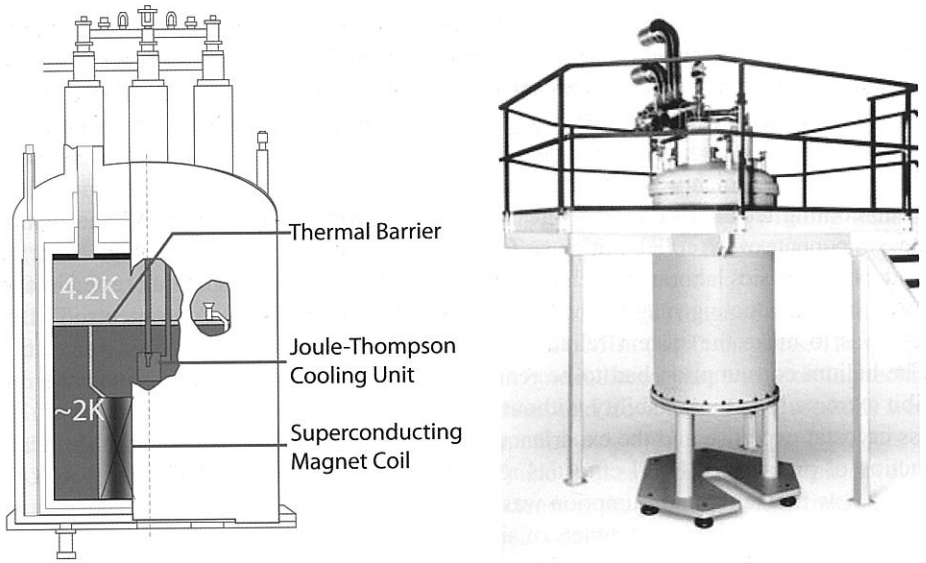

FIGURE 12.82: On the left, the sub-cooling scheme; on the right, the first 17.6 T magnet using this technology (1992), installed in Japan and in continuous operation since 1994. (Courtesy Bruker-Biospin.)

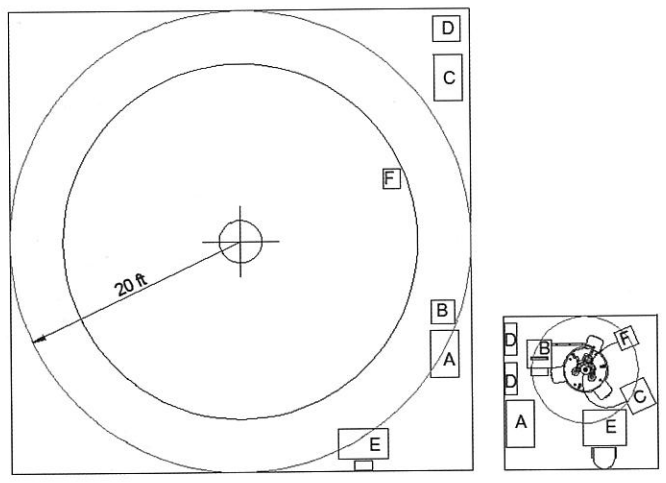

FIGURE 12.83: Space comparison of an 800 MHz unshielded magnet NMR spectrometer (1995, left); with an 800 MHz UltraShield Plus spectrometer in the same floor space (2006, right).

actively-shielded magnets was pushed up to 950 MHz (22.3 T), while in the same year it became possible to shrink the size of actively-shielded 18.8 T magnets to a much smaller format requiring only about 1/3 of the winding volume of the earlier models.

This second generation of actively shielded magnets clearly demonstrates how far reaching the small improvements in wire technology over time really are when applied simultaneously to developments in magnet technology. Concurrently these developments resulted in significant customer benefits with the result that today the installation of an 18 or 20 T magnet in an NMR lab is as

simple as the installation of a 7 T magnet was in former years. Figure 12.83 shows the space needed to set up an unshielded 800 MHz (18.8 T) system compared with the space necessary for today's actively shielded 800/850 MHz (18.8/20 T) systems. The 5 Gauss stray field line for an unshielded 18.8 T magnet needed an area of 12 m by 12 m with a ceiling height requiring two floors, or 4.9 m. Today in the same space one could set up eight 800 MHz spectrometers, and the 5 Gauss line would demand a clearance area of only 3 m by 3 m.

As the second generation actively shielded magnet fits into a single story floor, today one could in principle install sixteen 18.8 T magnets in the volume required by one first generation 800 MHz system. It would appear that at 950 MHz (22.3 T) the maximum field for actively shielded magnets using conventional LTS wire technology had been reached. The following Table 12.15 summarizes some of the characteristics of superconducting NMR magnets: the weight and the stored energy as a function of field strength. Note how the stored energy increases with increasing field strength.

TABLE 12.15: Stored Energies and Weights for High Resolution NMR Magnets from 7 to 23.5 T

Field Strength	Frequency	Weight	Stored Energy
7.05 T	300 MHz	~0.25 t	0.25 MJ
14.09 T	600 MHz	~1.2 t	0.8 MJ
19.97 T	850 MHz	~3.4 t	3.6 MJ
22.32 T	950 MHz	~6.7 t	14.6 MJ
23.49 T	1000 MHz	~15 t	50 MJ

It is technically possible to push the maximum field up to 1 GHz, as long as non-actively shielded versions of the systems are concerned because once the critical triad limit, current, temperature and magnetic field has been reached, a magnet with active shielding would become even more demanding and even more expensive. The table also illustrates the rate at which the mass of high resolution magnets increases as a function of field strength: raising the field from 20 T to 23.5 T increases the mass by a factor of more than 4; at the same time with the same advanced conductor technology in both cases, the superconductor mass increases by a factor of 8 and the amount of Nb_3Sn required increases by a factor of over 20! This dramatic increase is illustrated in Figure 12.84.

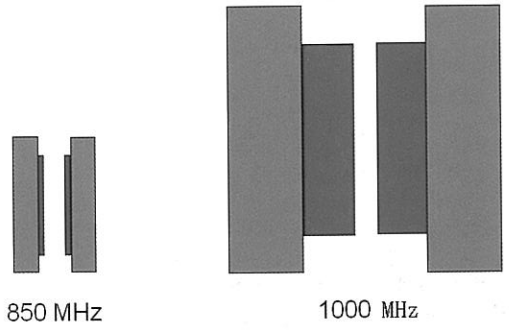

FIGURE 12.84: Illustrative comparison of the masses of a 20 T and a 23.5 T superconducting magnet using the same advanced wire technology.

Plans to break the 1 GHz barrier already exist; if one may speak of a barrier in this case, plans for which have been around for quite a while. The discovery of high temperature superconductors in 1986 raised expectations that the magnet world would change rapidly and that high fields substantially exceeding 1 GHz would become readily available. The high critical transition temperatures and the relatively high currents at high fields, publicized at that time, were very tempting and the task appeared to be easy.

From the point of the user unfortunately, the progress in handling HTS materials and in making their properties suitable for the desired applications proved to be very slow due to their complexity. The first generation of high temperature superconductors of the BSCCO type were ruled out as an unsuitable high field magnet material. The second generation of YBCO conductors on the other hand seems to be a very promising candidate. As the production of this material ramps up and becomes more of a routine manufacturing operation, our understanding of the stability requirements and mechanical properties will increase to the extent that the material may be ready for use in a practical application of the type that we have been reviewing. Optimistically we expect to be able to reach 1.2 GHz in about 5 to 7 years from now, a frequency region which promises to be of particular interest to the researchers in the life sciences.